ASTROCYTE-NEURON SIGNALING IN THE NUCLEUS ACCUMBENS: IMPLICATIONS FOR BRAIN REWARD CIRCUITRY

A DISSERTATION SUBMITTED TO THE FACULTY OF THE UNIVERSITY OF MINNESOTA BY

MICHELLE KORTO CORKRUM

IN PARTIAL FULFILLMENT OF THE REQUIREMENTS FOR THE DEGREE OF DOCTOR OF PHILOSSPHY

ADVISOR: ALFONSO ARAQUE, PhD

MAY 2019

Acknowledgements

I would like to thank my advisor, Alfonso Araque, for his enthusiastic approach to scientific discovery. In the Araque lab, I learned how to conduct rigorous science to address impactful questions as it relates to the role of astrocytes in health and disease.

I would like to thank my co-mentor, Mark Thomas, and my committee members, Eric Newman, Robert Meisel, and Michael Georgieff for invaluable guidance throughout my PhD training.

Thank you to the members of the Araque lab and Thomas lab for sharing your scientific insight and training.

My journey would not have been the same without the entering Neuroscience graduate class of 2014. I am inspired by each and every one of my classmates and look forward to remaining colleagues in the future.

The leadership of the Graduate Program of Neuroscience and the Medical Scientist Training Program aided me throughout my training journey, and I am forever thankful.

The research core facilities at the University of Minnesota propelled my experiments forward and I would like to thank the University Imaging Centers, E. Larson at the MnDRIVE Optogentics Core, M. Benneyworth at the Mouse Behavior Core and E. Marron at the Viral Vector and Cloning Core.

Work was supported by NIH 5 T32 GM 8471-22, NIH 5 T32 DA 7234-29, and F30DA042510

Dedication

In loving memory of my great aunt, Rita Padmore, who inspired me to reach for the stars and my grandfather, Wayne Turnquist, who encouraged me in my every endeavor.

Abstract

Dopamine is one of the major reward signaling molecules in the brain. Dopaminergic transmission contributes to physiological states such as learning, memory encoding, movement and motivated behaviors; and, the disruption of dopamine signaling can contribute to neuropsychiatric diseases such as substance use disorders. The majority of research on reward signaling has focused on neurons; however, astrocytes are emerging as key components of brain information processing. Astrocytes are a subset of glial cell, one of the most abundant cell types in the brain. Although astrocytes are not electrically excitable, in response to brain activity, they demonstrate increases in intracellular calcium and the subsequent release of neuroactive substances, termed gliotransmitters. Therefore, my dissertation aimed to investigate the hypothesis that astrocytes respond to brain reward signaling with elevations in cytoplasmic calcium, and subsequently modulate neuronal activity in the nucleus accumbens, one of the major reward centers of the brain. Utilizing fiber photometry, I found that astrocytes in the nucleus accumbens respond to dopamine and amphetamine with cytoplasmic calcium elevations *in vivo*. To elucidate the cellular mechanisms of this phenomenon and the consequences of astrocyte calcium signals on neuronal activity, we conducted experiments applying multiphoton calcium imaging and whole-cell patch clamp electrophysiology in acute brain slices containing the nucleus accumbens core. We found that astrocytes respond to dopamine, amphetamine and opioids with intracellular calcium elevations and subsequently modulate neuronal activity, either through adenosine signaling in the case of dopamine and amphetamine or glutamatergic signaling in the case of opioid exposure. Furthermore, we demonstrate that astrocytes contribute to the acute psychomotor behavioral effects of amphetamine, illustrating astrocyte modulation of drug-related behaviors. Overall, the current body of

work provides evidence that astrocytes actively contribute to brain reward processing via responding to dopamine and drugs of abuse with intracellular calcium increases and modulating neuronal and synaptic activity in the nucleus accumbens, one of the major nodes of the reward system.

Table of Contents

List of Tables

List of Figures

List of Abbreviations

ATP: adenosine triphosphate

Ca^{2+}: calcium

CPP: conditioned place preference

Cyclic AMP: cyclic adenosine monophosphate

D_1R: D1-like receptors

D_2R: D2-like receptors

DA: dopamine

DAMGO: [D-Ala^2, *N*-MePhe^4, Gly-ol]-enkephalin

DAT: dopamine transporter

DREADDs: Designer Receptors Exclusively Activated by Designer Drugs

EPSC: excitatory post synaptic potentials

GABA: Gamma-Aminobutyric acid

GFAP: glial fibrillary acidic protein

GFP: green fluorescent protein

GLT1: Glutamate transporter 1

IP_3: inositol triphosphate

MSNs: Medium Spiny Neurons

NAc: nucleus accumbens

NMDA: N-methyl-D-aspartate

PFC: prefrontal cortex

PPR: paired pulse ratio

SIC: slow inward currents

TRP channels: transient receptor potential channels

TRPA1: Transient receptor potential ankyrin type 1

VTA: ventral tegmental area

Chapter One: Introduction

Brain reward signaling is an integral component of the human experience. Through reward signaling we learn to associate salient stimuli that contribute to nutrition, reproduction and survival. Both natural rewards and drugs of abuse increase dopamine levels in the brain[12-15]; therefore, dopamine is a major reward signaling molecule. Dopamine signaling in the brain contributes to learning and memory, movement and reward; and when disrupted can result in pathological states such as Parkinson's disease and drug addiction.

Drug addiction is a devastating disease characterized as a substance use disorder in which there is persistent drug seeking despite harmful consequences. The propensity to relapse even after sustained periods of abstinence illustrates the chronicity of the disease and provides phenotypic evidence for persistent changes that occur in the brain. Fundamentally, drug addiction is a manifestation of alterations in synaptic transmission and plasticity. Therefore, research investigating the cellular mechanisms of synaptic signaling in the brain reward pathway will provide insight for the development of efficacious therapies to treat disruptions of dopaminergic signaling.

Dopamine receptors are G-protein coupled receptors with seven transmembrane domains (Figure 1.1). There are five subtypes of dopamine receptors belonging to the subcategories of D_1-like (D_1R; D_1 and D_5) receptors and D_2-like (D_2R; D_2, D_3, D_4) receptors. D_1Rs are coupled to the Gs protein to activate adenylyl cyclase and increase

cAMP production. Whereas, D_2Rs are coupled to Gi/o proteins that inhibit adenyl cyclase and lead to the decrease of cAMP production (Figure 1.1 and Box 1.1). Importantly, activation of both D_1Rs and D_2Rs can result in elevations of intracellular calcium via PLC signaling[8] (Box 1).

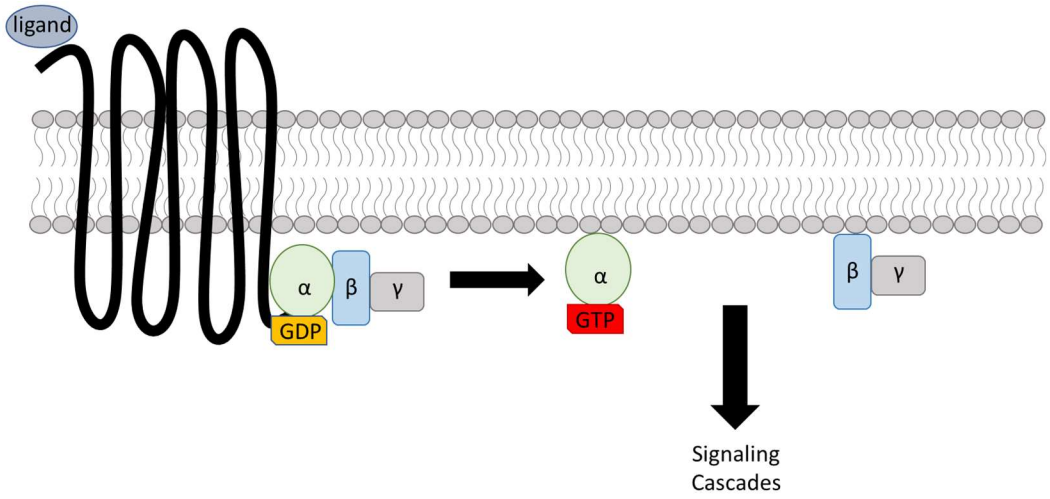

Figure 1.1. Schematic of G-protein signaling activation. In the inactive state, the G-protein coupled receptor (7-transmembrane receptor in black), is associated with the trimeric complex composed of the G-alpha (light green) and G-beta-gamma (light blue and light gray) subunits. Upon ligand binding, the GDP associated with the alpha subunit is released and converted to GTP with the addition of a phosphate group, resulting in the activation and disassociation of the alpha-subunit from the beta-gamma subunits resulting in downstream signaling events, including interactions with effectors such as adenylate cyclase. Hydrolysis of GTP back to GDP inactivates the G-protein signaling cascades.

Box 1.1. Dopamine Receptor Signaling

Traditionally, D_1Rs couple to the activation of adenyl cyclase via Gαs signaling and D_2Rs couple to the inhibition of adenyl cyclase via Gαi/o signaling. However, both classes of receptors can stimulate increases in cytoplasmic calcium. D_1Rs and D_1R-D_2R heterodimers can signal through the Gαq pathway to activate phospholipase C (PLC) and the subsequent hydrolysis of phosphatidylinositiol 4,5-biphosphate (PIP_2) to produce inositol triphosphate (IP_3) and diacylglycerol (DAG). Binding of IP_3 to its receptor on the endoplasmic reticulum results in cytoplasmic calcium elevations. D_2Rs can also stimulate PLC signaling and the consequent increases in cellular calcium via Gβγ signaling cascades.[8]

The majority of D_1Rs have a low affinity for dopamine and are activated by fast phasic signaling (from presynaptic dopaminergic neurons firing action potentials at >15 Hz) associated with memory consolidation, positive reinforcement and negative reinforcement[16]; whereas, most D_2Rs have a high affinity for dopamine and are activated by low concentrations of dopamine and the tonic firing of dopaminergic neurons (1-8Hz). D_2R activation is associated with motivational sensitivity to a stimulus[16]. Salient stimuli result in fast phasic signaling and activation of D_1Rs, and do not solely include rewarding reinforcing elements, but also novel stimuli and aversive stimuli. Therefore, dopaminergic activation does not only occur with reward, but also with aversive stimulation, such as foot shock and fear conditioning[17]. However, dopamine neurons respond preferentially to rewarding stimuli, given that approximately 75% of dopaminergic neurons respond to reward and approximately 14% signal in response to aversive stimuli[18].

Dopamine signaling in the brain contributes to reward related behaviors. Dopamine synaptic transmission can occur via synaptic contacts and extrasynaptic signaling via overflow of dopamine due to burst firing which can signal through dopamine receptors and transporters located extrasynaptically. There are four major circuits for dopaminergic transmission including: the mesolimbic system with projections from the ventral tegmental area (VTA) to the nucleus accumbens, amygdala and prefrontal cortex[19]; the mesocortical system with ventral tegmental projections to the cortex associated with cognition and executive function; the nigrostriatal pathway comprising projections from the substantia nigra pars compacta to the striatum—this pathway makes up approximately 80% of dopaminergic signaling and contributes to movement-related behaviors; and finally the tuberoinfundibular pathway which is comprised of dopaminergic signaling form the arcuate nucleus and periventricular nucleus to the infundibular region of the hypothalamus to modulate prolactin release from the anterior pituitary gland[8].

The mesolimbic dopamine system is primarily implicated in brain reward signaling. The primary source of dopamine related to reward behavior originates from the VTA. GABAergic regulation of dopaminergic cells includes modulation from local neurons, and projections from the nucleus accumbens and the globus pallidus. Afferents exhibit dopamine and glutamate co release[20,21], importantly this corelease appears to primarily happen within the mesolimbic pathway because it is not observed in the dorsal striatum, but it is observed within the nucleus accumbens[22].

The nucleus accumbens is one of the major loci for dopaminergic signaling within the mesolimbic dopamine system. The nucleus accumbens can be subdivided into a core region surrounded by a shell area. The two regions have differential expression of molecules. The shell exhibits increased expression of substance P, dopamine and serotonin and the core has increased expression of enkephalin and $GABA_A$ receptors[23]. The core sends projections within the basal ganglia whereas the shell sends projections to the amygdala and hypothalamus[23].

The nucleus accumbens core is involved with assessment of reward value and initiation of motor behavior related to reward[24]. Afferent projections for the nucleus accumbens core include**:** 1) glutamate afferents from the prefrontal cortex to provide motivational and associative information; 2) glutamatergic inputs from the parahippocampal formation to encode spatial and declarative information; 3) glutamatergic afferents from the thalamus; 4) GABAergic afferents from the ventral pallidum, VTA, lateral septum and medial prefrontal cortex; 5) dopaminergic afferents from the substantia nigra pars compacta and the VTA; 6) serotonergic input from the dorsal raphe. NAc core efferents include: output to basal ganglia GABAergic nuclei and to glutamatergic subthalamic neurons and VTA neurons[25].

The nucleus accumbens shell is involved with learning of reward and reward prediction and is associated with motivation and reward-related processes. Afferents to the nucleus accumbens shell include: 1) glutamatergic input from the prefrontal cortex; 2) afferents form the basal lateral amygdala, ventral hippocampus and the thalamus; 3)

dopaminergic input from the VTA; 4) noradrenaline input from the locus coeruleus and the nucleus of the solitary tract; and 5) serotonergic input from the dorsal raphe. Efferents from the nucleus accumbens shell include the ventral pallidum, mediodorsal thalamus, VTA, and lateral hypothalamus[25].

Interestingly, the nucleus accumbens core and nucleus accumbens shell appear to encode distinct components of dopamine signaling as it relates to reward. Saddoris et al. (2015)[26] aimed to investigate differential firing patterns of dopamine in the core and shell of the nucleus accumbens during task behavior as it relates to the predictive component of the reward (seeking the reward) and the salient component of the reward (taking the reward). Prediction error occurs in the core where dopamine encodes learning of associations and expected outcomes (predictive: seeking). During extinction, there was an attenuation of dopamine signals in the core indicating encoding for negative prediction error. Incentive salience occurs in the shell where dopamine is associated with providing value to stimuli and motivational drive (salient: taking). Work performed by Ito and colleagues (2000)[15] also illustrated distinctions between the two subregions of the nucleus accumbens, although both exhibit an increase in dopamine levels in response to cocaine self-administration, only the core showed an increase in dopamine levels in response to cues associated with cocaine administration. These data indicate that the subregions within the nucleus accumbens contribute differentially to reward related behaviors.

In addition to distinct subregions within the nucleus accumbens, there are also distinct cell types. The major cell type within the nucleus accumbens are GABAergic medium spiny neurons (MSNs) which compose over 90% of the neurons within the region.[25] The remaining neurons in the nucleus accumbens are interneurons. There are three types of GABAergic interneurons: parvalbumin positive, calretinin positive and interneurons that express: somatastatin, neuropeptide Y and neuronal nitric oxide synthase.[25] There is also a class of cholinergic interneurons that express choline acetyltransferase.[25] MSNs can express either D_1Rs or D_2Rs and there is a subpopulation of MSNs that express both D_1Rs and D_2Rs (less than 2%)[27]. Interestingly, D_1Rs constitute 80% of dopamine receptors in the nucleus accumbens[19]. D_1R MSNs express substance P, dynorphin and M4 cholinergic receptors. D_2R MSNs express enkephalin, A2a adenosine receptors and neurotensin.

D_1R and D_2R MSNs receive mesolimbic dopaminergic projections from the VTA. Based on studies that specifically blocked D_1R or D_2R neurons via a reversible neurotransmission blocking technique, researchers found that D_1R transmission is important for reward learning and D_2R signaling contributes to aversive learning.[28] D_2R signaling also contributes to learning flexibility given that when D_2R signaling is antagonized subjects exhibited greater difficulty learning the new locations of rewards[28].

Traditionally, D_1R and D_2R MSNs have been considered to be segregated into the direct and indirect pathway based on findings from the dorsal striatum. In the dorsal striatum D_1R neurons are part of the direct pathway and send projections to the globus pallidus

and substantia nigra and D_2R neurons are part of the indirect pathway because they make intermediate connections within the basal ganglia. D_1R neurons lead to disinhibition of thalamocortical output and increased movement; whereas, D_2R projections inhibit movement[29].

The demarcation for direct and indirect pathway for D_1R and D_2R MSNs in the nucleus accumbens does not appear to be as concrete. Kupchik and colleagues (2015)[27] found that D_1R and D_2R expressing MSNs project to the ventral pallidum (traditionally considered to be part of the indirect pathway). In the ventral pallidum, 50% of neurons received D_1R input and over 80% received D_2R input. Optogenetic stimulation of D_1R and D_2R neurons produced ventral pallidum responses and retrograde tracing experiments from the ventral pallidum indicated that 30% of cells projecting to the area were D_1R positive[27]. Therefore, the classic indirect pathway does not hold true for the NAc core because both D_1R and D_2R MSNs project to dorsal ventral pallidum en route to the ventral mesencephalon.

In addition to D_1R and D_2R MSNs, astrocytes are another cell type in the nucleus accumbens. **Astrocytes** are a subtype of glial cells, one of the most abundant cell types in the mammalian brain. Astrocytes can be characterized as either fibrous or protoplasmic depending on their location in the CNS (fibrous astrocytes reside in the white matter and protoplasmic astrocytes reside in the gray matter). Interestingly, astrocytes obtained their name due to their star-like shape with a cell body and processes that can extend to contact thousands of synapses[30]. In Ramón y Cajal's

(1899) rendition of human hippocampal astrocytes he depicted the cells as having integral connections with both blood vessels and neuronal synapses. These observations align with the traditional view of astrocytes as support cells and the more recent lines of evidence revealing astrocytes as key components of synaptic transmission and plasticity. Astrocytes contribute to maintaining brain homeostasis via maintenance of extracellular ion concentration, supplying trophic factors and metabolic support to neurons, preserving the blood-brain barrier, regulating blood flow and contributing to synaptogenesis[31]. Traditionally, these were the only roles astrocytes were believed to play in brain function because astrocytes are not electrically excitable—they do not generate action potentials in response to stimuli[31]. However, in the past decades, researchers have found that astrocytes demonstrate excitability and responsiveness to neuronal activity via increases in calcium—astrocytes exhibit calcium excitability[32]. Astrocytes contain both inotropic and metabotropic receptors for neurotransmitters[33] and multiple transmitters have been shown to increase calcium in astrocytes including: glutamate, ATP, epinephrine, norephinephrine, GABA, acetylcholine, serotonin, and substance P[34].

Mechanisms of astrocyte calcium increases

Intracellular calcium in astrocytes can be increased via the activation of G-protein coupled receptors located on astrocytes, such as receptors for glutamate, GABA and ATP. Activation of metabotropic G-protein coupled receptors can lead to the production of IP_3 through phospholipase C activation and the release of internal calcium stores when IP_3 binds to receptors on the endoplasmic reticulum[35] (Figure 1.2). Astrocyte

calcium levels can also increase via channels mediated by P2X receptors and NMDA receptors[36] (Figure 1.2). In addition to the soma, astrocytes also contain fine processes that exhibit increases in calcium. These processes are in close proximity to the synapse and distinct components of the process can demonstrate calcium elevations, in isolation, without affecting other components of the cell (these regions are considered microdomains[37-39].

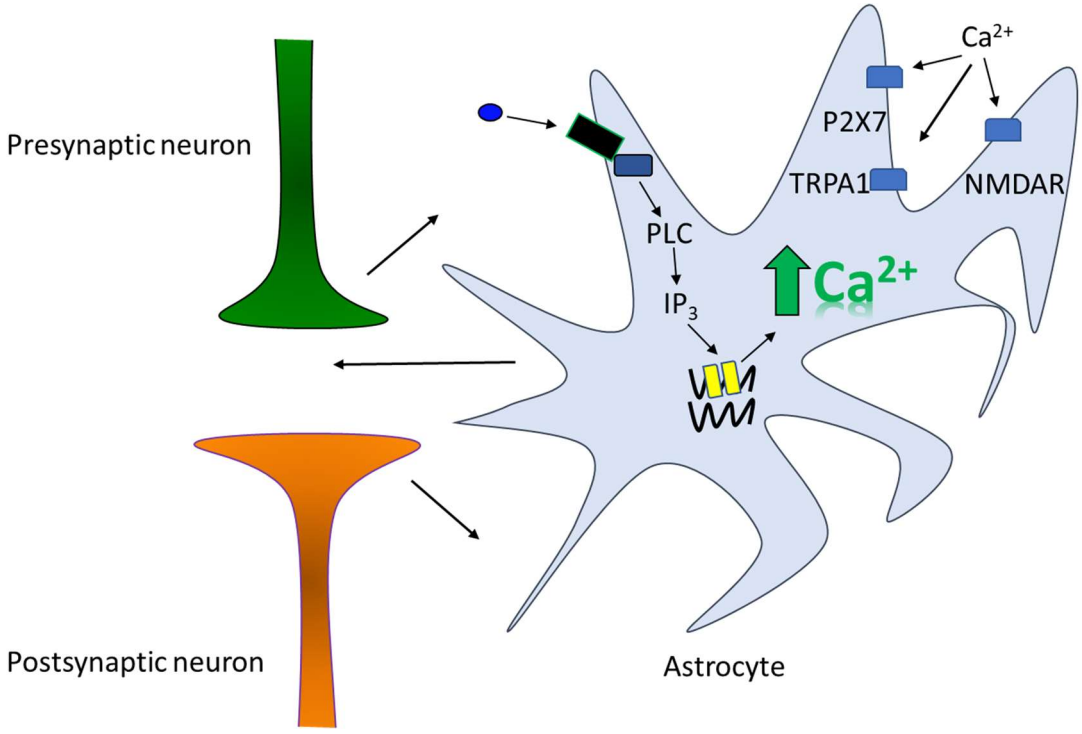

Figure 1.2. Mechanisms of astrocyte calcium increases.

Figure 1.2. Mechanisms of astrocyte calcium increases. Cytoplasmic calcium increases in astrocytes can occur via activation of G-protein coupled receptors and the subsequent release of calcium from internal endoplasmic reticulum stores via binding of IP_3 to IP_3 receptors. Astrocyte calcium increases can also occur via the influx of calcium from the extracellular space through receptors such as the P2X7, TRPA1 and NMDA.

Researchers have demonstrated that astrocytes can increase intracellular activity in the absence of neuronal activity[36]. Membrane induced calcium elevations in astrocytes can occur independent of neuronal activity via TRPA1 (transient receptor potential ankyrin type 1) receptors[36]. Calcium increases in astrocytes may also occur via reversal of the sodium/potassium exchanger located on the membrane of the astrocyte[36].

Mechanisms of gliotransmission

Astrocyte calcium elevations can subsequently lead to the release of neuroactive substances termed gliotransmitters[32], including glutamate, D-serine, GABA and ATP[35]. Calcium dependent mechanisms for gliotransmission include evidence for SNARE complex machinery given that glutamate release was inhibited in the presence of clostridial neurotoxins that inhibit exocytosis[40,41]. There is also evidence from cultured astrocytes for the presence of vesicular organelles for glutamate[42], ATP[43] and D-serine[44] (Box 1.2).

Calcium independent mechanisms of gliotransmitter release include organic anion channels that are volume sensitive, hemichannels, P2X7 receptor channels, reuptake

channel reversal and cystine-glutamate antiporter[35]. Glutamate has also been shown to be released via the volume-sensitive bestrophin-1 anion channel[45].

The bidirectional information flow between the presynaptic neuron, the post synaptic neuron and astrocytes has been deemed the tripartite synapse[31] (Figure 1.3).

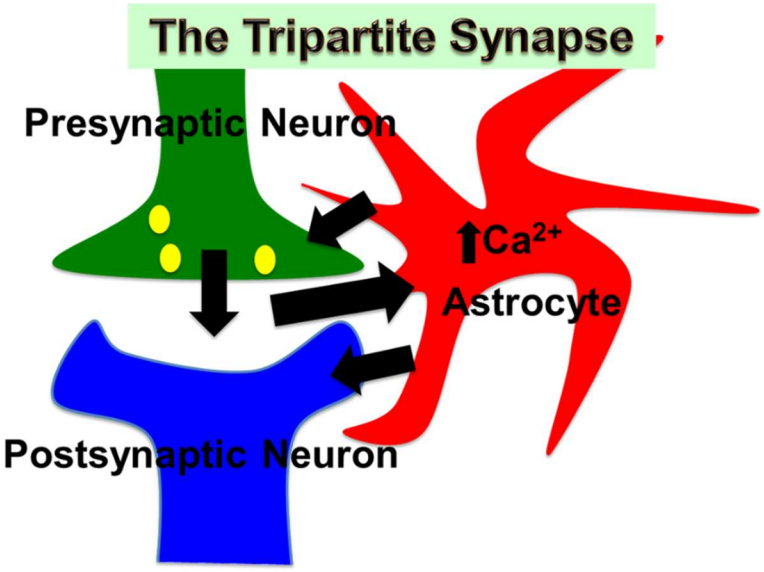

Figure 1.3. The tripartite synapse. Depiction of bidirectional signaling between the presynaptic neuron, post synaptic neuron and astrocytes at the synapse.

Box 1.2. Astrocyte glutamate signaling.

Astrocyte glutamate signaling can modulate neuronal excitability. Astrocytes can release glutamate via SNARE dependent vesicular glutamate release[1], resulting in neuronal slow inward currents (SICs). SICs are via the activation of extrasynaptic NMDA receptors that contain the GluN2B subunit, given that the frequency of SICs is attenuated by the NMDA receptor antagonist D-APV[2] and the amplitude of SICs is decreased by the specific GluN2B antagonist ifenprodil[2]. Paired recordings in the hippocampus and nucleus accumbens illustrate that SICs can result in neuronal synchrony[2,3] indicating that astrocytes meditate neuronal network activity. Interestingly, not all astrocyte calcium increases result in neuronal SICs, Shigetomi and colleagues (2008)[5] found that although both P2Y1 and PAR-1 receptor activation resulted in elevations of astrocyte cytoplasmic calcium, only PAR-1 activation induced SICs. These results may reflect the observation that astrocytes can release distinct gliotransmitters depending on the stimulus that induces the intracellular calcium increases[9]. Researchers have found that in addition to mediating slow neuronal currents, astrocytes can also mediate fast glutamate transmission via a two-pore domain potassium channel (TREK-1) localized to the microdomains of the astrocytes[10]. Interestingly, the researchers found that slow glutamate release can be mediated by a glutamate-permissive calcium-activated anion channel (Best-1). The results indicate that there are multiple mechanisms of astrocyte glutamate release including vesicular release and glutamate-permeable channels that can modulate neuronal activity.

However, some researchers have challenged the notion that IP_3 mediated increases in astrocyte calcium induces gliotransmisison, given that when the IP_3R2 (the receptor subtype preferentially expressed in astrocytes) is knocked out, there appears to be no impact on synaptic transmission or behavior[46-48]. Interestingly, although the majority of calcium transients are ablated in this model, 10% remain in the soma and 40% remain in the processes indicating a role for calcium increases independent of IP_3R2[49]. This research showed that in calcium free buffer, events at the processes were significantly reduced, suggesting calcium fluxes through the membrane may contribute to increases in intracellular calcium. This preservation of calcium may explain why synaptic

transmission changes were not observed in previous studies utilizing the $IP_3R2^{-/-}$ model. In agreement with this, researchers have found that when using approaches independent of IP_3R2 signaling to ablate astrocyte calcium signals, such as chelation of astrocyte calcium, there was an attenuation of spontaneous synaptic activity in the hippocampus[50]. However, many groups have seen ablation of synaptic changes with the $IP_3R2^{-/-}$ model[51,52] and behavioral changes associated with attenuation of IP_3R2 signaling[53]. Overall, when using the $IP_3R2^{-/-}$ mouse model it is important to recognize the caveats, i.e. calcium signaling is significantly reduced but a proportion remains in soma and processes of astrocytes; therefore, results have to be interpreted in light of this limitation and alternative approaches must also be used to verify the effects observed.

Astrocytes in the nucleus accumbens

Astrocytes have been specifically characterized in the nucleus accumbens. D'Ascenzo and colleagues (2007)[3] recorded from GFP expressing astrocytes in the nucleus accumbens and confirmed that astrocytes in this region were electrically inexcitable. Additionally, they found that the astrocytes had a mean resting membrane potential around -89 mV—illustrating that they were more hyperpolarized than the neurons in the region. They also found that the cells were coupled via gap junctions utilizing two methods: dye coupling of astrocytes after one cell was loaded with Alexa 568 and paired recordings illustrating depolarization induced current flow in a bidirectional manner. Overall, their study aimed to investigate astrocyte-neuron communication in the nucleus accumbens with a focus on mGluR5 activation. Activation of mGluR5 receptors increased calcium in astrocytes and stimulated glutamatergic transmission as

manifested as slow inward currents (SICs) mediated by NMDA receptors containing the NR2B subunit (the currents were sensitive to the selective NR2B subunit antagonist—ifenprodil).[3] Direct activation of astrocytes via caged calcium also induced SICs illustrating that SICs were mediated by calcium elevations in astrocytes. Importantly, mGluR5 activation only increased SICs in 56% of MSNs[3]—this may be due to the distinct neuronal populations in the nucleus accumbens (i.e. the data from the study was collected from pooled MSNs and astrocytes may modulate D_1R and D_2R MSN networks differentially as demonstrated by Martin et al., 2015[52]).

In addition to the evidence of bidirectional communication between astrocytes and neurons in the nucleus accumbens[3], astrocytes in the nucleus accumbens have also been implicated in contributing to the rewarding effects of drugs of abuse.

Ethanol

In 2014, Bull and colleagues published work investigating the role of astrocytes in ethanol seeking behavior[54]. The group utilized designer receptors specifically targeted to astrocytes in the nucleus accumbens core, and found that upon activation there was decrease ethanol self-administration. Importantly, this change in behavior was true for astrocyte manipulations in the nucleus accumbens core, but not the nucleus accumbens shell. The researchers also examined a marker for astrocyte activity, GFAP, and found that ethanol self-administration increased GFAP levels in nucleus accumbens core astrocytes, but not astrocytes located in the nucleus accumbens shell[54]. A study conducted in cultured astrocytes also suggests that astrocytes contribute to ethanol

induced dopaminergic signaling in the nucleus accumbens[55]. Additionally, Lee and colleagues (2013)[56] found that disruption of adenosine signaling in the striatum via ablating the mechanism of adenosine transport decreased overall expression of the glutamate transporter (EAAT2) and astrocyte expression of aquaporin-4, this led to increased ethanol consumption and decreased sensitivity to ethanol as well as attenuated glutamate clearance which was normalized with ceftriaxone treatment, an agent that can normalize glutamate transporter levels[56].

Psychostimulants

Cocaine self-administration and withdrawal increases GFAP levels but decreases astrocyte surface area and volume[57]. Interestingly, there was a decrease of coexpression of GFAP and synapsin I, suggesting decreased synaptic contacts between astrocytes and neurons in the NAc core after drug exposure, indicating a modulation of the machinery necessary for astrocyte-neuron communication[57]. Cocaine is also known to disrupt glutamatergic transmission via downregulation of GLT-1 expression (a glutamate transporter primarily expressed on astrocytes[58]), which can be restored with ceftriaxone treatment. Interestingly, ceftriaxone also recovered GFAP and synaptic changes observed with cocaine self-administration[57] and decreased drug seeking[58]. Future studies can focus on the electrophysiology correlates of the decrease in GFAP-synapsin I coexpression i.e. are the synaptic changes seen with all inputs to the nucleus accumbens or only specific inputs and cell types? Researchers have also found that attenuation of gliotransmission decreases reinstatement of drug seeking behaviors[59].

Opioids

Researchers have observed that astrocyte activation contributes to nucleus accumbens morphine signaling. Bland et al. (2009)[60] examined the effect of ibudilast which inhibits glial release of proinflammatory cytokines, nitric oxide and growth factors on morphine induced dopamine signaling in the nucleus accumbens and found that ibudilast decreased nucleus accumbens dopamine levels and morphine withdrawal symptoms.[60] Wu and colleagues (2017)[61] found that morphine disrupts astrocyte calcium signaling and D-serine signaling which is associated with an attenuation of excitability of inhibitory neurons. Narita and colleagues (2006)[62] also found that conditioned place preference of amphetamine and morphine was attenuated by systemic pretreatment of an inhibitor of astrocyte GFAP activation. Pretreatment of astrocyte conditioned media into the nucleus accumbens enhanced the rewarding effects of morphine and amphetamine[62], indicating that astrocytes contribute to drug seeking behavior.

The role of astrocytes in dopamine signaling

Drugs of abuse increase dopamine in the NAc which may contribute to the initial rewarding effects of the drugs[63,64]. Astrocytes express both D_1Rs and D_2Rs[65-67]. Importantly, dopamine receptor expression has also been found in human astrocytes[68,69].

Evidence for astrocyte signaling in dopaminergic transmission has been provided by cultured astrocyte studies. Researchers found that cultured cortical astrocytes

demonstrate responsiveness to dopamine[70]. Hansson and colleagues (1988)[71] found that D_1R agonism increased cyclic AMP levels in cultured astrocytes from the cortex and striatum and found that striatum astrocytes responded more robustly than cortical astrocytes, suggesting regional differences in astrocyte sensitivity to dopamine. Zanassi et al., (1999)[72] also found that D_1R activation increases cAMP levels in cultured striatal astrocytes and that neuronal presence influenced astrocyte responsiveness to dopamine, given that there were enhanced cAMP elevations when the astrocytes were cocultured with neurons from the substantia nigra, providing evidence for astrocyte-neuron communication in dopaminergic signaling systems. The researchers saw no increase in cAMP after dopamine exposure in the hippocampus, further suggesting that astrocytes in distinct regions of the brain respond to dopamine differently. Jennings and colleagues (2017)[73] found that hippocampal astrocytes respond to dopamine with increases in intracellular calcium. The data illuminate the variability and inability to generalize data across preparations, because the cAMP study was conducted in culture and the calcium study was conducted in acute brain slices. Additionally, the results suggest that cAMP alterations and calcium changes may not always be linked—this would have to be confirmed in controlled experiments looking at both calcium and cAMP in the same experimental preparation.

In addition to increasing cAMP levels, researchers have found that dopamine induced activation of astrocytes and increases in intracellular calcium are associated with PLC signaling[74]. Calcium imaging studies showed that cultured cortical astrocytes respond to D_2R activation with increases in calcium[68]. Vaarman and colleagues (2010)[75] found that

although astrocytes respond to dopamine with increases in calcium this was independent of dopamine receptors because when dopamine receptors were blocked astrocyte calcium increases persisted[75]. The researchers concluded that astrocyte increases in calcium was via reactive oxygen species produced by the breakdown of dopamine by monoamine oxidase[75]. Interestingly this increase in calcium was also via PLC signaling, the results are in contrast with previous studies that show a dopamine receptor dependent increase in astrocyte calcium in response to dopamine[74]. The conflicting results may be due to the conditions used to culture the astrocytes. One of the first *in-vitro* studies to investigate astrocyte responsiveness to dopamine in the hippocampus[73], partial contribution of monoamine oxidase was found to mediate astrocyte calcium increases, but this contribution was not as robust as the contribution of dopamine receptors.

Jennings and colleagues conducted one of the first studies investigating astrocyte responsiveness to dopamine in acute brain slices. This is an important advancement because acute brain slices do not exhibit the aberrant morphology and functional changes that are seen in cultured preparations[76]. The researchers found that astrocytes within the hippocampal stratum radiatum increase calcium in response to dopamine in a biphasic manner with the increase associated with D_1Rs and the decrease associated with D_2Rs. The increase in calcium was due to internal stores and decrease was associated with calcium channel activity. Astrocytes in the stratum lacunosum moleculare also responded to dopamine but in a receptor independent manner—similar to the results found by Vaarman et al. (2010)[75], future studies can investigate if this

increase was due to reactive oxygen species via metabolism of dopamine as proposed by Vaarman et al., (2010)[75]. Jennings and colleagues (2017)[73] also investigated synaptic transmission in the stratum lacunosum moleculare. They found that dopamine increased astrocyte calcium and depressed excitatory transmission. But the changes in synaptic transmission were mediated by dopamine receptors whereas the changes in astrocytes were not dependent on dopamine receptors. Additionally, clamping astrocyte calcium did not ablate depression of excitatory transmission suggesting that the depression is not mediated by calcium signaling in astrocytes[73]. Given that the astrocyte calcium signal was not ablated by the dopamine receptor antagonists, astrocyte responsiveness to dopamine in the stratum lacunosum moleculare may be mediated by reactive oxygen species[75]. Additionally, the researchers illustrated that these astrocytes are distinct when compared to stratum radiatum astrocytes, given that the astrocytes in the stratum radiatum required a lower concentration of dopamine for activation and the calcium increases were mediated by dopamine receptors. Because researchers did not find that dopamine receptors mediated calcium changes in astrocytes in the stratum lacunosum moleculare, it is not surprising that the calcium did not mediate dopamine-evoked depression of excitatory transmission in this brain region. The results suggest that in the stratum lacunosum moleculare, astrocytes are activated by a byproduct of dopamine and the calcium signal may be mediating the maintenance of the environment—a passive role rather than responding to synaptic activity via a receptor on the astrocyte. Therefore, astrocytes may only mediate neuronal activity when synaptic relevant receptors are activated on astrocytes. The study provides evidence that not all astrocyte calcium signals are the same—some may mediate maintenance of brain homeostasis

and other calcium signals may mediate synaptic transmission and plasticity. Specifically, astrocytes can increase calcium via dopamine receptors in one instance and in other instances via reactive oxygen species.

Martin et al., (2015)[52] conducted a pivotal study illustrating that astrocytes participate in distinct dopaminergic circuits in the striatum. The researchers found astrocytes that specifically modulate D_1R MSN signaling and a distinct group of astrocytes that specifically modulate D_2R MSN signaling (Martin et al., 2015)[52]. Although this study did not look at astrocyte responsiveness to dopamine it does illustrate an integral role of astrocytes in the dopaminergic system and illustrates distinct populations of astrocytes based on neuronal circuitry.

Future studies can look at what allows for the distinction between circuits within astrocytes. Factors that may influence astrocyte allocation into specific circuits include specific gene expression and proximity to synapses.

An additional study that investigated astrocyte contribution to dopaminergic tripartite synapses was conducted by Bosson et al., 2015[77]. The researchers showed that astrocytes are sensitive to dopaminergic signaling disruption and their contacts with neurons can be modulated by changes in dopaminergic signaling. The group investigated the impact of dopaminergic disruption on astrocyte signaling and structure of the tripartite synapse in the substantia nigra. Dopamine lesions increased GFAP levels and soma size of astrocytes. To specifically examine the tripartite synapse, the

researchers studied the presynaptic marker, synaptophysin, the post synaptic marker, PSD95, and a marker for perisynaptic astrocyte processes (phosphoezrin). The results indicated an increase in excitatory synapse number and an increase in the amount of synapses surrounded by perisynaptic astrocytes. In this study, D_1R and D_2R antagonists did not change the number of active astrocytes, but the frequency and amplitude of astrocyte calcium events increased with blockade of dopamine receptors and the number of gap junction coupled astrocytes also increased with D1/D2 antagonists on board[77], providing evidence that astrocytes respond to modulation of dopaminergic transmission.

However, there remains scarce research on the impact of dopamine on astrocyte-neuron signaling in the nucleus accumbens, one of the major reward centers of the brain. To understand the contribution of astrocytes to synaptic transmission and plasticity in the nucleus accumbens it is important to review the impact of dopamine and drugs of abuse on neuronal signaling in the nucleus accumbens. My thesis specifically examines the impact of dopamine, amphetamine and opioids on astrocyte calcium signaling and astrocyte-neuron interactions in the nucleus accumbens. One of the major effects of drugs of abuse in the brain is the modulation of synaptic transmission and plasticity. Drugs of abuse increase dopamine levels in the nucleus accumbens[12]. Amphetamine increases dopamine levels in the nucleus accumbens via blocking and reversing the dopamine transporter[4] (Box 1.3) and opioids increase dopamine via disinhibiting dopaminergic transmission from the VTA to the nucleus accumbens[78] (Box 1.3).

Box 1.3. Mechanism of action of amphetamine and opioids.

Amphetamine
Amphetamine is a powerful psychostimulant used to treat neuropsychiatric disorders such as attention deficit/hyperactivity disorder (ADHD). However, amphetamine also exhibits high abuse potential, given its ability to increase synaptic dopamine. The structure of amphetamine gives insight into its mechanism of action, amphetamine has high structural homology with monoamines (such as an aromatic ring and aryl side chain with a nitrogen attached), allowing the substance to compete for binding on monoamine reuptake transporters, including dopamine transporters. Amphetamine also reverses monoamine transporters via occluding the storage of monoamines into neuronal vesicles due to its high affinity for the vesicular monoamine transporter 2 (VMAT2). The actions of amphetamine cumulate into an increase of monoamines, such as dopamine, at the synapse.[4]

Opioids
Unlike amphetamine, opioids can directly bind to receptors in the brain to exert their effects. Opioids exert their effects in the brain via $G_{i/o}$-protein coupled receptor signaling. There are three major subtypes of opioid receptors, mu, kappa, and delta, and researchers have also characterized a nociception/orphanin FQ opioid peptide receptor[6]. Endogenous opioid peptides are derived from proenkephalin, proopiomelancortin, and prodynorphin[7]. Peptides with a high infinity for the mu opioid receptor and delta opioid receptor include: beta-endorphin and met-enkephalin. The endogenous peptide dynorphin 1-17 has a high affinity for kappa opioid receptors. Exogenous agonists include: DAMGO and morphine for mu opioid receptors, [D-Ala(2)]deltrophin-II for delta opioid receptors and U50,488 for kappa opioid receptors. After binding to its receptor, opioids induce their effects by hyperpolarizing cells and decreasing firing rates via opening inward rectifying potassium channels that are calcium dependent and closing N-type voltage gated calcium channels[11]. Overall, opioids can increase dopamine levels in the nucleus accumbens via disinhibiting dopaminergic transmission.

Dopamine acts in the nucleus accumbens to inhibit excitatory synaptic transmission and inhibitory synaptic transmission[79]. Psychostimulants, such as amphetamine have also been shown to attenuate excitatory transmission in the nucleus accumbens[80-82] and

opioids also exhibit the capacity to depress excitatory transmission in the nucleus accumbens[83]. Given that dopamine and abused substances can modulate synaptic transmission in the nucleus accumbens, and astrocytes have been shown to contribute to synaptic transmission and plasticity my thesis aimed to **test the hypothesis that astrocytes respond to dopamine, amphetamine and opioids with increases in cytoplasmic calcium and subsequently modulate excitatory neuronal transmission in the nucleus accumbens core.**

Aims of Dissertation

My dissertation aimed to investigate the role of astrocytes in dopaminergic signaling in the nucleus accumbens. 1) I aimed to examine if astrocytes in the nucleus accumbens respond to dopamine with increases in cytoplasmic calcium both *in vitro and in vivo.* 2) I aimed to investigate the consequences of astrocyte calcium signaling on neuronal synaptic transmission in the nucleus accumbens. 3) I aimed to determine the effects of amphetamine on astrocyte-neuron signaling in the nucleus accumbens. 4) I aimed to study the role of astrocytes in amphetamine-related drug seeking behaviors. 5) I aimed to examine the effects of opioids on astrocyte-neuron communication in the nucleus accumbens. Overall, my dissertation advances knowledge on astrocyte modulation of brain reward signaling and provides insight into potential novel therapeutics to treat diseases associated with disrupted dopaminergic transmission, such as drug addiction.

Chapter Two: Methods

2.1. Ethics Statement: All animal care and sacrifice procedures were approved by the University of Minnesota Institutional Animal Care and Use Committee (IACUC) with compliance to the National Institutes of Health guidelines for the care and use of laboratory animals.

2.2. Animals: Mice were housed under 12/12-h light/dark cycle and up to five animals per cage. The following animals (males and females) were used for the present study C57BL/6J, $IP_3R2^{-/-}$ (generously donated by Dr. J. Chen), DrD1 flox/flox (Drd1tm2.1Stl; JAX #025700), DAT-IRES-CRE, GLAST-GCaMP3 (generously donated by Dr. D. Bergles and Dr A. Agarwal), and Oprm1 flox/flox (MOR flox/flox; Jackson stock # 030074). Young (p15-p28) and adult (≥ 4 weeks) mice were used. GLAST-GCaMP3 mice were generated by crossing R26-lsl-GCaMP3 mice (JAX #014538)[84] with the GLAST-CreERT2 mice (MGI:3830051)[85]. As CreERT2 protein is inactive in the absence of tamoxifen treatment, expression of GCaMP3 was obtained in adult mice (8 weeks) by 8 daily injections of tamoxifen (1 mg, i.p.), dissolved in 90% sunflower oil, 10% ethanol to a final concentration of 10 mg/ml. The animals were used ≥ 2 weeks after tamoxifen treatment.

2.3. Slice preparation: Animals were rapidly decapitated and the brain was placed in ice-cold artificial cerebral spinal fluid (ACSF). For slow inward current experiments, animals were anesthetized with isoflurane and intracardially perused with ice cold ACSF.

ACSF contained (in mM): NaCl 124, KCl 2.69, KH_2PO_4 1.25, $MgSO_4$ 2, $NaHCO_3$ 26, $CaCl_2$ 2, and glucose 10, and was oxygenated with 95% O_2 / 5% CO_2 (pH = 7.3-7.4). 350 µm thick coronal slices containing the Nucleus Accumbens (NAc) core were made with a

vibratome (Leica VT 1200S) and incubated in oxygenated ACSF at room temperature for at least 30 minutes. Slices were placed in an immersion recording chamber and superfused (2 ml/min) with oxygenated ACSF and visualized with an Olympus BX50WI microscope (Olympus Optical, Japan), an Olympus BX61WI confocal microscope (Olympus Optical, Japan) or Leica SP5 multi-photon microscope.

2.4. Electrophysiology: The whole-cell patch clamp technique was used to make electrophysiological recordings of NAc core neurons. When filled with an internal solution containing (in mM): $KMeSO_4$ 135, KCl 10, HEPES 10, NaCl 5, ATP-Mg^{+2} 2.5, and GTP-Na^{+} 0.3 (pH = 7.3), patch electrodes exhibited a resistance of 3-10 MΩ. The membrane potential of neurons was held at -70 mV. Series and input resistances were monitored throughout the experiment using a -5 mV pulse. For slow-inward current (SIC) recordings the ACSF composition was the following (in mM): NaCl 124, KCl 2.69, KH_2PO_4 1.25, $NaHCO_3$ 26, $CaCl_2$ 4, glucose 10, glycine 10 μM. No magnesium was included in the solution to optimize activation of NMDA receptors and TTX (1 μ) was included to block sodium-dependent action potentials. For some experiments, astrocytes were patched with 4-9 MΩ electrodes filled with an internal solution containing (in mM): $KMeSO_4$ 100, KCl 50, HEPES-K 10, and ATP-Na^{+2} 4 (pH=7.3). Astrocytes membrane potential was held at -80 mV. GDPßS (10 mM) and 0.5% biocytin were included in the astrocyte patch pipette. Signals were recorded with PC-ONE amplifiers (Dagan Instruments, MN, US) and fed to a Pentium-based PC through a DigiData 1440A interface board. Signals were filtered at 1 KHz and acquired at 10 KHz sampling rate. The pCLAMP 10.4 (Axon instruments) software was used for stimulus generation, data display, acquisition and storage.

2.5. Synaptic stimulation and drug application: Synaptic currents were evoked using bipolar theta capillaries filled with ACSF placed in the brain region of study (NAc core). Paired pulses (2 ms duration with 50 ms interval) were continuously delivered at 0.33 Hz using a stimulator S-910 through an isolation unit. Excitatory post-synaptic currents (EPSCs) were isolated using picrotoxin (50 μM) and CGP5462 (1 μM) to block $GABA_A$ and $GABA_B$, respectively. The measures analyzed were mean amplitude of EPSC response and paired pulse ratio (PPR=2^{nd} EPSC/1^{st} EPSC). For exogenous dopamine (500 μM), adenosine (250 μM) and CNO (1 mM) application a borosilicate glass pipette containing the drug was placed over the NAc core and it was applied with a pressure pulse (0.5 bar, 5 s). For SKF 38393 (500 μM) or DAMGO (500 μM) application a borosilicate glass pipette containing SKF 38393 or DAMGO was placed over the NAc core and it was applied with a pressure pulse (0.5 bar, 60 s). For optical stimulation of dopamine axons, an optic fiber connected to an LED (620 nm) was placed over the NAc core and a light train (5ms pulses for 5 s) of 0.1, 1, 10, 20, 30 or 50 Hz was applied. EPSC amplitudes were grouped in 15 s time bins and EPSC obtained 15 s before and 15 s after dopamine were compared to assess changes in EPSC amplitude and PPR. For amphetamine experiments, EPSC amplitudes were grouped in 1 minute time bins and EPSC obtained 1 minute before and 20 minutes after amphetamine were compared to assess changes in EPSC amplitude. For SIC experiments the average number of SICs in a 10 minute baseline recording was compared to the average number of SICs in the 10 minute recording after DAMGO application for the first minute of the recording. Electrophysiology

analysis was done manually and semi automatically with custom MATLAB code for SIC analysis.

2.6. Ca^{2+} imaging: Cytoplasmic Ca^{2+} levels in astrocytes in the NAc core were monitored using epifluorescence, confocal, and multi-photon microscopy. Epifluorescence imaging utilized a CCD camera (Hammamatsu, Japan). Cells were illuminated during 100-200 ms with an LED at 490 nm (Prior Scientifics, MA, US) and images were acquired every 1-2 s. The LED and the CCD camera were controlled and synchronized by the MetaMorph software (Molecular devices). Confocal imaging utilized an Olympus BX61WI confocal microscope (Olympus Optical, Japan) controlled by the Fluoview software or a Leica SP5 multi-photon microscope (Leica Microsystems, USA) controlled by the Leica LAS software. Astrocytes were illuminated with 490 nm laser and images were acquired every 1-2 secs. Ca^{2+} was monitored using the following indicators: fluo-4 and the genetically encoded Ca^{2+} indicator dyes GCaMP3 under the glutamate aspartate transporter (GLAST) promoter and GCaMP6 under the glial fibrillary acidic protein (GFAP) promoter to specifically target astrocytes. For experiments using fluo-4, slices were incubated with fluo-4-AM (2 μM and 0.01 % of pluronic) for 60 min at room temperature. Where noted, Ca2+ experiments were performed in the presence of a cocktail containing: CNQX (20 μM), AP5 (50 μM), MPEP (50 μM), LY367385 (100 μM), picrotoxin (50 μM), CGP5462 (1 μM), atropine (50 μM), CPT (10 μM), and suramin (100 μM).

ImageJ software (NIH) was used to quantify fluorescence level measurements in astrocytes. Ca^{2+} variations recorded at the soma and processes of the cells were estimated as changes of the fluorescence signal over baseline ($\Delta F/F_0$), and cells were considered to show a Ca^{2+} event when the $\Delta F/F_0$ increase was at least two times the standard deviation of the baseline. Ca^{2+} event probability and Ca^{2+} oscillation (event) frequency measurements were used to quantify astrocyte activity. Ca^{2+} event probability was determined via calculating the number of events per astrocytes in a field of view in 10 second bins. To examine the difference in Ca^{2+} event probability in distinct conditions, the basal Ca^{2+} event probability (10 seconds before a stimulus) was averaged and compared to the average Ca^{2+} event probability (10 seconds after a stimulus). The Ca^{2+} oscillation (event) frequency was used for amphetamine and DAMGO experiments. The Ca^{2+} oscillation (event) frequency was determined via averaging the number of Ca^{2+} events per minute that occur during basal conditions and after exposure to amphetamine (10 μM) or averaging the number of Ca^{2+} events per thirty seconds that occur during basal conditions and after exposure to DAMGO (500 μM). Ca^{2+} analysis was done manually and semi automatically with custom MATLAB code.

2.7. Stereotaxic surgery: Animals at least four weeks of age were anesthetized with a ketamine (100 mg/kg)/ xylazine (10mg/kg) cocktail. Viral vectors (0.5μl-1μl) were injected bilaterally using a Hamilton syringe attached to a 29-gauge needle at a rate of 0.8-1.25 μl/min. To target the nucleus accumbens core, the following coordinates were used: anterior-posterior [AP]: +1.50 mm; medial-lateral [ML]: +/- 0.75 mm; dorsal-ventral [DV]: -4.50 mm). To target the ventral tegmental area, the following coordinates were

used: (anterior-posterior [AP]: -3 mm; medial-lateral [ML]: +/- 0.5 mm; dorsal-ventral [DV]: - 4.3 mm). Mice were used ≥ 2 weeks after stereotaxic surgeries. Below is a table of viral vectors used.

Table 2.1. Description of viral vector constructs

Viral Vector	**Goal**
AAV8-GFAP-hM3D(Gq)-mCherry (UNC vector core)	Target Gq designer receptor to astrocytes
AAV5-GfaABC1D-PI-LckGCaMP6.SV40 (Penn Vector Core)	Target GCaMP6 to the membrane of astrocytes
AAV5-GfaABC1D-cytoGCaMP6f-SV40 (Penn Vector Core)	Target GCaMP6 to the cytoplasm of astrocytes
AAV8-GFAP-mCherry-CRE (UNC vector core)	Target floxed genes in a astrocytic CRE dependent manner
AAV8-GFAP-mCherry (UMN vector core)	Target mCherry to astrocytes
AAV5-GfaABC1D-PI-Lck-GFP-SV40 (addgene)	Target GFP to membrane of astrocytes
AAV5-hSyn-FLEX-ChrimsonR-tdT (UNC vector core)	Target ChrimsonR to CRE-expressing neurons

2.8. Fiber photometry: We utilized fiber photometry to assess astrocyte Ca^{2+} activity and responsiveness to dopamine and amphetamine in freely behaving mice. In DAT-IRES-Cre mice, AAV5-hSyn-FLEX-ChrimsonR-tdT (0.5 µl; UNC vector core) was targeted to dopaminergic neurons in the VTA (anterior-posterior [AP]: -3 mm; medial-lateral [ML]: +/- 0.5 mm; dorsal-ventral [DV]: - 4.3 mm) and AAV5-GfaABC1D-cytoGCaMP6f-SV40 (1 µl; Penn Vector Core) or AAV5-GfaABC1D-PI-Lck-GFP-SV40 (1 µl; addgene) was targeted to NAc core astrocytes (anterior-posterior[AP]: +1.50 mm;

medial-lateral [ML]: +/- 0.75 mm; dorsal-ventral [DV]: -4.50 mm) and the optic fiber (400µm, Doric Lenses: MFC_400/430-0.48_6mm_MF2.5_FLT) was placed 0.02 mm dorsal to NAc core viral infusion. The implant was attached to the skull with a dual-cure resin-ionomer (DenMat). Experiments were performed ≥ 3 weeks after surgery.

For data acquisition, the RZ5P processor (Tucker Davis Technologies) was utilized. A fluorescence mini-cube (Doric Lenses) was coupled to a 470 nm LED (Thorlabs M470F3; modulated at 211 Hz), a 405 nm LED (Thorlabs M405F1; modulated at 531 Hz) and a 595 nm LED (Thorlabs M595F2; for optogenetic stimulation of dopaminergic terminals expressing ChrimsonR). The fluorescence mini-cube was coupled to a patch cable and the opposite end was connected to the implanted optic fiber on the mice. GCaMP6f fluorescence from astrocytes were transmitted back through the cable to the mini-cube and focused onto the photoreceiver (Newport Model 2151, FC adapter). The sampling rate for the signals was 6.1 kHz. For each stimulation parameter, mice were stimulated 3-5 times with a 2 minute inter-stimulation interval.

For data analysis, active (470 nm) and reference (405 nm) photometry signals were corrected for bleaching by fitting to an exponential function. The normalized signal was created via examining change in fluorescence ([470nm signal − fitted 405nm signal]/[fitted 405nm signal]). Custom MATLAB code was utilized to analyze the normalized data.

2.9. Amphetamine locomotor sensitization: $IP_3R2^{-/-}$ mice (n = 18; n = 8 males and n = 10 females) and control wild-type background mice (Black Swiss; n = 16; n = 5 males and n = 11 females) ≥ 5 weeks of age were used for behavioral experiments. For saline experiments ($IP_3R2^{-/-}$ mice: n =6; n = 3 males and n = 3 females; Black Swiss mice: n =6; n = 3 males and n = 3 females). Male and female GFAP-$D1^{-/-}$ mice (n = 12; n = 6 males and n = 6 females;) and GFAP-$D1^{-/-}$ control littermate mice (n = 11; n = 4 males and n = 7 females) were used for behavioral experiments. For saline experiments: GFAP-$D1^{-/-}$ mice (n = 13; n = 6 males and n = 7 females;) and GFAP-$D1^{-/-}$ control littermate mice (n = 9; n = 4 males and n = 5 females) Mice were ≥ 5 weeks of age. Mice were handled by the experimenter for at least two days before behavioral testing commenced. To habituate animals to i.p. injections and experimental conditions, mice were injected with saline for two consecutive days. Next, mice were injected for five consecutive days with amphetamine (2.5 mg/kg, i.p.). For examination of acute locomotor sanitization in D1 flox/flox mice 5 mg/kg amphetamine was administered (i.p.). On test days, mice were placed in locomotor chambers for 30 minutes to habituate to the environment, followed by drug administration (saline or amphetamine) and 60 minutes of locomotor tracking post-injection. Locomotor activity was tracked automatically using a camera tracking system and ANY-maze software (Stoelting Co.). A two-way repeated measures ANOVA was used to analyze the data.

2.10. Amphetamine conditioned place preference: Male and female $IP_3R2^{-/-}$ mice (n = 12; n = 6 males and n = 6 females), $IP_3R2^{-/-}$ control wild-type background mice (Black Swiss; n = 16; n = 5 males and n = 11 females), GFAP-$D1^{-/-}$ mice (n = 24; n = 12 males

and n = 12 females;) and GFAP-D1$^{-/-}$ control littermate mice (n = 19; n = 7 males and n = 12 females) were used for behavioral experiments. Mice were ≥ 5 weeks of age. The conditioned place preference apparatus was divided into two chambers with a guillotine-style door (black/white) separating the compartments. Chamber floors were distinct with one composed of separated stainless steel rods (grid) and the other composed of mesh flooring. Mice were handled by experimenter for at least two days before behavioral testing commenced. During pre-conditioning, the mice were allowed to freely explore the apparatus for 20 minutes, time spent in both chambers were recorded and averaged over the two pre-test days. During the conditioning phase mice were injected (s.c.) with either saline or amphetamine (2.5mg/kg) and immediately confined to the corresponding CS+/CS- chamber for 30 minutes.

2.11. Immunohistochemistry: The animals were anesthetized with Avertin (2,2,2 tribromoethanol, 240 mg/kg, i.p.) and intracardially perfused with ice cold phosphate buffered saline (PBS) and subsequently with 4% paraformaldehyde (PFA) in 0.1 M phosphate buffered saline (pH 7.4). The brain was removed and 40 µm coronal sections were made using a Leica VT1000S vibratome. Vibratome sections were incubated for one hour in blocking buffer (0.1% Triton X-100, 10% Donkey or Goat serum in PBS) at room temperature. The primary antibodies were diluted in the blocking solution and the sections were incubated overnight at 4°C. The following primary antibodies were used: Sheep anti-TH (Pel-Freez, 1:500), Mouse anti-NeuN (Millipore, 1:500), Rabbit anti-GFAP (Sigma, 1:500). The slices were washed three times for ten minutes each in 0.1M PBS. The secondary antibodies were diluted in the secondary antibody buffer (0.1% Triton X-

100, 5% Donkey or Goat serum in PBS) and incubated for 2 hours at room temperature. The following secondary antibodies were used: 488 donkey anti-sheep (Invitrogen, 1:500), 405 goat anti–mouse (Invitrogen, 1:500) 488 goat anti-rabbit (Invitrogen, 1:1000). The sections were then washed 3 times with 1xPBS for 10 minutes each and mounted using Vectashield Mounting media (Vector laboratories). Mounted slices were imaged using a Leica SP5 multi-photon microscope.

The cellular specificity of GCaMP3, GCaMP6, DREADD and CRE viral vectors was tested by immohistochemical analysis of randomly selected areas of the NAc. Out of the 511 cells expressing GCaMP3 from GLAST-GCaMP3 mice, 99% were astrocytes (identified by GFAP), 0.6% were neurons (identified by NeuN) 0% were oligodendrocytes (identified by NG2) and 0.4% were microglia (identified by Iba1). Out of the 192 cells expressing GCaMP6 from the AAV5-GfaABC1D-cytoGCaMP6f-SV40 viral vector, 99% were astrocytes (identified by GFAP), 0% were neurons (identified by NeuN) 0% were oligodendrocytes (identified by NG2) and 1% were microglia (identified by Iba1). Out of the 408 cells expressing mCherry from the AAV8-GFAP-hM3D(Gq)-mCherry viral vector, 99.01% were astrocytes (identified by GFAP), 0.25% were neurons (identified by NeuN), 0% were oligodendrocytes (identified by NG2) and 0.74% were microglia (identified by Iba1). Out of the 985 cells expressing mCherry from the AAV8-GFAP-mCherry-CRE viral vector, 87.6% were astrocytes (identified by GFAP), 11.9% were neurons (identified by NeuN), 0% were oligodendrocytes (identified by NG2) and 0.5% were microglia (identified by Iba1).

For biocytin labeling single astrocytes were recorded with patch pipettes and filled with internal solution containing 0.5% biocytin. Slices were fixed in 4% PFA in 0.1 PBS (pH 7.4) at 4°C. Slices were washed three times in 1xPBS (10 minutes each). To visualize biocytin slices were incubated with Alexa488-Streptavidin (RRID:AB 2315383; 1:500) for 48 hours at 4°C. Slices were then washed for 3 times with 1xPBS (10 minutes each) and mounted with Vectashield mounting media (Vector laboratories). All mounted slices were imaged using a Leica SP5 multi-photon microscope.

2.12. Tissue preparation for electron microscopy: Three mice, obtained from the Animal House Facility (School of Medicine, University of Castilla-La Mancha), were used in this study for pre-embedding immunohistochemical analyses. The care and handling of animals prior to and during the experimental procedures were in accordance with Spanish (RD 1201/2005) and European Union (86/609/EC) regulations, and the protocols were approved by the University's Animal Care and Use Committee. Animals were anaesthetized by intraperitoneal injection of ketamine／xylazine 1:1 (0.1 mL／kg b.w.) and transcardially perfused with ice-cold fixative containing 4% paraformaldehyde, with 0.05% glutaraldehyde and 15% (v/v) saturated picric acid made up in 0.1 M phosphate buffer (PB, pH 7.4). After perfusion, brains were removed and immersed in the same fixative for 2 hours or overnight at 4°C. Tissue blocks were washed thoroughly in 0.1 M PB. Coronal 60 µm thick sections were cut on a Vibratome (Leica V1000).

2.13. Antibodies and chemicals for electron microscopy: The following primary antibodies were used: guinea pig anti-D1R polyclonal (GP-Af500; C-terminus 45 aa. of mouse D1R, NM010076; Frontier Institute co., Japan). The characteristics and specificity of the antibody targeting D1R has been described elsewhere[86,87]. The secondary antibodies used were goat anti-guinea pig IgG coupled to 1.4 nm gold (1:100; Nanoprobes Inc., Stony Brook, NY, USA).

2.14. Immunohistochemistry for electron microscopy: Immunohistochemical reactions for electron microscopy were carried out using the pre-embedding immunogold method described previously[88]. Briefly, free-floating sections were incubated in 10% (v／v) NGS diluted in TBS. Sections were then incubated in anti-D1R antibodies [3-5 μg／mL diluted in TBS containing 1% (v／v) NGS], followed by incubation in goat anti-guinea pig IgG coupled to 1.4 nm gold (Nanoprobes Inc., Stony Brook, NY, USA), respectively. Sections were postfixed in 1% (v／v) glutaraldehyde and washed in double-distilled water, followed by silver enhancement of the gold particles with an HQ Silver kit (Nanoprobes Inc.). Sections were then treated with osmium tetraoxide (1% in 0.1 m phosphate buffer), block-stained with uranyl acetate, dehydrated in graded series of ethanol and flat-embedded on glass slides in Durcupan (Fluka) resin. Regions of interest were cut at 70-90 nm on an ultramicrotome (Reichert Ultracut E, Leica, Austria) and collected on single slot pioloform-coated copper grids. Staining was performed on drops of 1% aqueous uranyl acetate followed by Reynolds's lead citrate. Ultrastructural analyses were performed in a Jeol-1010 electron microscope.

2.15. Statistics: Data are expressed as mean ± standard error of the mean (SEM). Data normality was tested using a Kolmogorov-Smirnov test. Results were compared using a two-tailed Student's *t*-test or ANOVA (α = 0.05). One way ANOVA with a Fisher LSD method post hoc was used for normal distributed data and Kruskal-Wallis One Way ANOVA with Dunn's method post hoc was used for non-normal distributed data. A full report of the statistics used in every case is detailed in Extended Data Tables. Statistical differences were established with $p < 0.05$ (*), $p < 0.01$ (**) and $p < 0.001$ (***).

2.16. Pharmacology: 4-[3-[2-(Trifluoromethyl)-9*H*-thioxanthen-9-ylidene]propyl]-1-piperazineethanol dihydrochloride (flupenthixol dihydrochloride), [*S*-(*R**,*R**)]-[3-[[1-(3,4-Dichlorophenyl)ethyl]amino]-2-hydroxypropyl](cyclohexylmethyl) phosphinic acid (CGP 54626 hydrochloride), 8,8'-[Carbonyl*bis*[imino-3,1-phenylenecarbonylimino(4-methyl-3,1-phenylene)carbonylimino]]*bis*-1,3,5-naphthalenetrisulfonic acid hexasodium salt (suramin hexasodium salt), *N*-(Piperidin-1-yl)-5-(4-iodophenyl)-1-(2,4-dichlorophenyl)-4-methyl-1*H*-pyrazole-3-carboxamide (AM 251), D-(-)-2-Amino-5-phosphonopentanoic acid (D-AP5), 6-Cyano-7-nitroquinoxaline-2,3-dione disodium (CNQX disodium salt), (*S*)-(+)-α-Amino-4-carboxy-2-methylbenzeneacetic acid (LY367385), and 2-Methyl-6-(phenylethynyl)pyridine hydrochloride (MPEP hydrochloride), Octahydro-12-(hydroxymethyl)-2-imino-5,9:7,10a-dimethano-10a*H*-[1,3]dioxocino[6,5-*d*]pyrimidine-4,7,10,11,12-pentol (Tetrodotoxin: TTX) were purchased from Tocris Bioscience. Picrotoxin from Indofine Chemical Company (Hillsborough, NJ). Fluo-4-AM from Molecular Probes (Eugene, OR). All other drugs were purchased from Sigma.

Chapter Three: Astrocytes mediate dopamine-evoked synaptic regulation in the nucleus accumbens

Abstract

Dopamine is a key neurotransmitter involved in physiological processes, such as learning and memory, motor control and reward, as well as, pathological conditions, such as Parkinson's disease and drug abuse. In contrast to the extensive studies on neurons, the role of astrocytes in dopaminergic signaling remains largely unknown. Using transgenic mice, optogenetics and pharmacogenetics, we studied the role of astrocytes on the dopaminergic system. We show in freely-moving mice that astrocytes in the nucleus accumbens (NAc), a key reward center in the brain, respond with Ca^{2+} elevations to synaptically-released dopamine, a phenomenon that is enhanced by amphetamine, a psychostimulant drug that acts via increasing synaptic dopamine. In brain slices, synaptically-released dopamine increases astrocyte Ca^{2+} and stimulates the release of ATP/adenosine, which leads to excitatory synaptic depression through activation of presynaptic adenosine A_1 receptors. Amphetamine depresses neurotransmission through stimulation of astrocytes and the consequent activation of presynaptic A_1 receptors. Our results indicate that astrocyte activity is necessary and sufficient to mediate the synaptic regulation induced by dopamine and amphetamine in the NAc. We demonstrate that astrocyte-neuron interactions are involved in dopamine-mediated neuromodulation in the reward system, revealing a novel cellular pathway and target in brain reward signaling.

Introduction

Dopaminergic signaling plays fundamental roles in both physiologic and pathologic brain states. Dopamine is essential for movement, reward, learning and memory, and is implicated in brain disorders such as Parkinson's disease and drug addiction. The nucleus accumbens (NAc) is a key brain region in reward and addiction that receives extensive dopaminergic input from the ventral tegmental area (VTA)[89,90]. Dopamine depresses glutamatergic neurotransmission in the NAc, a phenomenon thought to be crucial in both reward and addiction[91,92], but the underlying mechanism remains unclear. While some reports indicate that dopamine acts on presynaptic D_1 receptors to directly depress excitatory transmission[80,81], adenosine signaling has also been implicated in dopamine-evoked excitatory depression[82,93,94]. In contrast to the extensive studies on the function of neurons in dopaminergic signaling in the NAc, the effects of dopamine on astrocyte activity and the consequences on neurotransmission are largely unknown.

Astrocytes have traditionally been considered support cells of the brain aiding in ion homeostasis, maintaining the blood-brain barrier and providing trophic support to neurons. Accumulating data shows that astrocytes also play active roles in brain physiology being key players in the tripartite synapse[31]. Astrocytes exhibit increases in intracellular Ca^{2+} in response to neurotransmitters[33,38,50,95-101] and, in turn, they release neuroactive substances termed gliotransmitters[100], that regulate synaptic transmission and plasticity[9,33,38,42,50,52,99-109]. The bidirectional signaling between neurons and astrocytes has been shown in many brain areas[33], however, the specific role of astrocytes in NAc dopamine signaling remains unknown. Here we show that optogenetic

stimulation of dopaminergic axons in freely moving animals evoke Ca^{2+} elevations in NAc astrocytes, and that these responses are altered by amphetamine. Using brain slices to identify the cellular signaling and physiological consequences, we show that astrocyte Ca^{2+} elevations evoked by synaptically-released dopamine stimulates the release of ATP/adenosine, which mediates dopamine- and psychostimulant-evoked depression of excitatory transmission through activation of A1 receptors. Selective pharmacogenetic activation of astrocytes mimic the dopamine-evoked synaptic regulation. Attenuation of astrocyte Ca^{2+} signaling decreases the acute psychomotor behavioral effects of amphetamine. This study reveals a novel cellular pathway in dopamine signaling in the brain reward system.

Results

Dopamine activates astrocyte Ca^{2+} signaling in the NAc.

Astrocytes in the globus pallidus and hippocampus[110,111] have been shown to respond to dopamine, but whether astrocytes respond *in vivo* to synaptically-released dopamine in reward centers such as the NAc remains unknown. To determine astrocyte responsiveness to synaptically-released dopamine *in vivo*, we monitored astrocyte Ca^{2+} levels in the NAc using a fiber-photometry system in freely behaving mice[112,113] and specifically stimulated dopaminergic afferents to the NAc using optogenetics (Fig. 1a, b). Mice expressing Cre under the dopamine transporter (DAT) promoter (DAT-IRES-CRE mice) were injected with the adeno associated virus AAV5-hSyn-FLEX-ChrimsonR-tdT into the VTA, to selectively express ChrimsonR (a red-shifted channelrhodopsin[114]) in dopaminergic neurons projecting to the NAc, as confirmed by immunohistochemical

colocalization of tdTomato with tyrosine hydroxylase (TH; the dopamine synthesis enzyme) in VTA neuronal cell bodies and axons in the NAc (Fig. 1a and Extended data Fig. 1a, b). Mice were also injected in the NAc with AAV5-GfaABC1D-cytoGCaMP6f-SV40 to express the Ca^{2+} indicator GCamp6f selectively in astrocytes, as confirmed by immunohistochemistry (Fig. 1a and Extended data Fig. 2c). Opto-stimulation of dopaminergic axons (5ms pulses for 5 s) reliably evoked Ca^{2+} elevations in NAc astrocytes in a stimulus frequency-dependent manner (Fig. 1c). These responses were abolished after i.p. injection of the broad dopamine receptor antagonist flupenthixol (5mg/kg) (Fig. 1d), and were absent in DAT-CRE mice injected with AAV5-GfaABC1D-GFP (i.e., lacking GCamp6f) confirming that the recorded signal was evoked by dopamine (Fig. 1d). Moreover, the amplitude (n = 19 responses from 5 animals), rise time (n = 19 responses from 5 animals) and response width (n = 19 responses from 5 animals) of the dopamine-evoked astrocyte calcium responses were enhanced 30 minutes after systemic amphetamine administration (2.5 mg/kg) (Fig. 1e, f), which is consistent with its known mode of action to increase synaptic dopamine[115]. Taken together, these *in vivo* results indicate that NAc astrocytes respond with Ca^{2+} elevations to dopamine released by synaptic terminals from the VTA, and that these responses are regulated by amphetamine.

We then performed electron microscopy studies to investigate whether astrocytes express dopamine receptors, and specifically D_1 dopamine receptors that are known to be coupled to G-proteins that mobilize Ca^{2+} [8]. Ultrastructural results indicate that D_1 receptors localize not only at the axon terminals and in the postsynaptic terminals, but

also in astrocytes (Fig. 1g), suggesting that astrocytes are able to sense dopamine and that the recorded responses could be from the direct activation of astrocytes by dopamine.

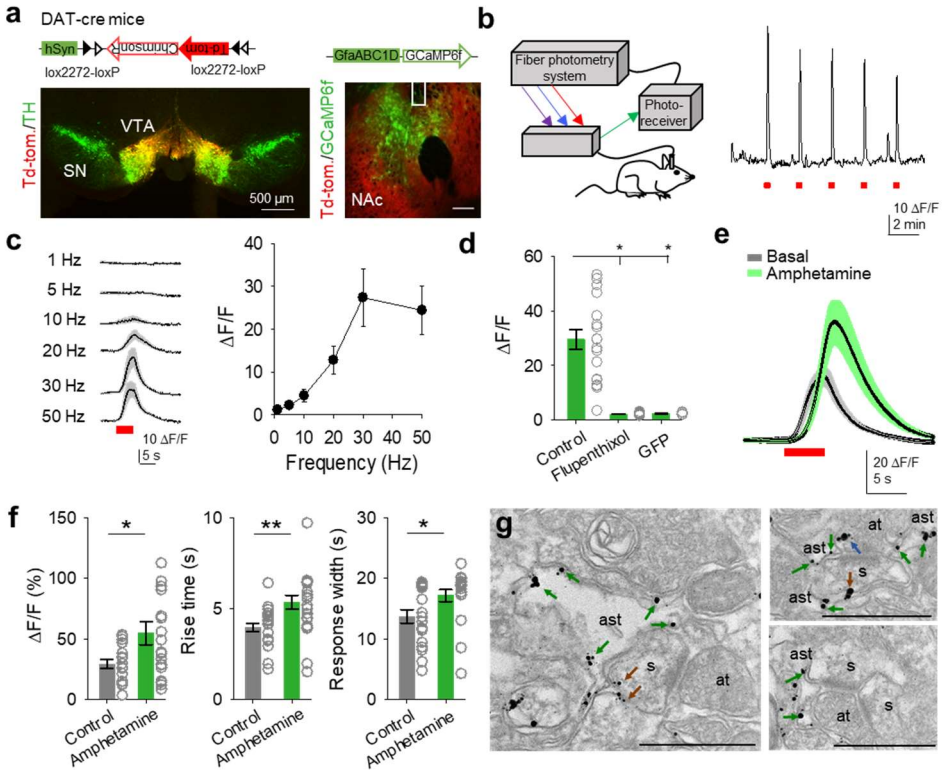

Fig. 3.1. Astrocytes respond to dopamine *in vivo*. a, Viral vectors used and fluorescence images from DAT-cre mice showing expression of ChrimsonR expression co-localized with TH in VTA dopaminergic neurons (*left*) and ChrimsonR in dopaminergic axons, astrocytes expressing GCaMP6f and the optic fiber track in the NAc (*right*). VTA: ventral tegmental area, SN: sustantia nigra, NAc: nucleus accumbens. **b,** Scheme showing the fiber photometry system (*left*) and astrocyte responses to ChrimsonR activation in the NAc (*right*). **c,** Mean astrocyte responses to different stimulation frequencies. **d,** Mean fluorescence amplitude in response to ChrimsonR activation in the different experimental conditions. **e,** Mean astrocyte responses to ChrimsonR activation before and after amphetamine administration. **f,** Mean fluorescence amplitude, response rise time and width before and after amphetamine administration. **g,** Electron microscopy images showing D_1 receptors in astrocytes (green arrows), spines (brown arrows) axon terminals (blue arrows). ast: astrocyte, s: spine, at: axon terminal (EM studies conducted by Rafael Lujan). Data are expressed as mean ± s.e.m., *p<0.05, **p<0.01.

To test this idea, we used brain slices to determine the astrocyte responsiveness to dopamine. First, we monitored the Ca^{2+} activity of NAc astrocytes in response to exogenous and endogenous dopamine. Local application of dopamine from a micropipette (500 μM, 5 s, 0.5 bar) elevated Ca^{2+} in 47 out of 75 astrocytes (n = 7), increasing the Ca^{2+} activity, quantified as Ca^{2+} event probability[9,52,99,101,109,116], in both somas (from 0.14 ± 0.05 to 0.63 ± 0.07, n = 7 slices, Fig. 2a, b) and processes (from 0.19 ± 0.04 to 0.54 ± 0.07, n = 7 slices, Fig. 2a, b). Astrocyte responsiveness to dopamine remained in the presence of a cocktail of neurotransmitter receptor antagonists (CNQX 20 μM, AP5 50 μM, MPEP 50 μM, LY367385 100 μM, picrotoxin 50 μM, CGP5462 1 μM, atropine 50 μM, CPT 10 μM, and suramin 100 μM) and TTX (1 μM), which blocks sodium-dependent action potentials (Fig. 2b), suggesting that dopamine acts directly on NAc astrocytes to elevate Ca^{2+} levels. The astrocyte Ca^{2+} responses to dopamine were abolished by the broad dopamine receptor antagonist flupenthixol (30 μM; n = 125 astrocytes from n = 11 slices), and by the D_1 receptor antagonist SCH 23390 (5 μM; n = 62 astrocytes from n = 4 slices), but unaffected by the D_2 receptor antagonist sulpiride (10 μM; n = 189 astrocytes from n = 14 slices (Fig. 2b), indicating that NAc astrocytes respond with Ca^{2+} elevations to exogenous dopamine through activation of D_1-like receptors.

We then investigated astrocyte responsiveness to synaptically released dopamine using the optogenetic approach described above. In the presence of the cocktail of neurotransmitter receptor antagonists, optogenetic stimulation of dopaminergic axons (5ms pulses for 5 s at 30 Hz) elevated astrocyte Ca^{2+} levels in 39 out of 110 astrocytes,

in both somas (from 0.11 ± 0.04 to 0.37 ± 0.06, n = 14 slices) and processes (from 0.19 ± 0.03 to 0.40 ± 0.03, n = 6 slices) in mice expressing ChrimsonR (Fig.2c-d), but not in control mice (Cre negative, i.e., wild-type DAT littermate mice lacking CRE injected with AAV5-hSyn-FLEX-ChrimsonR-tdTomato; n = 5; Fig. 2d). Consistent with results found *in vivo*, astrocytes responded to opto-stimulation in a stimulus frequency-dependent manner (Extended data Fig. 1c).

The astrocyte Ca^{2+} responses to synaptically-released dopamine were blocked by the global dopamine receptor antagonist flupenthixol (n = 143 astrocytes from n = 12 slices; Fig. 2d), and by the D_1 receptor antagonist SCH 23390 (n = 121 astrocytes from n = 6 slices; Fig. 2d), but not by the D_2 receptor antagonist sulpiride (n = 222 astrocytes from n = 13 slices; Fig. 2d). Taken together and consistent with ultrastructural evidence, these results indicate that NAc astrocytes express D_1 receptors and respond with Ca^{2+} elevations to synaptically-released dopamine through activation of D_1-like receptors.

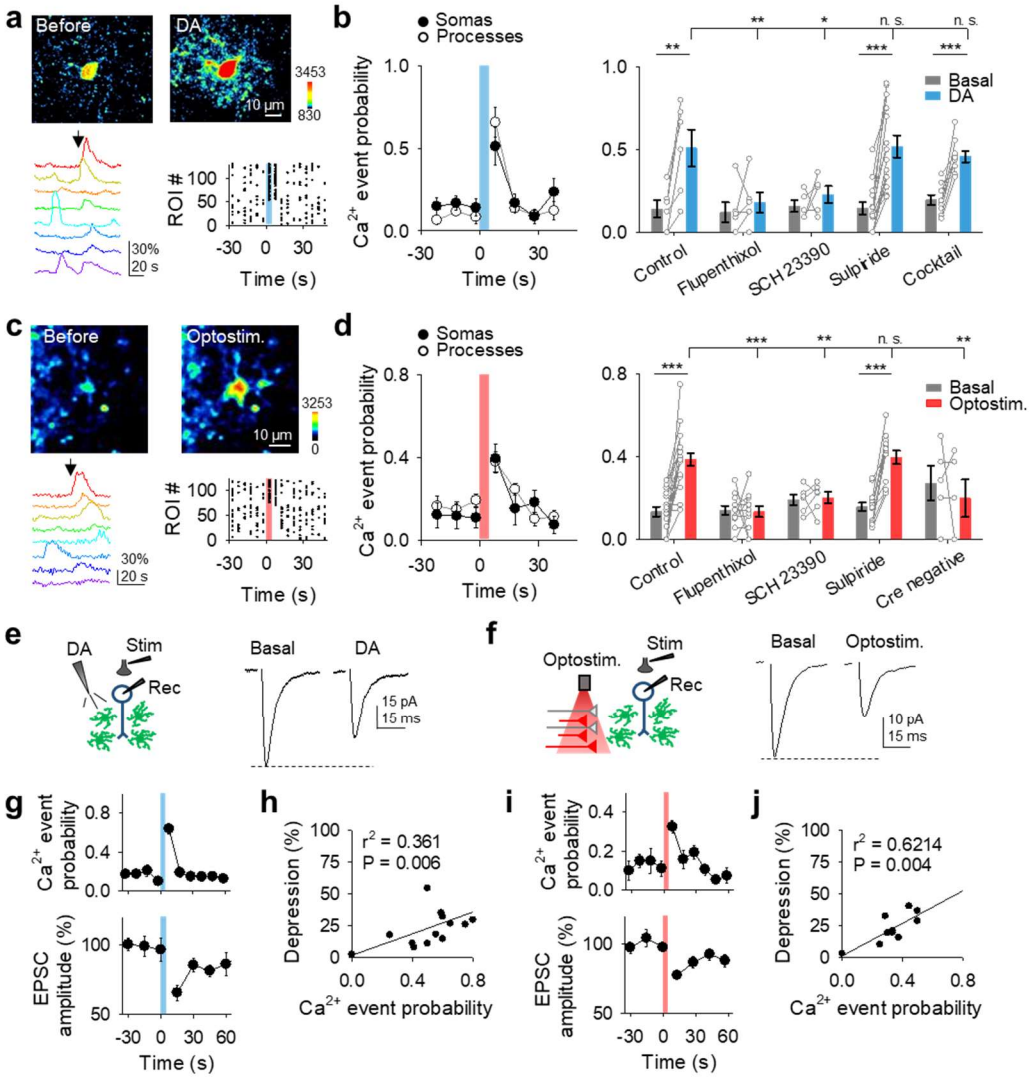

Fig. 3.2. Astrocytes respond to dopamine through D_1 receptors. a, Pseudocolor images showing the fluorescence intensities of a GCaMP3-expressing astrocytes before and after DA application (*top*), representative calcium traces of astrocytes (*bottom left*; arrow indicates DA application) and raster plot showing the calcium events recorded from all ROIs including astrocyte somas and processes (*bottom right*). **b,** Calcium event probability over time in somas and processes (*left*) and calcium event probability before (basal) and after DA application in different experimental conditions (*right*). **c** and **d,** The same as **a** and **b** but for optical stimulation. **e,** Scheme of the experimental approach (*left*) and representative EPSC traces before (basal) and after DA application (*right*). **f,** like **e** but for optical stimulation. **g,** Calcium event probability and relative EPSC amplitude over time. **h,** Relationship between calcium event probability and change in EPSC amplitude after DA application. **i** and **j,** The same as **g** and **h** but for optical stimulation. Blue and red shadows indicate DA application and optical stimulation, respectively. Data are expressed as mean ± s.e.m., *p<0.05, **p<0.01, ***p<0.001.

Dopamine-evoked excitatory synaptic regulation is mediated by astrocytes

We next investigated the consequences of the dopamine-induced astrocyte Ca^{2+} elevations on excitatory synaptic transmission in the NAc. We recorded excitatory postsynaptic currents (EPSCs) from medium spiny neurons (MSNs) before, during and after local application of dopamine while monitoring astrocyte Ca^{2+} levels (Fig. 2e). Local application of dopamine, which increased astrocytic Ca^{2+}¸ transiently depressed EPSC amplitude (from 97.6 ± 2.3 to 74.6 ± 6 .2%, n = 9; Fig. 2e, g and Extended data Fig. 3a-d)[80,81]. Likewise, synaptically-released dopamine evoked by optogenetic stimulation of dopaminergic afferents increased astrocytic Ca^{2+} and depressed excitatory synaptic transmission in mice that expressed ChrimsonR (from 98.3 ± 2.6 to 75.6 ± 2%, n = 13; Fig. 2f, i and Extended data Fig. 3e-h) but not in control littermate mice that underwent surgery (n = 6; Extended data Fig. 3h). The dopamine-induced EPSC depression was associated with an enhancement of the paired pulse ratio (PPR) (from 1.1 ± 0.05 to 1.4 ± 0.07, n = 15 for exogenous dopamine application; and 1.04 ± 0.08 to 1.32 ± 0.14, n = 11 for optical stimulation; Extended data Fig. 3c, g), suggesting a presynaptic mechanism. Interestingly, for both exogenous and synaptic dopamine there was a correlation between astrocyte Ca^{2+} elevation changes and percentage of EPSC depression (r^2 = 0. 393, n = 19 and r^2 = 0.6214, n = 11 for exogenous and synaptic dopamine, respectively; Fig. 2h and 2j), suggesting an interplay between astrocyte Ca^{2+} signaling and dopaminergic-induced depression of excitatory synaptic transmission. Consistent with the effects on astrocyte Ca^{2+}, the synaptic effects were abolished by the global dopamine receptor antagonist flupenthixol (n = 6 and n = 4 for exogenous and synaptic dopamine, respectively; Extended data Fig. 3d, h) and by the D_1 receptor antagonist

SCH 23390 (n = 9 and n = 6 for exogenous and synaptic dopamine, respectively; Extended data Fig. 3d, h), but preserved in the presence of the D_2 receptor antagonist sulpiride (n = 8 and n = 6 for exogenous and synaptic dopamine, respectively; Extended data Fig. 3d, h). These results indicate that dopamine acts via D_1-like receptors to presynaptically depress excitatory synaptic transmission[80,81], and that this synaptic regulation is associated with astrocyte Ca^{2+} elevations.

Next, we tested whether the astrocyte Ca^{2+} signal was necessary for the dopaminergic modulation of excitatory synaptic transmission. We used $IP_3R2^{-/-}$ mice[117], in which G protein-mediated Ca^{2+} elevations are largely impaired in astrocytes[46,52,116,118]. In slices from these mice, astrocyte Ca^{2+} levels and synaptic transmission were both unaffected by dopamine (Ca^{2+}: n = 135 astrocytes from n = 15 slices; EPSC: n = 8; Fig. 3b), suggesting that the dopamine-evoked synaptic regulation requires intact astrocyte Ca^{2+} signaling. To further test this hypothesis, we selectively ablated G protein signaling in astrocytes by injecting astrocytes through a whole-cell recording pipette with GDPßS which prevents G protein-mediated Ca^{2+} elevations (10 mM)[99,119]. GDPβS dialyzed in a single astrocyte spreads to a large number of gap-junction connected astrocytes (Fig. 3a). In MSNs located within the region of the GDPßS-loaded astrocyte network, dopamine did not affect astrocyte Ca^{2+} levels (n = 45 astrocytes from n = 4 slices; Fig. 3b) or synaptic transmission (n = 6; Fig. 3b). Taken together, these results indicate that G protein signaling and astrocyte Ca^{2+} elevations are necessary for dopaminergic depression of excitatory transmission in the NAc.

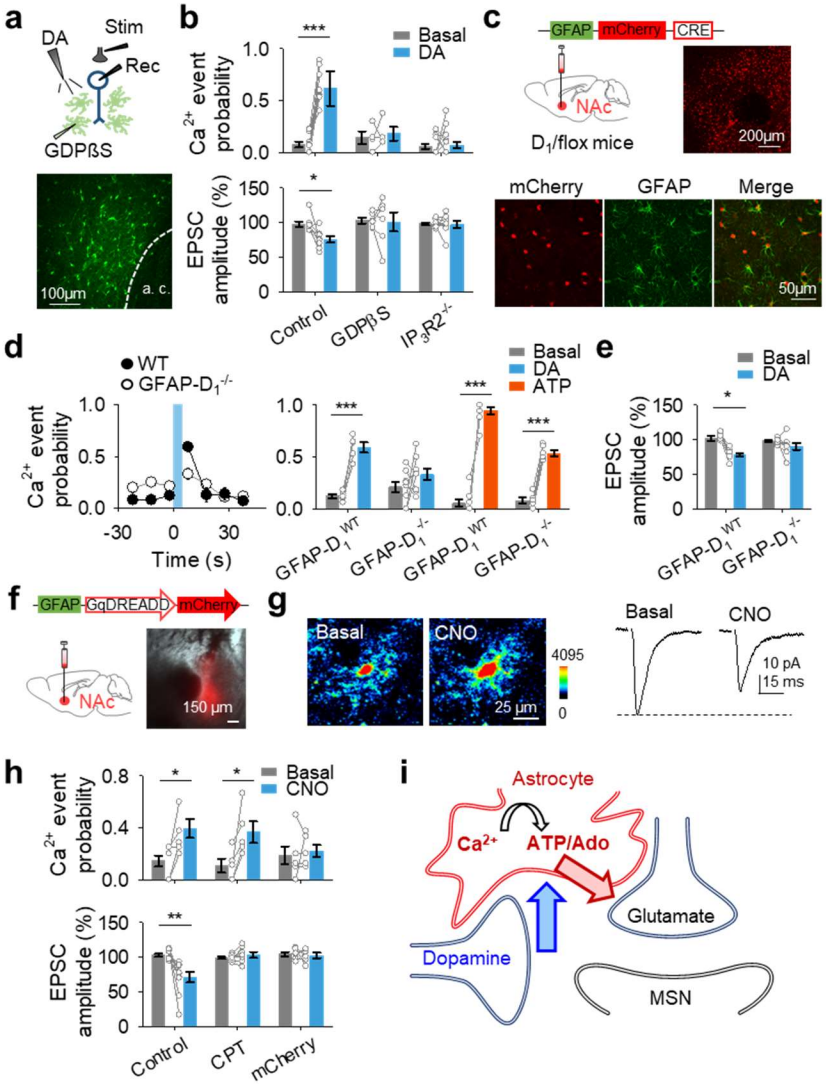

Fig. 3.3. Astrocyte calcium is necessary for DA-evoked synaptic depression.

Fig. 3.3. Astrocyte calcium is necessary for DA-evoked synaptic depression. a, Scheme of the experimental approach (*top*) and fluorescence image of an astrocyte network loaded with biocytin through a patched astrocyte (*bottom*). **b,** Calcium event probability and relative EPSC amplitude before (basal) and after DA application. **c,** Viral vector injected into the NAc of D1-flox mice and fluorescence image showing mCherry-Cre expression in the NAc (*top*), and immunohistochemistry images showing co-localization between mCherry-cre and GFAP (*bottom*). **d,** Calcium event probability over time (*left*) and calcium event probability before (basal) and after DA or ATP application (*right*). Blue shadow indicates DA application. **e,** Relative EPSC amplitude before (basal) and after DA application. **e,** Viral vector injected into the NAc and fluorescence image showing DREADD-mCherry expression in the NAc. **g,** Pseudocolor images showing the fluorescence intensities of a GCaMP6f-expressing astrocytes before and after CNO application (*left*) and representative EPSC traces before (basal) and after CNO application (*right*). **h,** Calcium event probability and relative EPSC amplitude before (basal) and after CNO application. **i,** Schematic summary depicting the signaling pathways involved in DA-evoked synaptic depression. Data are expressed as mean ± s.e.m., *p<0.05, **p<0.01, ***p<0.001.

D1 receptors specifically expressed in astrocytes mediate dopamine-evoked depression of synaptic transmission

To specifically examine the contribution of D_1 receptors expressed on astrocytes in the NAc, we selectively deleted astroglial D_1 receptors in the NAc. Mice containing the D_1 receptor gene floxed (DRD1 flox/flox mice) were injected with the viral vector (AAV8-GFAP-mCherry-CRE) into the NAc to generate a transgenic mouse model that lacks D_1 receptors specifically in NAc astrocytes (GFAP-$D_1^{-/-}$ mice; Fig. 3c and Extended data Fig. 4). As controls, virus-injected wild-type littermate mice (i.e., non-floxed DRD1mice; GFAP-D_1^{WT}) were used. We first confirmed that this approach was selective for astrocytes and not neurons. We tested neuronal responses to D_1 signaling by assessing Cd^{2+}-sensitive neuronal voltage-gated Ca^{2+} currents (Extended data Fig. 4c) that are known to be depressed by the D_1 agonist SKF 38393[120]. Consistent with this report, the amplitude of the Ca^{2+} current recorded from MSNs was depressed by SKF 38393 (500 µM, 60 s, 0.5 bar), an effect that was antagonized by the D_1 antagonist SCH 23390

(Extended data Fig. 4d, e). The SKF-evoked depression of the Ca^{2+} current was similar in MSNs of both DRD1 flox/flox wild-type littermate mice and GFAP-$D1^{-/-}$ mice (Extended data Fig. 4f), indicating that neuronal sensitivity to D_1 signaling remained intact in GFAP-$D1^{-/-}$ mice.

We next investigated the effects of astrocyte responsiveness to dopamine and dopamine-evoked synaptic regulation in GFAP-$D1^{-/-}$ mice and in GFAP-D_1^{WT} mice. Dopamine elevated Ca^{2+} in astrocytes from GFAP-D_1^{WT} mice (n = 136 astrocytes from n = 5 slices; Fig. 3d) but not from GFAP-$D_1^{-/-}$ mice (n = 88 astrocytes from n = 9 slices; Fig. 3d). In contrast, astrocytes from both GFAP-D_1^{WT} mice (n = 118 astrocytes form n = 9 slices; Fig. 3d) and GFAP-$D_1^{-/-}$ mice responded to ATP (n = 222 astrocytes from n = 6; Fig. 3d), indicating that the astrocyte Ca^{2+} machinery was preserved. In addition, to decreased astrocytic responsiveness to dopamine, the dopamine-evoked synaptic regulation was also absent in GFAP-$D_1^{-/-}$ mice (n = 8; Fig. 3e), while remaining present in GFAP-D_1^{WT} mice (n = 8; Fig. 3e). These results indicate that D_1 receptors specifically expressed on astrocytes mediate the dopamine-evoked depression of excitatory transmission in the NAc.

Astrocytes mediate synaptic depression via ATP/Adenosine signaling

Adenosine has been proposed to mediate the dopamine-induced synaptic depression in the NAc[82,93,94], but the source of adenosine remains unknown. Astrocyte Ca^{2+} signaling stimulates the release of different gliotransmitters[33], including ATP and its metabolic product adenosine, that regulate synaptic transmission in several brain areas[50,121-124].

Therefore, we hypothesized that ATP/adenosine was the gliotransmitter that mediates the dopamine-induced synaptic regulation. We first confirmed that the dopamine-evoked synaptic depression was prevented by the adenosine A_1 receptor antagonist CPT (2 μM; n = 7 and n = 7 for exogenous and synaptic dopamine, respectively; Extended data Fig. 5a, b), without affecting the astrocyte Ca^{2+} signaling (n = 85 astrocytes from n = 6 slices and n = 60 astrocytes from n = 5 slices for exogenous and synaptic dopamine, respectively; Extended data Fig. 5a, b). Moreover, exogenous adenosine application (250 μM, 5 s, 0.5 bar) evoked a similar neurotransmission depression as dopamine (n = 6 and n = 6, respectively; Extended data Fig. 5d, e), confirming that A_1 receptors mediate dopamine-induced depression of excitatory transmission. We then tested whether astrocyte Ca^{2+} was necessary for the dopamine-evoked depression of excitatory transmission. The synaptic depression evoked by dopamine was prevented by blocking the astrocyte Ca^{2+} signal after loading the astrocyte network with GDPßS and in $IP_3R2^{-/-}$ mice (Extended data Fig. 5c-e). Notably, in these conditions, adenosine was still able to depress the neurotransmission, indicating that it acts downstream of the astrocyte Ca^{2+} signal. Taken together, these results indicate that dopamine-evoked synaptic depression is mediated by activation of astrocytes, and that it occurs through sequential steps that involve astrocyte Ca^{2+} elevations, ATP/adenosine release and activation of presynaptic A_1 receptors (Fig. 3i).

Astrocyte Ca^{2+} elevations are sufficient to depress excitatory transmission in the NAc

To further test the involvement of astrocytes in synaptic depression regulation, we investigated if astrocyte Ca^{2+} elevations were sufficient to depress excitatory transmission in the NAc by directly and selectively activating astrocytes using designer receptors exclusively activated by designer drugs (DREADDs). We targeted astrocytes in the NAc with the viral vector AAV8-GFAP-Gq-DREADD-mCherry, as confirmed by immunohistochemistry (Fig. 3f and Extended data Fig. 6a-c). Activation of Gq-DREADD expressing astrocytes with clozapine-N-oxide (CNO) induced both astrocyte Ca^{2+} elevations (n = 43 astrocytes from n = 8 slices; Fig. 3g, h) and synaptic transmission depression (n = 10; Fig. 3g, h) in Gq-DREADD expressing slices. No changes in astrocytic Ca^{2+} (n = 46 astrocytes from n = 6 slices) or synaptic transmission (n = 6) were observed in response to CNO in slices from control AAV8-GFAP-mCherry injected animals (Fig. 3h). Similar to dopamine-evoked depression of neurotransmission, the synaptic depression associated with the selective DREADD activation of astrocytes resulted in an increase in PPR (n = 10; Extended data Fig. 6d), indicating a presynaptic mechanism. In addition, the DREADD-mediated synaptic regulation was also prevented by CPT (n = 7; Fig. 3h), while the astrocyte Ca^{2+} elevations were still present (n = 32 astrocytes from n = 5 slices; Fig. 3h). Taken together, these results indicate that astrocyte activation depresses excitatory transmission in the NAc via A_1 receptor signaling.

The psychostimulant amphetamine modulates excitatory synaptic transmission through activation of astrocytes

The results above indicate that astrocytes are key elements in dopaminergic signaling in the NAc. We then investigated the effects of the psychostimulant amphetamine, which is known to increase dopamine levels through the reversal and blockade of dopamine transporters[115], on astrocyte Ca^{2+} signaling and synaptic transmission. Amphetamine (10 μM) increased the Ca^{2+}-oscillation frequency in astrocytes (n = 32 astrocytes from n = 6 slices; Fig. 4a-d) and depressed excitatory synaptic transmission (n = 5; Fig. 4e-g). Both effects were absent in the presence of the global dopamine receptor antagonist flupenthixol (Ca^{2+}: n = 24 astrocytes from n = 4 slices, Fig. 4d; EPSC: n = 5, Fig. 4g). These results suggest that both amphetamine-evoked increases of Ca^{2+} activity in astrocytes and depression of synaptic transmission are via dopamine receptors. We then tested whether astrocyte Ca^{2+} signaling is necessary for amphetamine actions on excitatory synaptic transmission. First, we found that in $IP_3R2^{-/-}$ mice, which did not undergo amphetamine-induced astrocyte Ca^{2+} increases (n = 83 astrocytes from n = 7 slices, Fig. 4d), amphetamine-mediated depression of excitatory synaptic transmission was also absent (n = 6; Fig. 4g). Additionally, when G protein signaling in astrocytes was selectively ablated, utilizing GDPßS, amphetamine-induced astrocyte Ca^{2+} elevations (n = 66 astrocytes from n = 5 slices, Fig. 4d) and amphetamine-evoked depression of excitatory synaptic transmission was no longer present (n = 6, Fig. 4g), further supporting the hypothesis that astrocyte Ca^{2+} increases are necessary for amphetamine modulation of excitatory synaptic transmission. Finally, we found that when we ablated D_1 receptors on astrocytes utilizing the NAc GFAP-$D_1^{-/-}$ mice, astrocytes no longer

exhibited an increase in cytoplasmic Ca^{2+} oscillations and the depression of excitatory synaptic transmission was no longer present (Ca^{2+}: n = 119 astrocytes from n = 11 slices, Fig. 4d; EPSC: n = 5, Fig. 4g). These data are consistent with the hypothesis that amphetamine-mediated increases in dopamine levels, activate astrocytes which, in turn, stimulate gliotransmitter release and the depression of excitatory synaptic transmission. Moreover, amphetamine-induced synaptic depression was abolished by the adenosine A_1 receptor antagonist CPT (n = 7; Fig. 4g), without affecting Ca^{2+} elevations in astrocytes (n = 96 astrocytes from n = 8, Fig. 4d). Taken together, these results indicate that amphetamine acts via the activation of astrocytes and the subsequent release of ATP/adenosine to depress excitatory synaptic transmission.

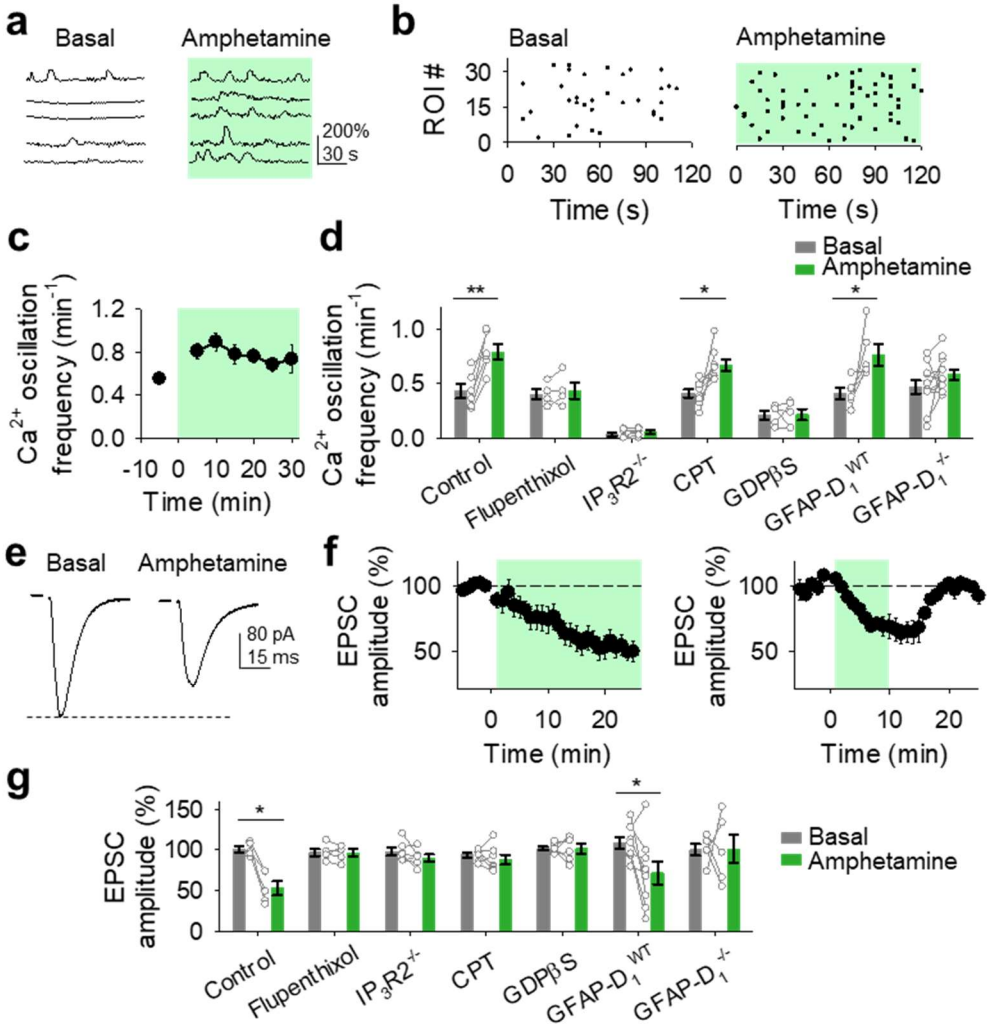

Fig. 3.4: Astrocytes are involved in amphetamine synaptic effects. a, Representative calcium traces of astrocytes in control (basal) and the presence of amphetamine. **b,** Raster plots showing the calcium events recorded from all ROIs including astrocyte somas and processes in control (basal) and the presence of amphetamine. **c,** Calcium oscillation frequency over time. **d,** Calcium oscillation frequency in control (basal) and in the presence of amphetamine in different experimental conditions. **e,** Representative EPSC traces before (basal) and after amphetamine application. **f,** Relative EPSC amplitude over time. **g,** Relative EPSC amplitude before (basal) and in the presence of amphetamine in different experimental conditions. Data are expressed as mean ± s.e.m., *p<0.05, **p<0.01, ***p<0.001.

Discussion

Present results demonstrate that astrocytes in the NAc core are key elements of the dopaminergic system. Using transgenic mice, optogenetics and DREADDs, we found that NAc astrocytes respond to dopamine with increases in cytoplasmic Ca^{2+} and release ATP/adenosine that mediates dopamine and amphetamine effects on excitatory synaptic transmission. Therefore, the present results show that astrocytes are crucially involved in the brain reward system.

In addition to passive support roles, astrocytes have been shown to play crucial roles in mediating synaptic transmission and plasticity in various brain regions such as the hippocampus, amygdala and dorsal striatum[9,50,109,122,123]. In this study we investigated the involvement of astrocytes in the reward system. Although previous studies have failed to find astrocyte Ca^{2+} responses to dopamine receptor agonists in the NAc[3], we found that astrocytes respond to dopamine through D_1 receptors. Our findings are in line with previous studies showing that astrocytes respond to dopamine with cytoplasmic Ca^{2+} increases in the hippocampus[110] and that dopamine regulates astrocyte Ca^{2+} activity in the globus pallidus[111]. We now provide evidence showing that astrocytes in the NAc, a key reward brain region, sense synaptically-released dopamine *in vivo*, and that the physiological consequences of the dopamine-evoked astrocyte Ca^{2+} increases lead to the synaptic depression of excitatory transmission, a crucial neurophysiological signal involved in reward. We show that astrocytes express D_1 receptors and that their activation leads to intracellular Ca^{2+} increases and the release of ATP/adenosine that

depresses synaptic transmission. Therefore, astrocytes can be considered integral elements of the dopaminergic system.

Dopamine has been known to depress excitatory transmission in the NAc[91,92], however, the exact mechanism of dopamine-evoked depression has been debated. Some researchers have proposed a presynaptic mechanism of action[79]; whereas others have suggested the intermediate signaling molecule ATP/adenosine to mediate dopamine effects in the NAc[82,93,94], although the exact source of ATP/adenosine remained unknown. The present results show that dopamine effects on excitatory synaptic transmission is mainly mediated by D_1 receptors. However, while previous reports had proposed that the dopamine-evoked synaptic depression was mediated by presynaptic D_1 receptors[80,81], our present results indicate that synaptic depression is mediated by astrocytic D_1 receptors. This is based on the following observations: i) astrocytes respond to dopamine with cytoplasmic Ca^{2+} elevations that are mediated though D_1 receptors; ii) dopamine-evoked synaptic depression was absent when we blocked astrocyte Ca^{2+} signal with GDPβS and in the $IP_3R2^{-/-}$ mice; iii) dopamine-evoked synaptic depression was absent in the GFAP-$D_1^{-/-}$ mice that lacked D_1 receptors specifically in astrocytes. In addition, the present results show that astrocytes release ATP/adenosine downstream of the Ca^{2+} signal and, therefore, astrocytes are the source of ATP/adenosine that leads to the dopamine-evoked synaptic depression.

Astrocytes in the NAc have been proposed to regulate neuronal excitability and addiction through the release of glutamate[3,125]. Interestingly, these studies have found astrocytic

glutamate release in response to mGluR5 or to long-term activation with DREADDs. The present study focused on astrocytic ATP/adenosine signaling in response to dopamine or to acute activation with DREADDs. Hippocampal astrocytes can release distinct gliotransmitters in response to different neuronal stimuli[9], thus, it is possible that NAc astrocytes release both gliotransmitters depending on the input signal they receive.

Dopamine signaling and excitatory synaptic regulation in the NAc are key events in reward and addiction[91,92]. Astrocytes have been proposed to be involved in drug seeking behavior[125], but the synaptic mechanism of action has not been completely elucidated. Present results show that astrocytes respond to synaptically-released dopamine and consequently regulate excitatory neurotransmission through the release of gliotransmitters ATP/adenosine and activation of neuronal A_1 adenosine receptors. In addition, they also show that astrocytes are responsible for the synaptic effects of the psychostimulant amphetamine. Additionally, the present study is the first to demonstrate astrocyte responsiveness to dopamine in freely behaving mice. Our results show that astrocytes are key elements in dopaminergic signaling in the NAc, are modulated by amphetamine and mediate its actions, indicating that they play critical roles in the synaptic regulation in the reward system. Elucidating the cellular mechanisms involved in dopamine neuromodulation is essential for developing efficacious therapies for diseases involving disrupted dopaminergic transmission such as Parkinson's disease and drug addiction. Hence, astrocytes may be potential novel cellular targets for treatment of neuropsychiatric disorders associated with disrupted dopaminergic signaling, such as motivation disorders and drug addiction.

Chapter 3: Extended Figures

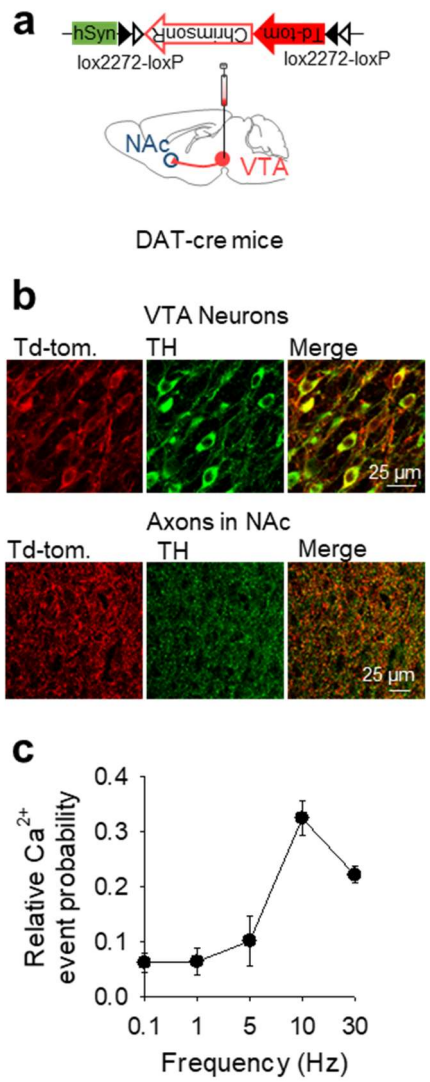

Extended data Fig. 3.1: ChrimsonR expression in dopaminergic neurons. a, Viral vector injected into the VTA of DAT-cre mice. **b,** Immunohistochemical images showing expression of AAV5-hSyn-ChrimsonR-TdTomato in neuronal somas in the VTA (*top*) and axon terminals in the NAc (*bottom*). *From left to right*: TdTomato, TH and merge. **c,** Mean astrocyte responses to different stimulation frequencies.

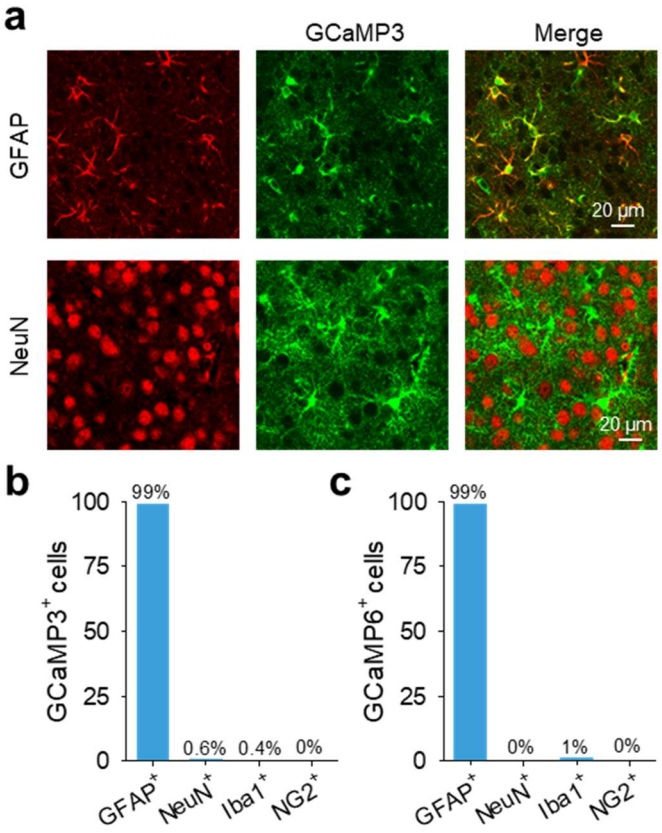

Extended data Fig. 3.2: GCaMP expression in astrocytes. a, Immunohistochemical images showing expression of GCaMP3 in NAc astrocytes and co-stained with GFAP or NeuN. *From left to right*: cell marker, GCaMP3 and merge. **b,** Percent distribution of GCaMP3⁺ cells. **c,** Percent distribution of GCaMP6f⁺ cells.

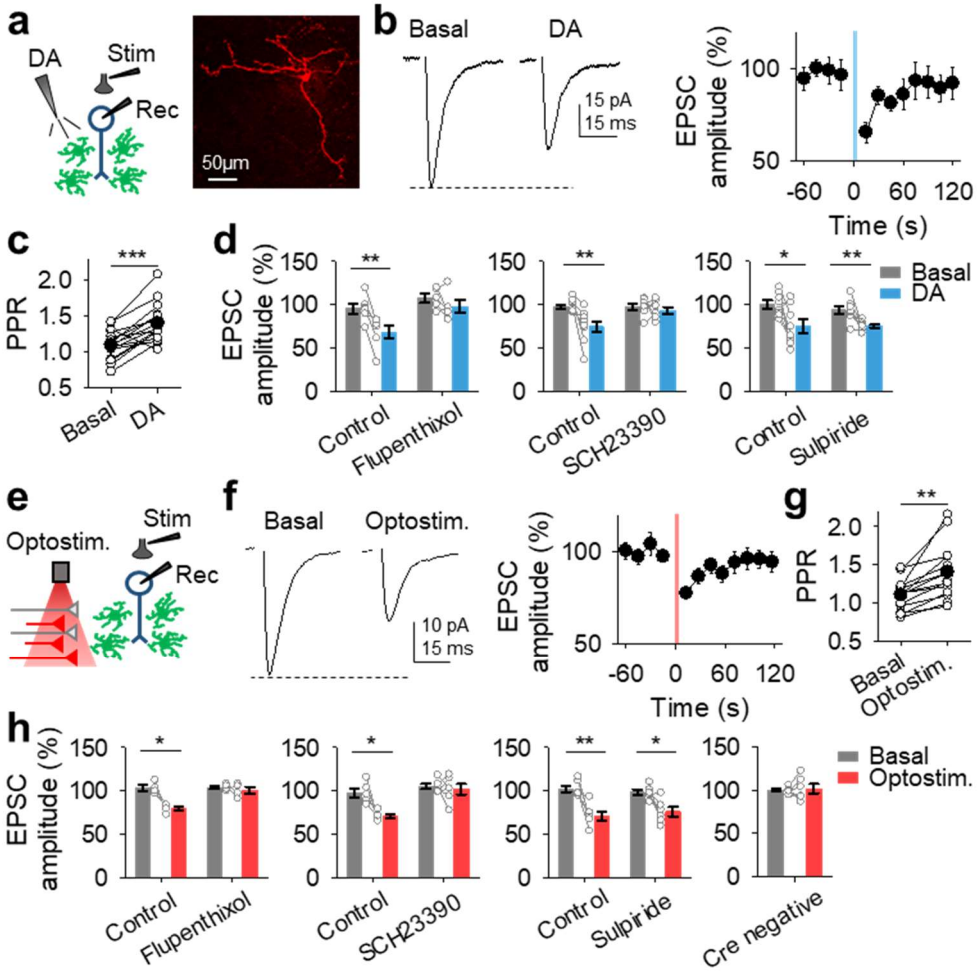

Extended Data Fig. 3.3. Dopamine depresses excitatory transmission. a, Experimental scheme *(right)* and image of nucleus accumbens medium spiny neuron (*left)*. **b,** Representative excitatory postsynaptic current (EPSC) traces before (basal) and after DA application (*right*) and relative EPSC amplitude over time. **c,** Paired pulse ratio (PPR) before (basal) and after dopamine application. **d,** Relative EPSC amplitude. **e-h,** as a-d, but for optical stimulation. Blue and red shadows indicate DA application and optical stimulation, respectively. Data are expressed as mean ± s.e.m., *p<0.05, **p<0.01, ***p<0.001.

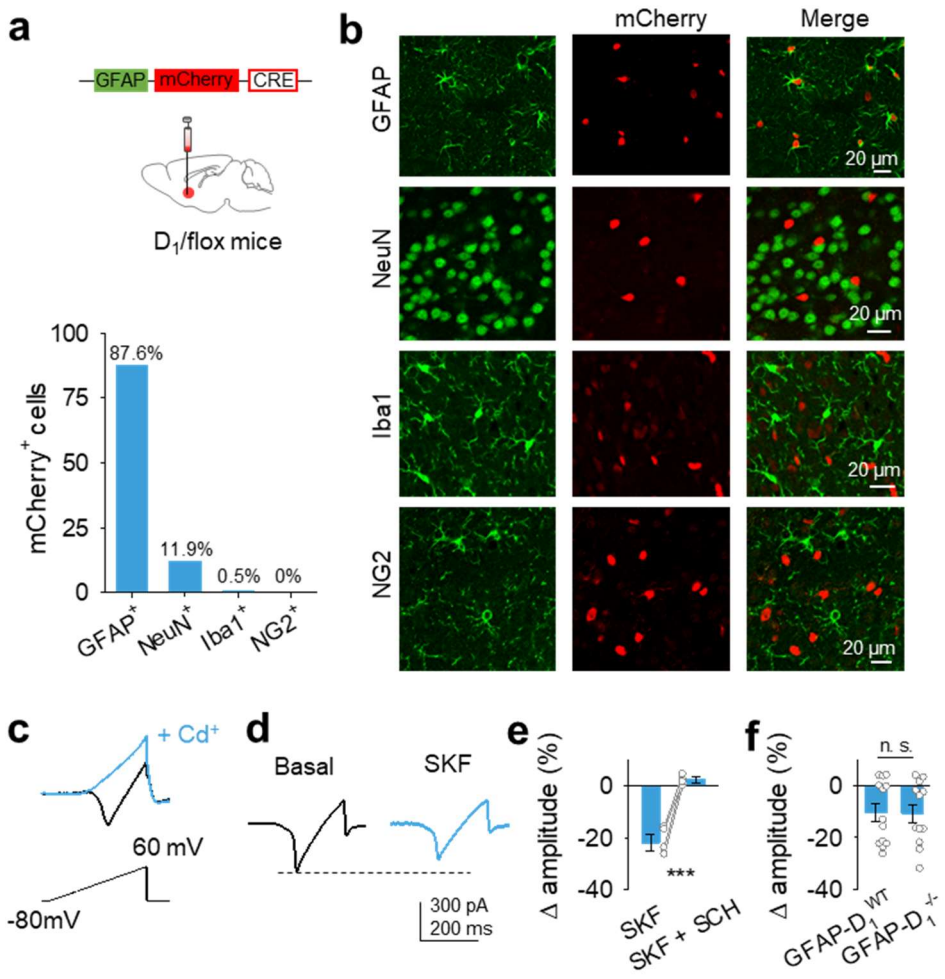

Extended Data Fig. 3.4. AAV8-GFAP-mCherry-CRE targets astrocytes. a, Experimental scheme (*top*) and percent distribution of mCherry⁺ cells (*bottom*). **b,** Immunohistochemistry images of mCherry⁺ cells co-stained with GFAP, NeuN, Iba1 or NG2. *From left to right:* cell marker, mCherry, and merge. **c,** Representative Cd^+ sensitive currents. **d,** Cd^+ sensitive current before (basal) and after SKF 38393 application. **d,** Relative change in amplitude of Cd^+ sensitive current in SKF 38393 only conditions (SKF) or in SKF 38393 and SCH 23390 conditions (SKF + SCH). **e,** Relative change in amplitude of Cd^+ sensitive current in response to SKF 38393. Data are expressed as mean ± s.e.m., ***p<0.001.

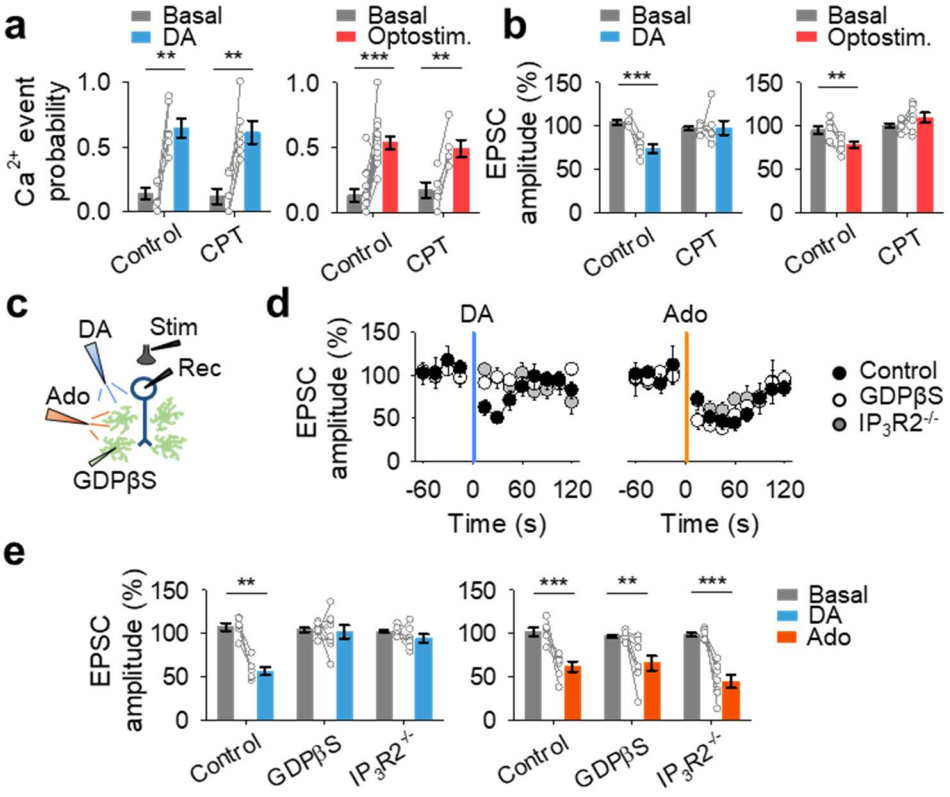

Extended Data Fig. 3.5: Astrocytes mediate DA-evoked synaptic depression via adenosine signaling. a, Calcium event probability before (basal) and after DA application or optogenetic stimulation. **b,** Relative EPSC amplitude before (basal) and after DA application or optogenetic stimulation. **c.** Scheme of experimental approach. **d.** Relative EPSC amplitude over time. Blue and red shadows indicate DA application and adenosine application, respectively. **e.** Relative EPSC amplitude before (basal) and after DA application or adenosine application. Data are expressed as mean ± s.e.m., **p<0.01, ***p<0.001.

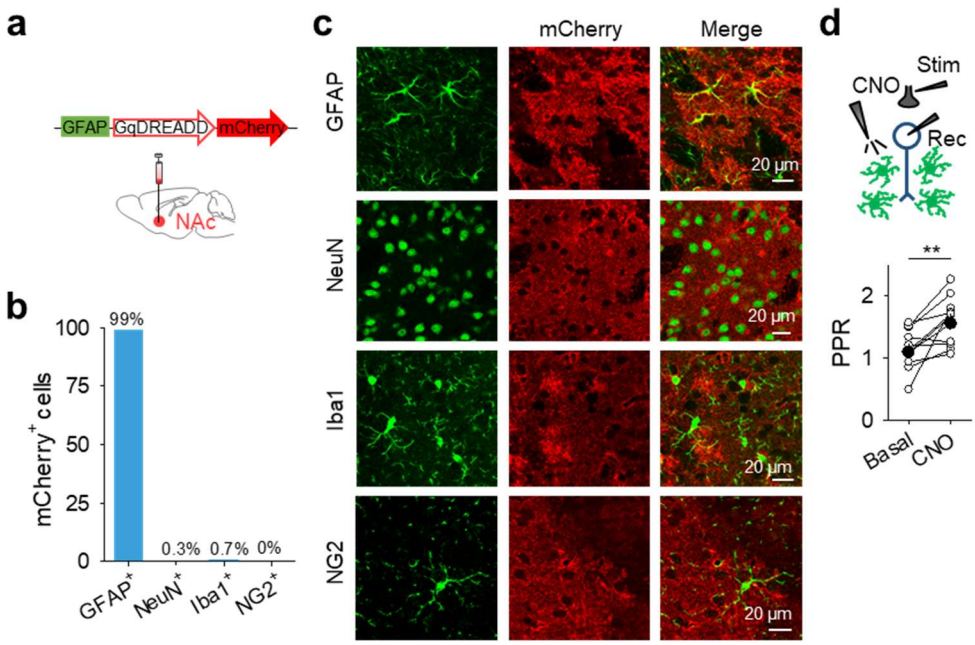

Extended Data Fig. 3.6: AAV8-GFAP-hM3D(Gq)-mCherry is specifically expressed in astrocytes. a, Scheme of experimental approach. **b,** Percent distribution of mCherry⁺ cells. **c,** Immunohistochemistry images of mCherry⁺ cells co-stained with GFAP, NeuN, Iba1 or NG2. *From left to right:* cell marker, mCherry, and merge. **d,** Experimental scheme (*top*) and paired pulse ratio (PPR) before (basal) and after CNO application (*bottom*). Data are expressed as mean ± s.e.m., **p<0.01.

Chapter Three: Statistics

Kruskal-Wallis One Way ANOVA values					
	H value	DF	P value	Post hoc	q and p values
Fig. 1d	28.912	2	<0.001	Dunn's Method	Control vs Flupenthixol: q=5.122, p<0.05; Control vs GFP: q=3.184, p<0.05; Flupenthixol vs GFP: q=0.642, p>0.05

Extended data table 1. Full report of Kruskal-Wallis One Way ANOVA values. Full report of H values, degrees of freedom (DF) and p value for the Kruskal-Wallis One Way ANOVA tests performed on non-parametric data and the post hoc analysis q and p values.

One way ANOVA values					
	F value	DF	p value	Post hoc	p values
Fig. 2b	4.539	4	0.005	Fisher LSD Method	Control vs Flupenthixol: p=0.007; Control vs SCH23390: p=0.027; Control vs Sulpiride: p=0.921; Control vs Cocktail: p=0.631
Fig. 2d	10.724	4	<0.001	Fisher LSD Method	Control vs Flupenthixol: p<0.001; Control vs SCH23390: p=0.003; Control vs Sulpiride: p=0.858; Control vs Cre Negative: p=0.005

Extended data table 2. Full report of One way ANOVA values. Full report of F values, degrees of freedom (DF) and p value for the One way ANOVA tests performed and the post hoc analysis p values.

Student's t test				
	Comparison	Condition	Test	t and p values
Fig. 1f	Control vs amphetamine	Fluorescence amplitude (AU)	Two-tailed Student's unpaired t-test	t=-2.48, p=0.017
Fig. 1f	Control vs amphetamine	Rise time (s)	Two-tailed Student's unpaired t-test	t=-3.19, p=0.002
Fig. 1f	Control vs amphetamine	Response width (s)	Two-tailed Student's unpaired t-test	t=-3.19, p=0.026
Fig. 2b	Basal vs DA	Control	Two-tailed Student's paired t-test	t=-4.32, p=0.007
Fig. 2b	Basal vs DA	Flupenthixol	Two-tailed Student's paired t-test	t=-0.81, p=0.811
Fig. 2b	Basal vs DA	SCH23390	Two-tailed Student's paired t-test	t=-0.88, p=0.428
Fig. 2b	Basal vs DA	Sulpiride	Two-tailed Student's paired t-test	t=-7.4, p<0.001
Fig. 2b	Basal vs DA	Cocktail	Two-tailed Student's paired t-test	t=-6, p<0.001
Fig. 2d	Basal vs Optostim.	Control	Two-tailed Student's paired t-test	t=-6.22, p<0.001
Fig. 2d	Basal vs Optostim.	Flupenthixol	Two-tailed Student's paired t-test	t=0.139, p=0.892
Fig. 2d	Basal vs Optostim.	SCH23390	Two-tailed Student's paired t-test	t=-0.337, p=0.75

Fig. 2d	Basal vs Optostim.	Sulpiride	Two-tailed Student's paired t-test	t=-7.587, p<0.001
Fig. 2d	Basal vs Optostim.	Cre negative	Two-tailed Student's paired t-test	t=0.645, p=0.554
Fig. 3b	Basal vs DA	Calcium event probability: Control	Two-tailed Student's paired t-test	t=-8.836, p<0.001
Fig. 3b	Basal vs DA	Calcium event probility: GDPβS	Two-tailed Student's paired t-test	t=-0.397, p=0.718
Fig. 3b	Basal vs DA	Calcium event probility: $IP_3R2^{-/-}$	Two-tailed Student's paired t-test	t=-0.312, p=0.76
Fig. 3b	Basal vs DA	EPSC amplitude (%): Control	Two-tailed Student's paired t-test	t=3.731, p=0.007
Fig. 3b	Basal vs DA	EPSC amplitude (%): GDPβS	Two-tailed Student's paired t-test	t=0.152, p=0.885
Fig. 3b	Basal vs DA	EPSC amplitude (%): $IP_3R2^{-/-}$	Two-tailed Student's paired t-test	t=0.188, p=0.856
Fig. 3d	Basal vs DA	GFAP-D_1^{WT}	Two-tailed Student's paired t-test	t=-8.725, p<0.001
Fig. 3d	Basal vs DA	GFAP-$D_1^{-/-}$	Two-tailed Student's paired t-test	t=-1.335, p=0.219
Fig. 3d	Basal vs ATP	GFAP-D_1^{WT}	Two-tailed Student's paired t-test	t=-13.241, p<0.001
Fig. 3d	Basal vs ATP	GFAP-$D_1^{-/-}$	Two-tailed Student's paired t-test	t=-21.548, p<0.001
Fig. 3e	Basal vs DA	GFAP-D_1^{WT}	Two-tailed Student's paired t-test	t=10.203, p<0.001
Fig. 3e	Basal vs DA	GFAP-$D_1^{-/-}$	Two-tailed Student's paired t-test	t=1.867, p=0.104
Fig. 3h	Basal vs CON	Calcium event probility: Control	Two-tailed Student's paired t-test	t=-2.965, p=0.041
Fig. 3h	Basal vs CON	Calcium event probility: CPT	Two-tailed Student's paired t-test	t=-3.355, p=0.028
Fig. 3h	Basal vs CON	Calcium event probility: mCherry	Two-tailed Student's paired t-test	t=-0.474, p=0.656
Fig. 3h	Basal vs CON	EPSC amplitude (%): Control	Two-tailed Student's paired t-test	t=3.468, p=0.007
Fig. 3h	Basal vs CON	EPSC amplitude (%): CPT	Two-tailed Student's paired t-test	t=-1.244, p=0.260
Fig. 3h	Basal vs CON	EPSC amplitude (%): mCherry	Two-tailed Student's paired t-test	t=0.326, p=0.757
Fig. 4d	Basal vs Amphetamine	Control	Two-tailed Student's paired t-test	t=-4.752, p=0.005
Fig. 4d	Basal vs Amphetamine	Flupenthixol	Two-tailed Student's paired t-test	t=-0.776, p=0.494
Fig. 4d	Basal vs Amphetamine	$IP_3R2^{-/-}$	Two-tailed Student's paired t-test	t=-1.089, p=0.318
Fig. 4d	Basal vs Amphetamine	CPT	Two-tailed Student's paired t-test	t=-3.295 , p=0.013
Fig. 4d	Basal vs Amphetamine	GDPβS	Two-tailed Student's paired t-test	t=-0.0473, p=0.962

Fig. 4d	Basal vs Amphetamine	GFAP-D_1^{WT}	Two-tailed Student's paired t-test	t=-2.68, p=0.044
Fig. 4d	Basal vs Amphetamine	GFAP-$D_1^{-/-}$	Two-tailed Student's paired t-test	t=-1.581, p=0.145
Fig. 4g	Basal vs Amphetamine	Control	Two-tailed Student's paired t-test	t=5.444, p=0.006
Fig. 4g	Basal vs Amphetamine	Flupenthixol	Two-tailed Student's paired t-test	t=0.228, p=0.831
Fig. 4g	Basal vs Amphetamine	$IP_3R2^{-/-}$	Two-tailed Student's paired t-test	t=1.509, p=0.192
Fig. 4g	Basal vs Amphetamine	CPT	Two-tailed Student's paired t-test	t=1.036, p=0.34
Fig. 4g	Basal vs Amphetamine	GDPβS	Two-tailed Student's paired t-test	t=0.08, p=0.939
Fig. 4g	Basal vs Amphetamine	GFAP-D_1^{WT}	Two-tailed Student's paired t-test	t=2.824, p=0.022
Fig. 4g	Basal vs Amphetamine	GFAP-$D_1^{-/-}$	Two-tailed Student's paired t-test	t=-0.031, p=0.977
Fig. 4i	WT vs $IP_3R2^{-/-}$	Saline	Two-tailed Student's unpaired t-test	t=-0.796, p=0.432
Fig. 4i	WT vs $IP_3R2^{-/-}$	Amphetamine	Two-tailed Student's unpaired t-test	t=4.604, p<0.001
Fig. 4i	GFAP-D_1^{WT} vs GFAP-$D_1^{-/-}$	Saline	Two-tailed Student's unpaired t-test	t=0.051, p=0.96
Fig. 4i	GFAP-D_1^{WT} vs GFAP-$D_1^{-/-}$	Amphetamine	Two-tailed Student's unpaired t-test	t=2.395, p=0.038
E.D. Fig. 3c	Basal vs DA	PPR	Two-tailed Student's paired t-test	t=-4.98, p<0.001
E.D. Fig. 3d	Basal vs DA	Control	Two-tailed Student's paired t-test	t=5.23, p=0.003
E.D. Fig. 3d	Basal vs DA	Flupenthixol	Two-tailed Student's paired t-test	t=1.348, p=0.249
E.D. Fig. 3d	Basal vs DA	Control	Two-tailed Student's paired t-test	t=3.808, p=0.005
E.D. Fig. 3d	Basal vs DA	SCH23390	Two-tailed Student's paired t-test	t=0.72, p=0.498
E.D. Fig. 3d	Basal vs DA	Control	Two-tailed Student's paired t-test	t=2.743, p=0.029
E.D. Fig. 3d	Basal vs DA	Sulpiride	Two-tailed Student's paired t-test	t=4.178, p=0.004
E.D. Fig. 3g	Basal vs Optostim.	PPR	Two-tailed Student's paired t-test	t=-4.321, p<0.001
E.D. Fig. 3h	Basal vs Optostim.	Control	Two-tailed Student's paired t-test	t=4.081, p=0.027
E.D. Fig. 3h	Basal vs Optostim.	Flupenthixol	Two-tailed Student's paired t-test	t=0.599, p=0.591
E.D. Fig. 3h	Basal vs Optostim.	Control	Two-tailed Student's paired t-test	t=3.692, p=0.021

E.D. Fig. 3h	Basal vs Optostim.	SCH23390	Two-tailed Student's paired t-test	t=0.46, p=0.665
E.D. Fig. 3h	Basal vs Optostim.	Control	Two-tailed Student's paired t-test	t=4.44, p=0.007
E.D. Fig. 3h	Basal vs Optostim.	Sulpiride	Two-tailed Student's paired t-test	t=2.943, p=0.032
E.D. Fig. 3h	Basal vs Optostim.	Cre negative	Two-tailed Student's paired t-test	t= -0.441, p=0.667
E.D. Fig. 4e	SKF vs SKF+SCH	Δ amplitude (%)	Two-tailed Student's unpaired t-test	t=-8.209, p<0.001
E.D. Fig. 4e	GFAP-D_1^{WT} vs GFAP-$D_1^{-/-}$	Δ amplitude (%)	Two-tailed Student's unpaired t-test	t=-0.046, p=0.964
E.D. Fig. 5a	Basal vs DA	Control	Two-tailed Student's paired t-test	t=-5.679, p=0.002
E.D. Fig. 5a	Basal vs DA	CPT	Two-tailed Student's paired t-test	t=-4.74, p=0.005
E.D. Fig. 5a	Basal vs Optostim.	Control	Two-tailed Student's paired t-test	t=-5.425, p<0.001
E.D. Fig. 5a	Basal vs Optostim.	CPT	Two-tailed Student's paired t-test	t=-7.752, p=0.001
E.D. Fig. 5b	Basal vs DA	Control	Two-tailed Student's paired t-test	t=10.279, p<0.001
E.D. Fig. 5b	Basal vs DA	CPT	Two-tailed Student's paired t-test	t=-0.0938, p=0.929
E.D. Fig. 5b	Basal vs Optostim.	Control	Two-tailed Student's paired t-test	t=5.474, p=0.002
E.D. Fig. 5b	Basal vs Optostim.	CPT	Two-tailed Student's paired t-test	t=-1.451, p=0.197
E.D. Fig. 5e	Basal vs DA	Control	Two-tailed Student's paired t-test	t=6.607, p=0.001
E.D. Fig. 5e	Basal vs DA	GDPβS	Two-tailed Student's paired t-test	t=0.26, p=0.802
E.D. Fig. 5e	Basal vs DA	$IP_3R2^{-/-}$	Two-tailed Student's paired t-test	t=1.804, p=0.121
E.D. Fig. 5e	Basal vs Ado	Control	Two-tailed Student's paired t-test	t=4.282, p=0.008
E.D. Fig. 5e	Basal vs Ado	GDPβS	Two-tailed Student's paired t-test	t=3.804, p=0.007
E.D. Fig. 5e	Basal vs Ado	$IP_3R2^{-/-}$	Two-tailed Student's paired t-test	t=6.753, p<0.001
E.D. Fig. 6d	Basal vs CON	PPR	Two-tailed Student's paired t-test	t=-3.264, p=0.009

Extended data table 3. Full report of Student's t-tests t and p values. Full report of all the Student's t-tests t and p values from main and extended data (E.D. figures).

Chapter Four: The role of astrocyte calcium signaling in drug-related behaviors

Abstract

The findings presented in the previous chapter indicate that astrocytes play a pivotal role in mediating dopamine-evoked depression of synaptic transmission and amphetamine-mediated depression of synaptic transmission in the nucleus accumbens. The current chapter aims to investigate the extent to which astrocyte mediation of synaptic transmission translates into preclinical models of drug-seeking behavior. We conducted amphetamine locomotor sensitization and amphetamine conditioned place preference in $IP_3R2^{-/-}$ mice and nucleus accumbens core GFAP-$D1^{-/-}$ mice and found that nucleus accumbens core astrocytes modulate the psychomotor behavioral effects of amphetamine. The results of the study illustrate that astrocytes contribute to drug-related behaviors and may serve as therapeutic targets for substance use disorders.

Introduction

Drug addiction is characterized by sustained drug seeking despite harmful consequences and a susceptibility to relapse into drug seeking behavior. The mediation of drug seeking is via both positive reinforcement (the rewarding effects of the drug) and negative reinforcement (the drive to circumvent adverse stimuli such as withdrawal symptoms). Preclinical behavioral models of addiction attempt to examine the multifactorial components that contribute to drug seeking behavior to elucidate the cellular and molecular components contributing to this devastating disease. There are three major behavioral paradigms used to investigate drug seeking behavior including:

locomotor sensitization, conditioned place preference and drug self-administration. Importantly, these paradigms include either non-contingent (experimenter administered) and contingent administration of the drug and this can influence the translational validity of the study given that human addicts contingently administer drugs of abuse. However, all three paradigms can provide insight into the neural basis of drug seeking behavior.

Locomotor sensitization examines a compelling characteristic of drugs of abuse, such as psychostimulants and opioids, which is the enhanced responsiveness to a stimulus after repeated exposure when compared to the first exposure to the same stimulus. This paradigm is primarily conducted via a noncontingent manner and studies have found that sensitization to a drug is associated with increased dopamine activity in the nucleus accumbens[126] and dysregulated extracellular glutamate levels[127]. The level of locomotor sensitization is associated with the maintenance of drug seeking behavior[59] and the sensitizing effects of amphetamine have been observed in human subjects[128,129], providing translational validity to the behavioral paradigm.

Conditioned place preference (CPP) can also be used in preclinical models to investigate the neural mechanisms of drug seeking behavior. CPP utilizes classical conditioning to associate an environment with the rewarding effects of the drug. For the paradigm, there is a conditioned stimulus (context or cue) that was previously neutral associated with an unconditioned stimulus (noncontingent drug delivery). Both psychostimulants and opioids have been shown to produce CPP. The magnitude of preference for the context paired with drug indicates the motivational state of the animal

produced by drug delivery.[25] Like sensitization, amphetamine conditioned place preference has also been demonstrated in humans[130], illustrating the translational validity of the preclinical model.

Drug self-administration is one of the closest models to human drug use given the contingent nature of drug delivery. Animals are trained in operant chambers to either lever press or nose poke for drug delivery (oral or intravenous drug administration). Interestingly, one of the first models of self-administration was not with drugs, but with self-administration of electrical stimulation to the brain[131], providing evidence for a locus of reinforcement and reward processing in the brain.

Given that the current study aimed to examine the contribution of astrocyte signaling to the psychomotor effects of amphetamine, we utilized locomotor sensitization. We also aimed to examine the role of astrocytes in the rewarding effects of amphetamine utilizing conditioned place preference.

Studies utilizing behavioral paradigms to investigate circuit changes associated with drugs of abuse have primarily focused on neurons. However, researchers have found that astrocytes may also play a role in drug seeking behavior. One of the major hallmarks of drug induced plasticity is changes in glutamatergic homeostasis. Researchers have found that astrocytes regulate glutamate via glutamate transporters and the cysteine glutamate exchanger. These substrates are down regulated after drug exposure and normalization reduces reinstatement of drug seeking behavior[25].

Furthermore, researchers have found that deficient gliotransmission via disruption of vesicular mediated astrocyte transmitter release decreases reinstatement of drug seeking behavior[59] indicating that astrocytes play a key role in drug related behaviors.

Additionally, our results have illustrated that astrocytes in the nucleus accumbens core contribute to dopamine-evoked and amphetamine-mediated depression of excitatory transmission (Chapter 3) suggesting that astrocytes may also contribute to the behavioral phenotypes manifested by amphetamine administration. The current work aimed to test the hypothesis that astrocytes contribute to amphetamine-related behaviors associated with locomotor sensitization and conditioned place preference utilizing $IP_3R2^{-/-}$ mice and NAc core GFAP-$D1^{-/-}$ mice. We found that astrocytes in the nucleus accumbens core preferentially contribute to the acute psychomotor effects of amphetamine, but not the rewarding effects of amphetamine as measured by conditioned place preference. The results illustrate that astrocyte contribution to the behavioral effects of amphetamine may be circuit dependent (i.e. astrocytes are involved in the locomotor circuit associated with amphetamine psychomotor behavior, but nucleus accumbens core astrocytes may not be involved in the motivational circuit associated with conditioned place preference).

Overall, our findings indicate that astrocytes modulate the psychomotor effects of amphetamine and may serve as a treatment target for drug-related behaviors.

Results

A manifestation of astrocyte signaling is cytoplasmic calcium elevations mediated by the activation of IP_3R2 and the release of internal calcium stores. Astrocyte calcium signaling and gliotransmission can be attenuated by ablating IP_3R2 in astrocytes[48,49,52,109]. To investigate the contribution of astrocyte calcium signaling and gliotransmission on drug related behaviors we utilized $IP_3R2^{-/-}$ mice. We found that when compared to wild-type mice, $IP_3R2^{-/-}$ mice demonstrated attenuated behavioral sensitivity to amphetamine ($p > 0.001$; 2.5 mg/kg, i.p.; Figure 4.1a-b), indicating that astrocyte calcium signaling contributes to the locomotor effects of amphetamine in behaving animals. The extent of sensitization that occurred from day 1 to day 5 was also significantly different between the two groups ($p = 0.001$; Figure 4.1b, Extended table 4.3), suggesting that IP_3R2 calcium signaling in astrocytes contributes to the locomotor effects of amphetamine and the mechanisms involved in sensitization to the drug. As a control, we investigated the effects of repeated saline injections on locomotor activity and saw no differences between groups or days ($p = 0.335$; Figure 4.1b), indicating that the locomotor activity produced by amphetamine are due to the psychomotor effects of the drug and not the stress of repeated i.p. injections. Overall, these findings suggest that calcium signaling in astrocytes mediated by IP_3R2 contributes to behavioral responsiveness to amphetamine.

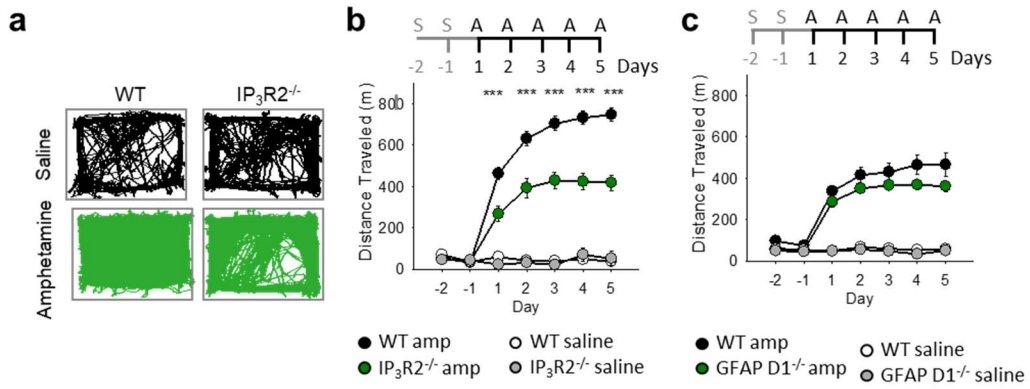

Figure 4.1. Astrocyte calcium signaling contributes to amphetamine psychomotor behavior. a, Representative traces of locomotor activity in animals injected with saline or amphetamine. **b,** Distance traveled in $IP_3R^{-/-}$ mice after saline or amphetamine (2.5. mg/kg) injections. **c,** Distance traveled in $D1R^{-/-}$ mice after saline or amphetamine (2.5 mg/kg) injections. ***p<0.001

Next, we investigated the role of astrocyte D1-like receptors (D_1Rs) on behavioral sensitivity to amphetamine. Amphetamine increases synaptic dopamine levels by blocking and reversing the dopamine transporter; therefore, we examined if astrocyte dopamine receptors contribute to amphetamine locomotor enhancement. To ablate D_1Rs in astrocytes, we conducted stereotaxic surgeries in D1 flox mice and targeted the AAV8-GFAP-mCherry-CRE viral vector to NAc core astrocytes. D1 flox mice that received the AAV8-GFAP-mCherry-CRE viral vector are referred to as GFAP-$D1^{-/-}$ mice and control experiments utilized wild-type littermate mice injected with the AAV8-GFAP-mCherry-CRE viral vector (GFAP-$D1^{WT}$). We found a dose dependent effect of amphetamine on GFAP-$D1^{-/-}$ mice locomotor activity. There was no significant difference in behavioral sensitivity to amphetamine with 2.5 mg/kg i.p. injection in GFAP-$D1^{-/-}$ mice

when compared to GFAP-D1^{WT} mice (p = 0.997; Figure 4.1c); however, there was a difference in acute locomotor responsiveness to amphetamine when we increased the dose to 5mg/kg i.p. injection (p = 0.03; Figure 4.2a-b). These results indicate that D_1Rs expressed on astrocytes contribute to behavioral sensitivity to amphetamine at higher doses.

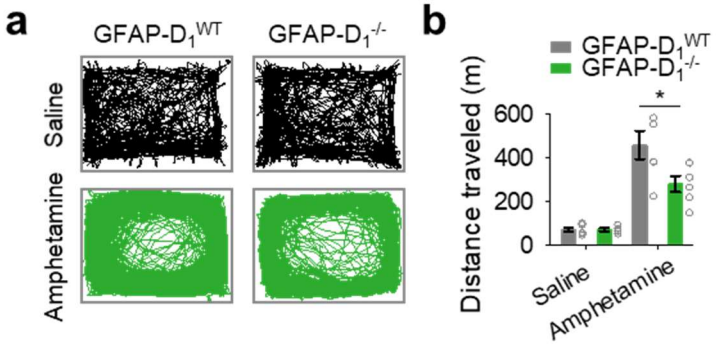

Figure 4.2. Astrocyte D_1R signaling contributes to amphetamine psychomotor behavior. a, Representative traces of locomotor activity in animals injected with saline or amphetamine. **b,** Distance traveled in D1R$^{-/-}$ mice after saline or amphetamine (5 mg/kg) injections. *p<0.05

Finally, we investigated the contribution of astrocyte calcium signaling and astrocyte D_1Rs on amphetamine-induced conditioned place preference. We found that there was no significant difference between IP$_3$R2$^{-/-}$ mice and wild-type control mice for preference

of the amphetamine-paired environment (p = 0.711; Figure 4.3a). Furthermore, we found that GFAP-D1$^{-/-}$ mice and GFAP-D1^{WT} mice demonstrated preference for the amphetamine-paired environment equally (p = 0.896; Figure 4.3b). These results indicate that astrocyte calcium signaling and D_1Rs expressed on NAc core astrocytes do not significantly contribute to learning of the cues associated with the rewarding properties of amphetamine.

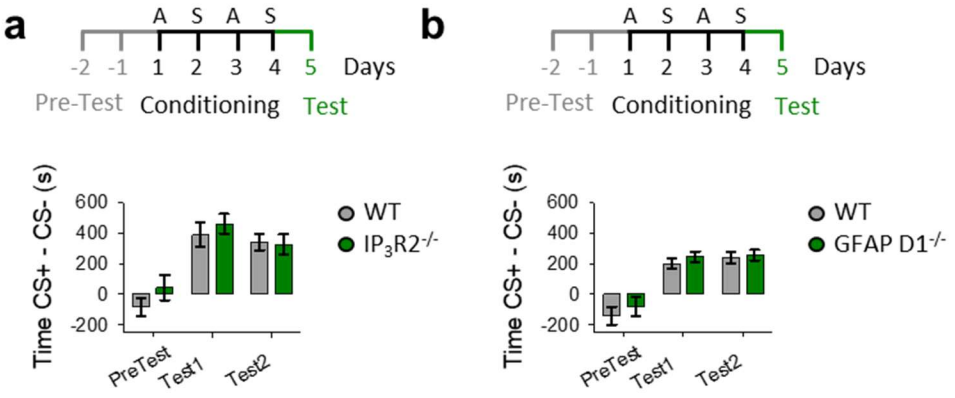

Figure 4.3. Amphetamine conditioned place preference in IP$_3$R$^{-/-}$ mice and GFAP D1R$^{-/-}$ mice. a, Relative preference of amphetamine paired environment in IP$_3$R$^{-/-}$ mice. **b,** Relative preference of amphetamine paired environment in GFAP D1R$^{-/-}$ mice.

Discussion

The investigation of drug related behaviors in preclinical models provides insight into the cellular and molecular mechanisms contributing to drug addiction. In the present study,

we utilized two behavioral paradigms to elucidate the role of astrocytes in the behavioral manifestation of the rewarding effects of amphetamine. We found that astrocytes specifically contribute to the psychomotor enhancement associated with amphetamine administration, as revealed by attenuated acute locomotor responses to amphetamine in $IP_3R2^{-/-}$ mice and GFAP-$D1^{-/-}$ mice when compared to wild-type control mice. However, we did not observe a difference in amphetamine-associated place preference in $IP_3R2^{-/-}$ mice and GFAP-$D1^{-/-}$ mice when compared to wild-type control mice. Interestingly, studies targeting neuronal dopaminergic signaling have also observed a noncongruence between deficits in locomotor sensitization and conditioned place preference. For example, researchers observed that in dopamine-transporter knock-out mice, acute psychomotor sensitivity to cocaine was attenuated, but conditioned place preference to both cocaine and amphetamine was preserved[132]. Furthermore, conditioned place preference remained in dopamine deficient mice for both cocaine[133] and morphine[134]; whereas, locomotor sensitivity to morphine was attenuated[134]. In mice deficient for the D_1 receptor, enhanced locomotor responses to cocaine were absent, but cocaine conditioned place preference was observed[135]. These results illustrate that dopaminergic signaling differentially modulates locomotor sensitization and conditioned place preference.

Importantly, locomotor sensitization and conditioned place preference target distinct neural circuits for expression of psychomotor enhancement and place preference. Psychomotor enhancement is associated with innate limbic and movement circuits[136] that can be hijacked by drugs of abuse; whereas, place preference involves circuits

implicated in learning and memory to associate a specific environment with a drug stimulus, i.e. the hippocampus.

The results indicate that astrocytes specifically mediate distinct circuits implicated in drug related behaviors. These results correspond with electrophysiology data obtained from the dorsal striatum, in which specific populations of astrocytes mediate neuronal activity of D_1R expressing medium spiny neurons versus D_2R expressing medium spiny neurons[52]. Interestingly, in the present study we specifically manipulated D_1Rs in astrocytes in the nucleus accumbens core. The core of the nucleus accumbens is associated with motor-related behaviors pertaining to reward[137], and we found a decrease in these motor-related behaviors when the D_1Rs in nucleus accumbens core astrocytes were ablated. The shell of the nucleus accumbens is associated with motivation and cue-associated learning; therefore, future studies specifically designed to ablate D_1Rs in astrocytes of the nucleus accumbens shell may provide further insight into the circuit specific modulation of astrocytes in brain reward signaling. Interestingly, past studies have also found a distinction in nucleus accumbens core astrocytes versus nucleus accumbens shell astrocytes in mediating drug seeking behavior; specifically, the modulation of core astrocytes disrupted ethanol self-administration, but shell astrocyte activity did not contribute to the phenotype[54]. Therefore, future studies can test the hypothesis that NAc core astrocytes mediate motor-related behaviors associated with amphetamine and NAc shell astrocytes contribute to the motivational aspects of amphetamine-related behaviors.

Our results indicate that IP_3R2 signaling in astrocytes contribute to behavioral phenotypes. This is in contrast to a study conducted in which a battery of behavioral testing found no difference between $IP_3R2^{-/-}$ mice and control mice[47]. Importantly, in the study no drug related behaviors were tested suggesting that although IP_3R2 signaling may not be implicated in physiologic processes or depression/anxiety related phenotypes examined, it may be implicated in pathologies associated with drug abuse.

In contrast to findings utilizing the dnSNARE model to ablate gliotransmission[59], we found deficits in psychomotor induced locomotor enhancement. Differences between the present study and the dnSNARE study include the approach to ablate gliotransmission (i.e. $IP_3R2^{-/-}$ mice vs. dnSNARE mice) and the psychostimulant drug used (amphetamine vs. cocaine). Turner and colleagues (2013)[59] did not find a significant difference in cocaine locomotor enhancement or sensitization in dnSANRE mice when compared to control mice. However, we found an attenuation of locomotor sensitivity to amphetamine. These results indicate that astrocytes may differentially influence drug-related behaviors to specific drugs, given that amphetamine and cocaine differentially modulate locomotor sensitization[138]. Alternatively, astrocytes may differentially modulate drug-related circuits via IP_3R2 compared to dnSNARE related gliotransmission, suggesting that unique gliotransmission pathways may govern specific drug-related behaviors. Future studies will need to be conducted in both transgenic mice using multiple drugs of abuse to investigate the hypothesis, that astrocytes are implicated in drug-related behaviors of specific drugs.

Overall, the present study provides evidence that astrocytes contribute to the psychomotor effects of amphetamine. Given that astrocyte signaling manipulation modulated locomotor sensitization, but not CPP suggests that astrocytes modulate specific circuits of drug related behaviors.

Chapter Four: Statistics

Two-Way ANOVA Values			
	F value	DF	P value
Fig 4.1 IP_3 (amp)	10.057	6	< 0.001
Fig 4.1 IP_3 (sal)	1.154	6	0.335
Fig 4.1 $D_1^{-/-}$ (amp)	0.0958	6	0.997
Fig 4.1 $D_1^{-/-}$ (amp)	0.486	6	0.843
Fig 4.3 IP_3	0.345	2	0.711
Fig 4.3 $D_1^{-/-}$	0.11	2	0.896

Extended table 4.1. Two-way ANOVA values report

Student's t test (two-tailed, unpaired)			
	Comparison	t value	p value
Fig 4.1 $D_1^{-/-}$ (amp)	Dif Day 1 v Day 5	0.499	0.623
Fig 4.2 $D_1^{-/-}$ (amp)	amp $D1^{WT}$ vs $D1^{-/-}$	2.395	0.03

Extended table 4.2. Student's t test (two-tailed, unpaired) values report

Mann-Whitney Rank Sum Test			
	Comparison	T value	p value
Fig 4.1 IP_3 (amp)	Dif Day 1 v Day 5	374	0.001

Extended table 4.3. Mann-Whitney Rank Sum Test values report

Chapter Five: Opioid effects on astrocyte-neuron signaling in the nucleus accumbens

Abstract

Major hallmarks of astrocyte physiology are the elevation of intracellular calcium in response to neurotransmitters and the release of neuroactive substances, gliotransmitters, that modulate neuronal activity. While μ opioid receptor expression has been identified in astrocytes of the nucleus accumbens, the functional consequences on astrocyte-neuron communication remains unknown. The present study has investigated the astrocyte responsiveness to μ opioid signaling and the regulation of gliotransmission in the nucleus accumbens. Through the combination of calcium imaging and whole-cell patch clamp electrophysiology in brain slices, we have found μ opioid receptor activation in astrocytes elevate their cytoplasmic calcium and stimulates the release of the gliotransmitter glutamate, which evoked slow inward currents through activation of neuronal NMDA receptors. These results indicate the existence of molecular mechanisms underlying opioid-mediated astrocyte-neuron signaling in the nucleus accumbens.

Introduction

Opioids are efficacious compounds used as analgesics in the medical setting[139,140]; however, opioids are also deadly addictive substances due to their rewarding actions in the brain[141]. Opioid substance use disorder has grown exponentially in the past decades, resulting in tens of thousands of overdose deaths[142]. Opioids are both naturally occurring and synthetically derived substances such as morphine, heroin, oxycodone and fentanyl. The rewarding and addicting effects of opioids are mediated by their activation of inhibitory G-protein coupled receptors ($G_{i/o}$)[11]. There are three main subtypes of opioid receptors: μ, δ and *κ* receptors[11].

While the majority of research on opioids has focused on neurons, very little is known about the involvement of astrocytes in opioid signaling. Recent evidence demonstrates the expression of μ opioid receptors on astrocytes in the hippocampus, ventral tegmental area and the nucleus accumbens[143]. The μ opioid receptors localized to astrocytes in the hippocampus were found to evoke astrocytic glutamate release through TREK-1-containing two-pore potassium (K2P) channels[144]. In addition, opioid receptor activation in cultured astrocytes has been shown to increase intracellular calcium via IP_3 signaling[145]. However, whether astrocytes in situ respond to opioid signaling in the nucleus accumbens, a primary brain area involved in reward and addiction remains unknown.

Historically, astrocytes have been considered support cells of the brain, contributing to ion homeostasis, maintaining the blood-brain barrier and providing trophic and metabolic support to neurons[31]. However, accumulating evidence indicates that astrocytes contribute to brain information processing through functional signaling interaction with neuronal synaptic elements establishing tripartite synapses[31]. A single astrocyte can make synaptic contacts with tens of thousands of synapses and over 50% of excitatory synapses in the hippocampus exhibit close proximity to an astrocyte process[146]. Astrocytes express a large variety of neurotransmitter receptors that bind neurotransmitters and eventually result in an increase in cytoplasmic calcium and the

release of neuroactive substances (termed gliotransmitters) that modulate neuronal activity and synaptic transmission and plasticity[32,147-149].

Using brain slices, we have investigated whether nucleus accumbens astrocytes respond to opioids and whether opioid signaling in astrocytes stimulates gliotransmission. Since opioids are known to exert both their analgesic and rewarding effects via activation of μ opioid receptors, we focused the present study on this subtype of opioid receptors. We have found that astrocytes respond to μ-opioid receptors with intracellular calcium elevations. These calcium elevations were associated with the release of glutamate that evoked NMDAR-mediated slow inward currents (SICs) in neurons. These results indicate that astrocytes participate in opioid signaling in the nucleus accumbens.

Results

To examine the role of astrocytes in μ opioid signaling in the nucleus accumbens we aimed to confirm that astrocytes in this region expressed μ opioid receptors[143]. Immunohistochemistry experiments demonstrated μ opioid receptor expression in astrocytes in the nucleus accumbens core (Figure 1A).

Astrocyte excitability manifests as cytoplasmic calcium elevations[36,150,151]; therefore, we aimed to test the hypothesis that the selective μ opioid receptor agonist, DAMGO, would increase astrocyte calcium levels. To monitor astrocyte calcium, we used the genetically encoded calcium indicator (GCaMP6f) selectively expressed in NAc core astrocytes (Fig. 1B). Local application of DAMGO with a micropipette (500 μM, 60 s, 0.5 bar) increased cytoplasmic calcium levels in both the soma and processes of astrocytes (Figure 1C-D). We found that astrocyte calcium events significantly increased after DAMGO application (n = 257 astrocytes from n = 19 experimental planes of view, p = 0.02; Figure 1E-F; Table 1) when compared to baseline levels, indicating that astrocytes respond to μ opioid signaling with increases in calcium.

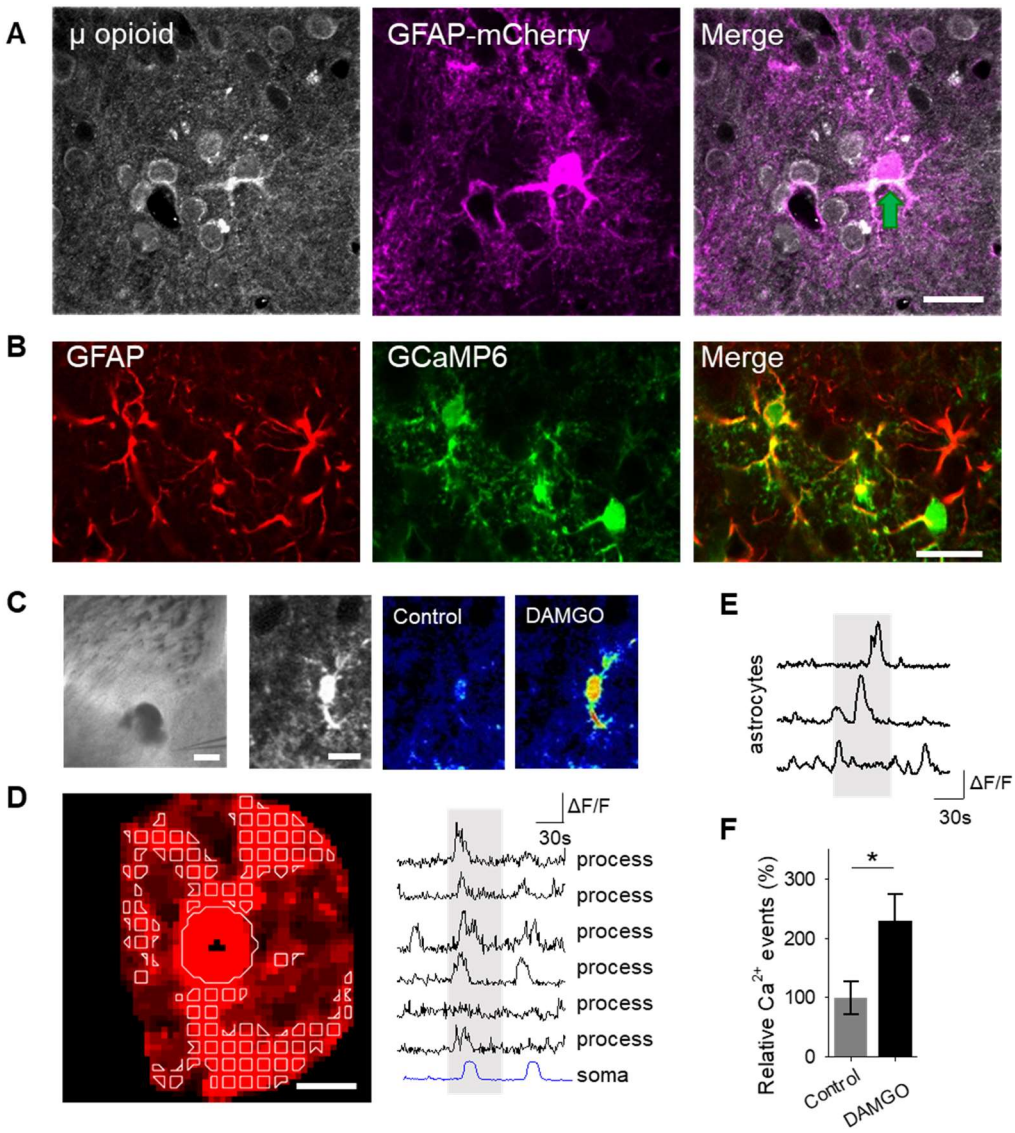

Figure 5.1. μ opioid receptor activation increases astrocyte cytoplasmic calcium levels. (A) Immunohistochemical images of μ opioid receptor expression in mCherry-expressing astrocytes and merged image. Scale bar 20 μm. Green arrow indicates colocalization. **(B)** Immunohistochemical images of GCaMP6 expression in GFAP-expressing cells. Scale bar 20 μm. **(C)** Image (scale bar 200 μm) illustrating experimental approach and pseudocolor images (scale bar 10 μm) showing the fluorescence intensities of a GCaMP6-expressing astrocytes before and after DAMGO application.

Figure 1 continued. (D) Representative image of soma and process regions of interests (sale bar 10 μm) and calcium traces of astrocyte processes and soma (gray shading indicates DAMGO application). **(E)** Calcium traces of astrocytes (gray shading indicates DAMGO application). **(F) R**elative calcium events before (control) and after DAMGO application. Data are expressed as mean ± s.e.m., *p<0.05.

A consequence of astrocyte calcium elevations is the release of neuroactive substances, such as glutamate, which modulate neuronal activity[152]. Astrocyte glutamate has been shown to activate extrasynaptic NMDA receptors to produce slow inward currents (SICs) in different brain areas[3,153,154]. SICs are distinct from excitatory post synaptic currents due to their slower time course and sensitivity to the NMDA receptor antagonist D-AP5 (50 μM; Figure 2A-C). We recorded whole-cell currents in neurons in the presence of tetrodotoxin (TTX) to block sodium-dependent action potentials, before and after applying DAMGO. We found that in addition to modulating astrocyte calcium, local delivery of DAMGO increased the frequency of SICs (n = 17, p = 0.01; Figure 2C-D; Table 1), indicating μ opioid signaling in astrocytes stimulates the release of astrocytic glutamate.

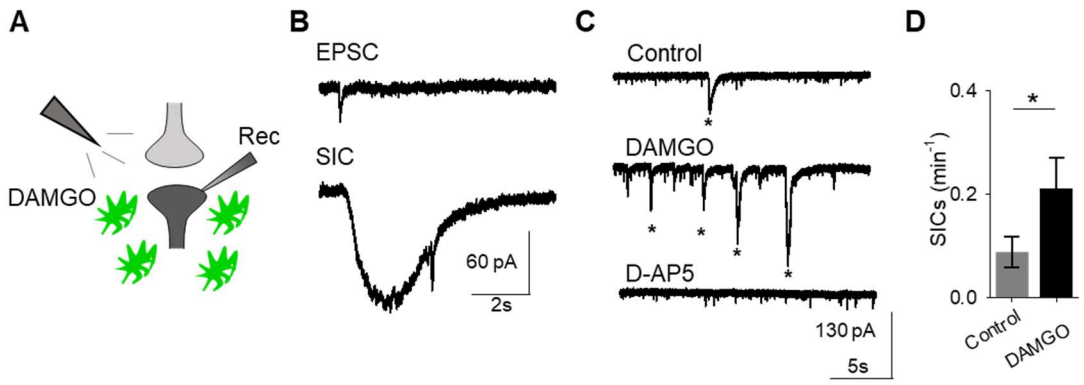

Figure 5.2. μ opioid receptor activation mediates slow inward currents in neurons. **(A)** Scheme of electrophysiology experimental approach. **(B)** Representative traces of excitatory post synaptic potential (EPSC; top) and slow inward current (SIC; bottom). **(C)** Representative electrophysiology recordings in control conditions (top) after DAMGO application (middle), and in the presence of the D-AP5 (bottom). Stars indicate SICs. **(D)** SICs per minute before (control) and after DAMGO application. Data are expressed as mean ± s.e.m., *p<0.05.

To confirm that the effects of DAMGO were mediated by activation of opioid receptors, we conducted experiments in the presence of the global opioid receptor antagonist naltrexone (10 μM). We found that in the presence of naltrexone, DAMGO no longer induced astrocytic calcium elevations (n = 55 astrocytes from n = 7 experimental planes of view, p = 0.77; Figure 3A-C; Table 1) nor affected neuronal SICs (n = 5, p = 0.62; Figure 3D-F; Table 1), suggesting that DAMGO actions are via opioid receptors to modulate astrocyte calcium signaling and the generation of neuronal SICs.

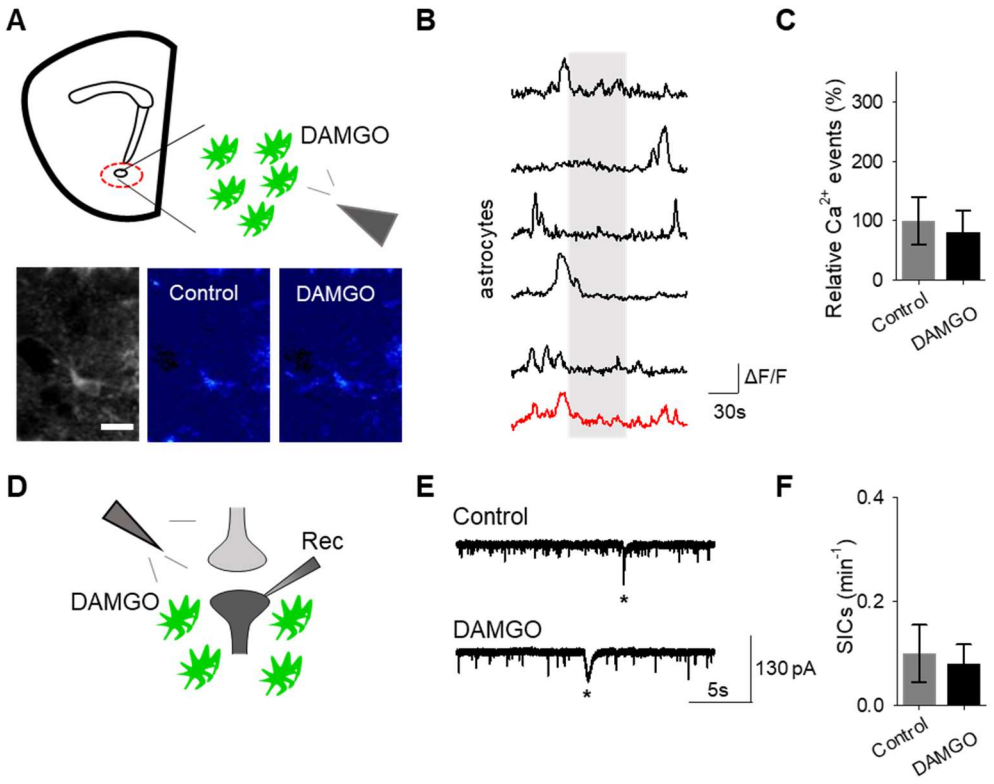

Figure 5.3. The opioid receptor antagonist naltrexone attenuates DAMGO actions on astrocytes and neurons. (A) Scheme of experimental approach and pseudocolor images showing the fluorescence intensities of a GCaMP6-expressing astrocytes before and after DAMGO application in the presence of naltrexone (10 μM). **(B)** Calcium traces of astrocytes (gray shading indicates DAMGO application; red trace: average) in the presence of naltrexone. **(C)** Relative calcium events before (control) and after DAMGO application in the presence of naltrexone. **(D)** Scheme of electrophysiology experimental approach. **(E)** Representative electrophysiology recordings in control conditions and after DAMGO application in the presence of naltrexone. **(F)** SICs per minute before (control) and after DAMGO application in the presence of naltrexone. Data are expressed as mean ± s.e.m., scale bar 10 μm.

Next, we investigated if the actions of DAMGO were mediated by μ opioid receptors expressed on astrocytes. We generated NAc core GFAP-MOR$^{-/-}$ mice via targeting the viral vector, AAV8-GFAP-mCherry-CRE, to transgenic mice with a floxed μ opioid receptor gene (MOR flox/flox mice; Figure 4A). We confirmed that the AAV8-GFAP-mcherry-CRE viral vector was targeted to GFAP-expressing and GCaMP6f- expressing astrocytes (Figure 4B). Additionally, we confirmed that the AAV8-GFAP-mCherry-CRE was not targeted to NeuN-expressing neurons (Figure 4C). Next, we conducted calcium imaging experiments, and observed no significant astrocyte calcium elevations in response to DAMGO (n = 92 astrocytes form n = 8 experimental planes of view, p = 0.21; Figure 5A-C; Table 1), suggesting that DAMGO acted directly on μ opioid receptors expressed on astrocytes to produce calcium increases. Additionally, in the NAc core of GFAP-MOR$^{-/-}$ mice we did not observe DAMGO-induced SIC elevations (n = 9, p = 0.78; Figure 5D-F; Table 1), indicating the DAMGO-evoked gliotransmission was mediated by μ opioid receptors expressed on astrocytes.

Finally, we investigated the intracellular signaling cascade that mediates the astrocyte responsiveness to DAMGO and the subsequent gliotransmission. A primary pathway of astrocyte calcium signaling is via IP_3 mediated calcium elevations governed by the activation of IP_3 receptors on the endoplasmic reticulum to induce the release of internal calcium stores[36]. We examined the contribution of IP_3 signaling using $IP_3R2^{-/-}$ mice, which have impaired G protein-coupled receptor mediated astrocyte calcium signaling[48,52,109]. No significant changes in astrocyte calcium signaling (n = 54 astrocytes form n = 8 experimental planes of view, p = 0.78 Figure 6A-C; Table 1) and SIC frequency (n = 6, p = 0.74 Figure 6D-F; Table 1) were evoked by DAMGO in $IP_3R2^{-/-}$ mice, indicating that DAMGO-evoked astrocyte calcium increases and neuronal SICs were mediated by IP_3 signaling in astrocytes.

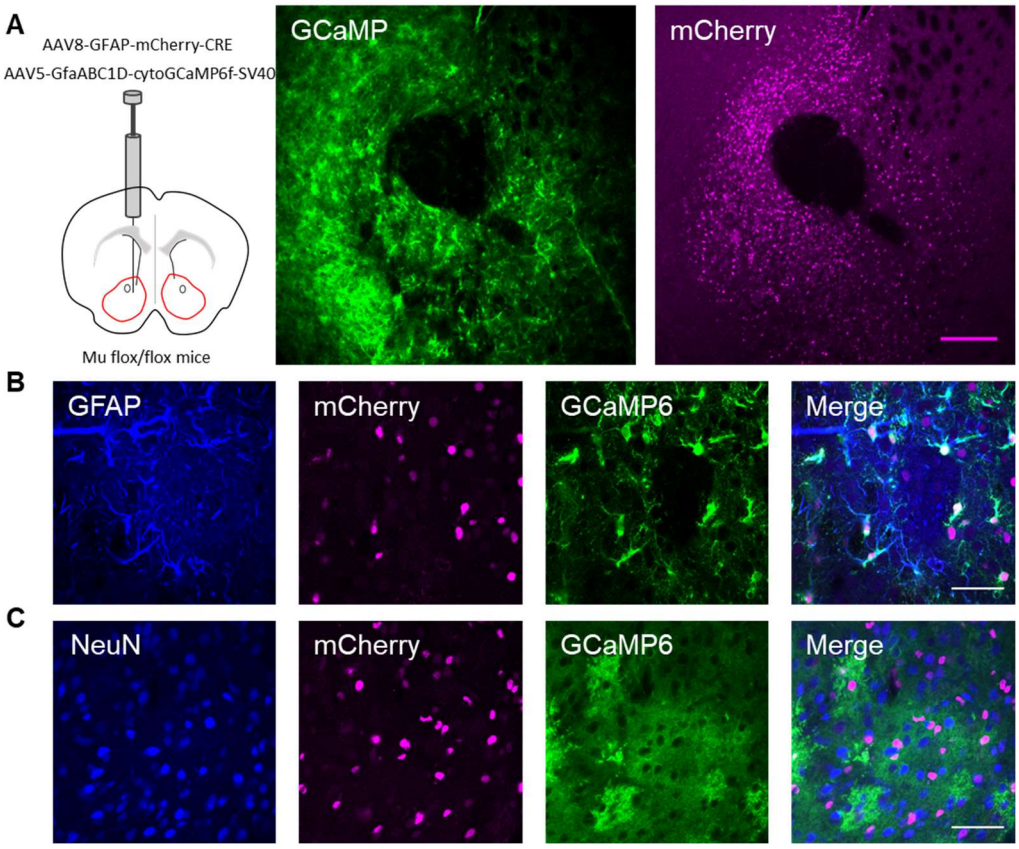

Figure 5.4. Targeting AAV8-GFAP-mCherry-CRE to astrocytes in the nucleus accumbens of μ flox mice. (A) Scheme of viral targeting experimental approach and immunohistochemistry images of GCaMP6 (green) and AAV8-GFAP-mCherry-CRE (magenta) in the nucleus accumbens. **(B)** Immunohistochemistry images of mCherry^{+} cells co-stained with GFAP, and GCaMP6 and merge image. **(C)** Immunohistochemistry images of mCherry^{+} cells co-stained with NeuN and GCaMP6 and merge image. Magenta scale bar 200 μm, white scale bar 50 μm.

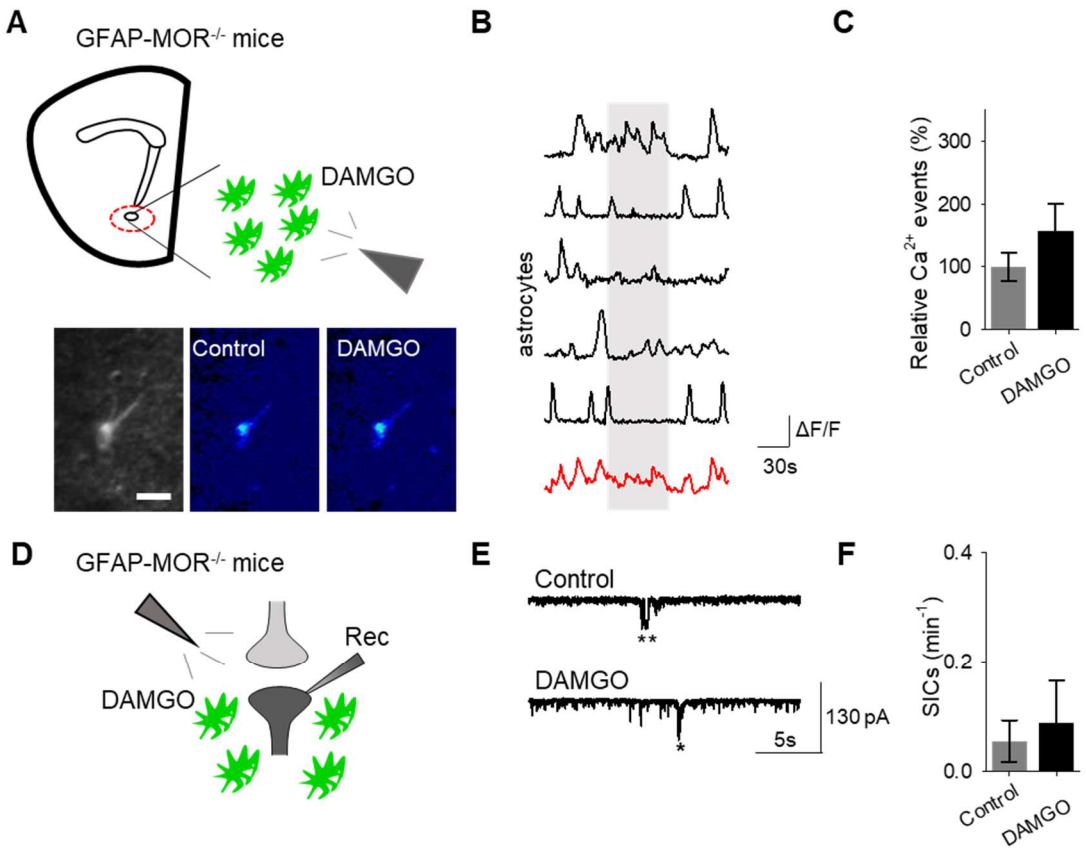

Figure 5.5. Astrocyte μ opioid receptors mediate DAMGO actions on astrocytes and DAMGO-evoked neuronal slow inward currents. (A) Scheme of experimental approach and pseudocolor images showing the fluorescence intensities of a GCaMP6-expressing astrocytes before and after DAMGO application in slices from GFAP-MOR$^{-/-}$ mice. **(B)** Calcium traces of astrocytes (gray shading indicates DAMGO application; red trace: average) in slices from GFAP-MOR$^{-/-}$ mice. **(C)** Relative calcium events before (control) and after DAMGO application in slices from GFAP-MOR$^{-/-}$ mice. **(D)** Scheme of electrophysiology experimental approach in slices from GFAP-MOR$^{-/-}$ mice. **(E)** Representative electrophysiology recordings in control conditions and after DAMGO application in slices from GFAP-MOR$^{-/-}$ mice. **(F)** SICs per minute before (control) and after DAMGO application in slices from GFAP-MOR$^{-/-}$ mice. Data are expressed as mean ± s.e.m., scale bar 10 μm.

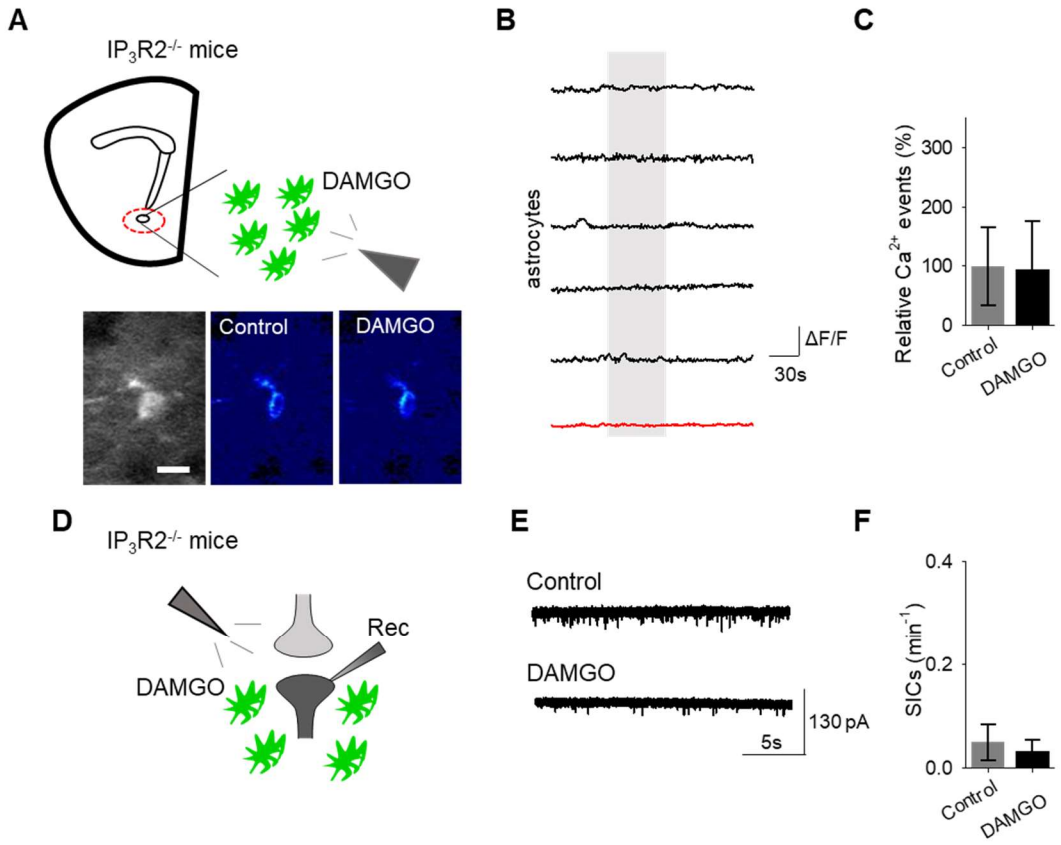

Figure 5.6. IP_3 signaling in astrocytes mediates DAMGO actions on astrocytes and neuronal slow inward currents. (A) Scheme of experimental approach and pseudocolor images showing the fluorescence intensities of a GCaMP6-expressing astrocytes before and after DAMGO application in slices from $IP_3R2^{-/-}$ mice. **(B)** Calcium traces of astrocytes (gray shading indicates DAMGO application; red trace: average) in slices from $IP_3R2^{-/-}$ mice. **(C)** Relative calcium events before (control) and after DAMGO application in slices from $IP_3R2^{-/-}$ mice. **(D)** Scheme of electrophysiology experimental approach in slices from $IP_3R2^{-/-}$ mice. **(E)** Representative electrophysiology recordings in control conditions and after DAMGO application in slices from $IP_3R2^{-/-}$ mice. **(F)** SICs per minute before (control) and after DAMGO application in slices from $IP_3R2^{-/-}$ mice. Data are expressed as mean ± s.e.m., scale bar 10 μm.

Table 1. Summary Statistics.

Figure	N (# animals)	Test	T value	Z statistic	P value
5.1c	19(8)	Two-tailed student's paired t-test	-2.496	-	0.0225
5.2d	17 (7)	Two-tailed student's paired t-test	-2.651	-	0.0174
5.3c	7 (3)	Two-tailed student's paired t-test	0.294	-	0.779
5.3f	5 (3)	Two-tailed student's paired t-test	0.535	-	0.621
5.5c	8 (2)	Two-tailed student's paired t-test	-1.354	-	0.218
5.5f	9 (2)	Wilcox Signed Rank Test	-	0	0.789
5.6c	8 (2)	Wilcox Signed Rank Test	-	0	0.789
5.6f	6 (2)	Two-tailed student's paired t-test	0.349	-	0.741

Discussion

The current study demonstrates that astrocytes in the nucleus accumbens core express μ opioid receptors and respond to μ opioid receptor activation with increases in cytoplasmic calcium. Furthermore, the μ-opioid signaling in astrocytes is able to stimulate the release of the gliotransmitter glutamate, which activate neuronal NMDARs, as evidenced by the increase in neuronal SICs. Indeed, the astrocytic increases in calcium and neuronal slow inward currents were mediated by opioid receptors as indicated by the attenuation of the response in the presence of the global opioid receptor antagonist naltrexone. Specifically, the DAMGO-induced astrocyte calcium increases and slow inward currents were mediated by the release of internal stores of calcium mediated by activation of IP_3R2, given that the responses were no longer present in $IP_3R2^{-/-}$ mice. Additionally, the selective ablation of μ opioid receptors on astrocytes decreased astrocyte calcium responses to DAMGO and DAMGO-induced slow inward currents. Taken together, this experimental evidence obtained with pharmacological and transgenic approaches, suggest that astrocytes can be involved in opioid signaling in the nucleus accumbens.

The present study advances the literature on the consequences of opioid signaling on astrocyte structure and function. Past research has demonstrated that in response to opioids, such as morphine, astrocytes exhibit increased GFAP levels, a marker for astrocyte activation[155]. Additional functional evidence implicating astrocytes in opioid signaling was obtained via the investigation of astrocyte glutamate transporter expression in response to opioid exposure. Morphine dependence was associated with decreased expression of the astrocyte glutamate transporter, GLT-1[156]. Furthermore, activation of GLT-1 decreased drug-related behaviors associated with morphine such as place preference[157]. Whether these effects are mediated indirectly through neuronal signaling or directly through activation of astrocyte receptors remains to investigated. The present demonstration of direct astrocyte responsiveness to opioids through activation of μ-opioid receptors, suggest that these functional changes associated with morphine-related behaviors may be directly mediated by astrocytes, which would suggest that astrocytes are actively involved in drug-related behaviors.

One of the first studies investigating the physiological consequence of μ opioid receptor activation on astrocytes found that activation of these receptors in the hippocampus led to astrocytic glutamate release through TREK-1-containing two-pore potassium (K2P) channels[144]. Our present results suggest the calcium-dependent glutamate release in NAc astrocytes. Although regional differences might account for these different mechanisms of opioid-induced glutamate release, it is more likely that these alternative mechanisms of release, which are not be mutually exclusive, may coexist. Further studies are required to elucidate whether these different mechanisms represent an additional feature of the astrocyte heterogeneity[52,158] or the heterogenous mechanisms of gliotransmitter release[159].

Astrocyte calcium elevations are associated with gliotransmission, such as glutamate release to modulate synaptic transmission and plasticity. SICs result from the activation of extrasynaptic NMDA receptors that contain the GluN2B subunit. Neuronal synchronization following SICs has been observed in the hippocampus and nucleus accumbens[3,160], indicating that astrocytes responding to opioids are able to impact neuronal network activity.

The current results demonstrate that opioids and opioid signaling impact astrocyte-neuron communication in the nucleus accumbens. Therefore, since astrocytes can be involved in opioid signaling, they may serve as a potential target for therapeutics designed to treat opioid use disorders.

Chapter Six: Discussion

The current work provides several lines of evidence supporting the hypothesis that astrocytes actively contribute to brain reward signaling (Figure 6.1). One of the primary reward transmitters in the brain is dopamine, and our work illustrates that nucleus accumbens core astrocytes respond to dopamine with increases in cytoplasmic calcium (Chapter 3). Furthermore, we illustrate that astrocyte calcium signaling can be modulated by amphetamine (Chapter 3) and opioids (Chapter 5), indicating that astrocytes respond to pharmacologic manipulations of dopamine levels and potential drugs of abuse. Astrocyte calcium elevations in response to dopamine (Chapter 3), amphetamine (Chapter 3) and opioids (Chapter 5) are associated with modulation of neuronal signaling providing evidence for astrocyte-neuron communication in the brain reward pathway. Furthermore, we provide evidence that astrocytes contribute to the psychomotor behavioral phenotype associated with amphetamine administration (Chapter 4) indicating astrocytic modulation of drug seeking behavior. Overall, the results indicate the potential role of astrocytes as therapeutic targets of diseases associated with dopamine dysregulation, such as substance use disorders.

6.1. Clinical Implications

The results from the present study suggest that astrocytes are potential therapeutic targets for diseases related to dopaminergic dysregulation, such as substance use disorders. Below I discuss treatment approaches for astrocyte targeting that can be implemented in the clinical setting.

6.2. Therapeutic Intervention: Pharmacology

The current study illustrates that astrocytes contribute to the actions of drugs of abuse in the nucleus accumbens with regards to glutamatergic transmission. In addition to actively modulating excitatory synaptic transmission via adenosine signaling (Chapter 3) and glutamatergic signaling (Chapter 4), astrocytes also regulate synaptic glutamate levels via transporters expressed on the cell[137]. Astrocytes express both the cystine-glutamate exchanger and glutamate transporters, such as GLT-1. Extended exposure to both psychostimulants and opioids downregulate these regulatory mechanisms, resulting in increased extracellular glutamate and dysregulated synaptic transmission and plasticity[137]. Researchers have investigated drugs that can target this disruption, including ceftriaxone (a commonly used antibiotic) and n-acetyl-cysteine (a readily available nutritional supplement)—both drugs normalize the system via increasing cystine-glutamate exchanger and GLT-1 expression levels and exhibit functional outcomes of decreased drug seeking behavior[25]. A structural analog of ceftriaxone, without antibiotic activity, is clavulanic acid which has been shown to decrease psychostimulant and opioid drug seeking. Ibudilast (readily used in the clinic to treat asthma) regulates glial activity via inhibiting phosphodiesterase activity and has been shown to modulate responses to amphetamine[161] and morphine[162].

6.3. Therapeutic Intervention: Noninvasive neuromodulation

Preclinical models have demonstrated that modulation of astrocytic activity may be efficacious for attenuating drug seeking and reinstatement of drug related behaviors[54,125]. Although these studies utilized invasive approaches via pharmacogenetics, non-invasive

modulation of astrocytes may also provide a potential avenue to treating diseases associated with dopamine disruption. For example, transcranial direct current stimulation (tDCS) has been shown to stimulate astrocyte calcium signaling[163]. Although tDCS is not yet an FDA approved treatment, it has potential therapeutic effects for enhancing cognition and treating neuropsychiatric disorders such as depression, chronic pain and addiction. Monai and colleagues (2016)[163] found that tDCS induced IP_3R2 dependent calcium elevations in astrocytes mediated by noradrenergic signaling. Importantly, the researchers did not observe elevations in neuronal calcium suggesting that tDCS exerts its effects directly on astrocytes to modulate synaptic plasticity. Interestingly, tDCS mediated plasticity measured in both the visual cortex and barrel cortex was mediated by noradrenergic signaling and astrocyte calcium elevations, given that the plasticity was not observed in $IP_3R2^{-/-}$ mice. The visual evoked potential was seen in neurons and not astrocytes suggesting that tDCS acts on astrocytes which then subsequently modulate neuronal plasticity. Importantly, Monai and collegues (2018)[164] also observed alleviation of depression symptoms in mice with tDCS which was not observed in $IP_3R2^{-/-}$ mice suggesting that astrocytes play a role in the therapeutic effects of tDCS as well as the plasticity inducing components of tDCS. Overall, the results provide evidence that astrocytes may be modulated by non-invasive neuromodulation and serve as important targets for the development of therapeutics to treat neuropsychiatric disorders.

6.4. Future Experiments

The nucleus accumbens integrates reward signaling in a complex array of distinct circuit signaling mechanisms, including multiple glutamatergic inputs to discrete cell types within the region. The current project specifically examined astrocyte-neuron signaling in

the nucleus accumbens core examining activity from a mixed neuronal population. Given that there are differences in the core and the shell subregions of the nucleus accumbens and D_1R and D_2R MSNs as it pertains to synaptic adaptations associated with reward signaling, future experiments can be designed to compare and contrast astrocyte-neuron signaling in these discrete circuits.

Additionally, the current project investigated excitatory transmission in the nucleus accumbens via electrical stimulation of glutamatergic afferents (Chapter 3). Researchers have found that specific glutamatergic inputs, have distinct impacts on synaptic transmission and plasticity associated with drugs of abuse (Reviewed by Scofield et al., 2016[25]); therefore, future studies utilizing circuit manipulations such as optogenetics and pharmacogenetics for specific glutamatergic inputs (i.e. hippocampus, prefrontal cortex and amygdala) will provide further insight into astrocyte-neuron signaling in the nucleus accumbens.

Drugs of abuse induce plasticity within the brain, the majority of research has focused on neuronal plasticity; however, it would be interesting to investigate astrocyte plasticity as it pertains to brain reward signaling. Specifically, is there plasticity in the astrocyte calcium signal in response to drugs of abuse? To investigate this question, future studies can chronically image a population of astrocytes over the course of drug exposure (acute, chronic, withdrawal and reinstatement) utilizing miniscopes or fiber photometry in awake behaving animals. Parameters of astrocyte calcium signal to examine include: amplitude of calcium response and frequency of events. With miniscopes, researchers

can also study population dynamics of astrocytes, do the identity of astrocytes that are responding remain the same, do the astrocytes that are responsiveness during acute exposure to a drug remain active during withdrawal, or does a new subset of astrocytes become active?

In addition to calcium signals, astrocyte plasticity may also manifest as changes in molecular markers, such as GFAP and c-Fos. Researchers have found that in response to drugs of abuse, GFAP levels are modulated[62,165]. Additionally, activation of astrocytes with pharmacogenetics results in increased c-Fos expression[166,167]. In neuronal research, synaptic plasticity can be measured by markers of dendritic spine density, it would be interesting to investigate the correlation of these neuronal markers with changes in astrocytic markers. Furthermore, to truly understand how the molecular changes translate to synaptic transmission and plasticity, experiments designed to correlate GFAP and c-Fos changes to calcium signaling and neuronal activity would provide insightful advances to the field. These experiments may include biomarkers that can be visualized *in vivo* to track the changes over time while correlating them to astrocyte and neuronal physiology.

An important future experiment includes investigating astrocyte responsiveness to natural rewards. The current study demonstrated that astrocytes respond with increases in calcium to dopamine, amphetamine and opioids. Knowledge of astrocyte responsiveness to natural rewards, such as food reward will provide further insight into astrocyte signaling in brain reward circuits.

Interestingly, the current results indicate that astrocytes regulate neuronal activity in the nucleus accumbens either through glutamatergic signaling in response to opioid receptor activation (Chapter 5, Figure 6.1) or adenosine signaling in response to dopamine receptor activation (Chapter 3, Figure 6.1). A single astrocyte can release multiple gliotransmitters in response to specific inputs to the cell[9]; therefore, future studies can investigate if a single synapse can be modulated in the nucleus accumbens differentially depending on the input to astrocytes (i.e. can dopamine and opioids modulate the same neuronal synapse through astrocytes differentially?) This study will provide further insight into astrocyte-neuron communication in the brain reward system.

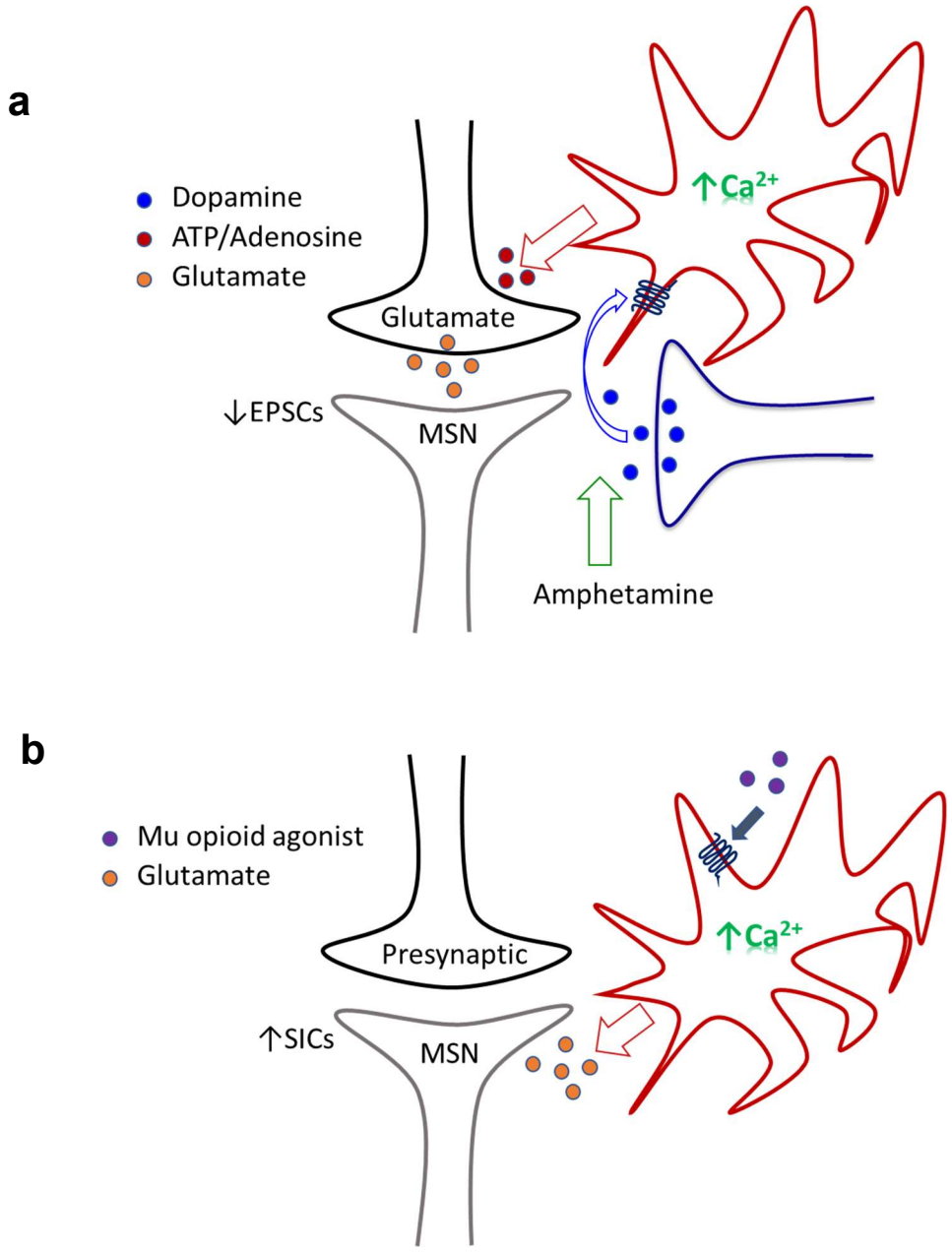

Figure 6.1. Schematic of the role of astrocytes in dopaminergic and opioid signaling. a, Summary from findings in chapter 3 indicating that astrocytes respond to dopamine and amphetamine-mediated dopamine increases with elevations of cytoplasmic calcium and subsequent depression of excitatory post synaptic currents (EPSCs) via adenosine signaling. **b,** Summary of experimental conclusions from chapter 5 suggesting that astrocytes respond to mu opioid receptor activation with increases in cytoplasmic calcium and the subsequent regulation of neuronal slow inward currents (SICs).

References

1 Araque, A., Li, N., Doyle, R. T. & Haydon, P. G. SNARE protein-dependent glutamate release from astrocytes. *The Journal of neuroscience : the official journal of the Society for Neuroscience* **20**, 666-673 (2000).

2 Fellin, T. *et al.* Neuronal synchrony mediated by astrocytic glutamate through activation of extrasynaptic NMDA receptors. *Neuron* **43**, 729-743, doi:10.1016/j.neuron.2004.08.011 (2004).

3 D'Ascenzo, M. *et al.* mGluR5 stimulates gliotransmission in the nucleus accumbens. *Proceedings of the National Academy of Sciences of the United States of America* **104**, 1995-2000, doi:10.1073/pnas.0609408104 (2007).

4 Heal, D. J., Smith, S. L., Gosden, J. & Nutt, D. J. Amphetamine, past and present--a pharmacological and clinical perspective. *Journal of psychopharmacology* **27**, 479-496, doi:10.1177/0269881113482532 (2013).

5 Shigetomi, E., Bowser, D. N., Sofroniew, M. V. & Khakh, B. S. Two forms of astrocyte calcium excitability have distinct effects on NMDA receptor-mediated slow inward currents in pyramidal neurons. *The Journal of neuroscience : the official journal of the Society for Neuroscience* **28**, 6659-6663, doi:10.1523/JNEUROSCI.1717-08.2008 (2008).

6 Reinscheid, R. K. *et al.* Orphanin FQ: a neuropeptide that activates an opioidlike G protein-coupled receptor. *Science* **270**, 792-794 (1995).

7 Shippenberg, T. S., LeFevour, A. & Chefer, V. I. Targeting endogenous mu- and delta-opioid receptor systems for the treatment of drug addiction. *CNS & neurological disorders drug targets* **7**, 442-453 (2008).

8 Beaulieu, J. M. & Gainetdinov, R. R. The physiology, signaling, and pharmacology of dopamine receptors. *Pharmacological reviews* **63**, 182-217, doi:10.1124/pr.110.002642 (2011).

9 Covelo, A. & Araque, A. Neuronal activity determines distinct gliotransmitter release from a single astrocyte. *eLife* **7**, doi:10.7554/eLife.32237 (2018).

10 Woo, D. H. *et al.* TREK-1 and Best1 channels mediate fast and slow glutamate release in astrocytes upon GPCR activation. *Cell* **151**, 25-40, doi:10.1016/j.cell.2012.09.005 (2012).

11 Al-Hasani, R. & Bruchas, M. R. Molecular mechanisms of opioid receptor-dependent signaling and behavior. *Anesthesiology* **115**, 1363-1381, doi:10.1097/ALN.0b013e318238bba6 (2011).

12 Di Chiara, G. & Imperato, A. Drugs abused by humans preferentially increase synaptic dopamine concentrations in the mesolimbic system of freely moving rats. *Proceedings of the National Academy of Sciences of the United States of America* **85**, 5274-5278 (1988).

13 Hyland, B. I., et al. . Firing modes of midbrain dopamine cells in the freely moving rat. *Neuroscience* **114.2** 475-492 (2002).

14 Pettit, H. O., and Joseph B. Justice Jr. . Dopamine in the nucleus accumbens during cocaine self-administration as studied by in vivo microdialysis. *Pharmacology Biochemistry and Behavior* **34.4** 899-904 (1989).

15 Ito, R., et al. Dissociation in conditioned dopamine release in the nucleus accumbens core and shell in response to cocaine cues and during cocaine-seeking behavior in rats. *Journal of Neuroscience* **20.19** (2000).
16 Volkow, N. D., Wise, R. A. & Baler, R. The dopamine motive system: implications for drug and food addiction. *Nature reviews. Neuroscience* **18**, 741-752, doi:10.1038/nrn.2017.130 (2017).
17 Badrinarayan, A. *et al.* Aversive stimuli differentially modulate real-time dopamine transmission dynamics within the nucleus accumbens core and shell. *The Journal of neuroscience : the official journal of the Society for Neuroscience* **32**, 15779-15790, doi:10.1523/JNEUROSCI.3557-12.2012 (2012).
18 Schultz, W. Predictive reward signal of dopamine neurons. *J Neurophysiol* **80**, 1-27, doi:10.1152/jn.1998.80.1.1 (1998).
19 Wightman, R. M. & Robinson, D. L. Transient changes in mesolimbic dopamine and their association with 'reward'. *Journal of neurochemistry* **82**, 721-735 (2002).
20 Chuhma, N. *et al.* Dopamine neurons mediate a fast excitatory signal via their glutamatergic synapses. *The Journal of neuroscience : the official journal of the Society for Neuroscience* **24**, 972-981, doi:10.1523/JNEUROSCI.4317-03.2004 (2004).
21 Yamaguchi, T., Wang, H. L., Li, X., Ng, T. H. & Morales, M. Mesocorticolimbic glutamatergic pathway. *The Journal of neuroscience : the official journal of the Society for Neuroscience* **31**, 8476-8490, doi:10.1523/JNEUROSCI.1598-11.2011 (2011).
22 Stuber, G. D., Hnasko, T. S., Britt, J. P., Edwards, R. H. & Bonci, A. Dopaminergic terminals in the nucleus accumbens but not the dorsal striatum corelease glutamate. *The Journal of neuroscience : the official journal of the Society for Neuroscience* **30**, 8229-8233, doi:10.1523/JNEUROSCI.1754-10.2010 (2010).
23 Salgado, S. & Kaplitt, M. G. The Nucleus Accumbens: A Comprehensive Review. *Stereotactic and functional neurosurgery* **93**, 75-93, doi:10.1159/000368279 (2015).
24 Voorn, P., Vanderschuren, L. J., Groenewegen, H. J., Robbins, T. W. & Pennartz, C. M. Putting a spin on the dorsal-ventral divide of the striatum. *Trends in neurosciences* **27**, 468-474, doi:10.1016/j.tins.2004.06.006 (2004).
25 Scofield, M. D. *et al.* The Nucleus Accumbens: Mechanisms of Addiction across Drug Classes Reflect the Importance of Glutamate Homeostasis. *Pharmacological reviews* **68**, 816-871, doi:10.1124/pr.116.012484 (2016).
26 Saddoris, M. P., Cacciapaglia, F., Wightman, R. M. & Carelli, R. M. Differential Dopamine Release Dynamics in the Nucleus Accumbens Core and Shell Reveal Complementary Signals for Error Prediction and Incentive Motivation. *The Journal of neuroscience : the official journal of the Society for Neuroscience* **35**, 11572-11582, doi:10.1523/JNEUROSCI.2344-15.2015 (2015).
27 Kupchik, Y. M. *et al.* Coding the direct/indirect pathways by D1 and D2 receptors is not valid for accumbens projections. *Nature neuroscience* **18**, 1230-1232, doi:10.1038/nn.4068 (2015).
28 Hikida, T., Morita, M. & Macpherson, T. Neural mechanisms of the nucleus accumbens circuit in reward and aversive learning. *Neuroscience research* **108**, 1-5, doi:10.1016/j.neures.2016.01.004 (2016).

29 Calabresi, P., Picconi, B., Tozzi, A., Ghiglieri, V. & Di Filippo, M. Direct and indirect pathways of basal ganglia: a critical reappraisal. *Nature neuroscience* **17**, 1022-1030, doi:10.1038/nn.3743 (2014).
30 Bushong, E. A., Martone, M. E., Jones, Y. Z. & Ellisman, M. H. Protoplasmic astrocytes in CA1 stratum radiatum occupy separate anatomical domains. *The Journal of neuroscience : the official journal of the Society for Neuroscience* **22**, 183-192 (2002).
31 Araque, A., Parpura, V., Sanzgiri, R. P. & Haydon, P. G. Tripartite synapses: glia, the unacknowledged partner. *Trends in neurosciences* **22**, 208-215 (1999).
32 Bezzi, P. & Volterra, A. A neuron-glia signalling network in the active brain. *Current opinion in neurobiology* **11**, 387-394 (2001).
33 Araque, A. *et al.* Gliotransmitters travel in time and space. *Neuron* **81**, 728-739, doi:10.1016/j.neuron.2014.02.007 (2014).
34 Verkhratsky, A., Orkand, R. K. & Kettenmann, H. Glial calcium: homeostasis and signaling function. *Physiological reviews* **78**, 99-141, doi:10.1152/physrev.1998.78.1.99 (1998).
35 Santello, M., Cali, C. & Bezzi, P. Gliotransmission and the tripartite synapse. *Advances in experimental medicine and biology* **970**, 307-331, doi:10.1007/978-3-7091-0932-8_14 (2012).
36 Bazargani, N. & Attwell, D. Astrocyte calcium signaling: the third wave. *Nature neuroscience* **19**, 182-189, doi:10.1038/nn.4201 (2016).
37 Grosche, J. *et al.* Microdomains for neuron-glia interaction: parallel fiber signaling to Bergmann glial cells. *Nature neuroscience* **2**, 139-143, doi:10.1038/5692 (1999).
38 Di Castro, M. A. *et al.* Local Ca2+ detection and modulation of synaptic release by astrocytes. *Nature neuroscience* **14**, 1276-1284, doi:10.1038/nn.2929 (2011).
39 Kanemaru, K. *et al.* In vivo visualization of subtle, transient, and local activity of astrocytes using an ultrasensitive Ca(2+) indicator. *Cell reports* **8**, 311-318, doi:10.1016/j.celrep.2014.05.056 (2014).
40 Pascual, M., Climent, E. & Guerri, C. BDNF induces glutamate release in cerebrocortical nerve terminals and in cortical astrocytes. *Neuroreport* **12**, 2673-2677 (2001).
41 Bezzi, P. *et al.* Prostaglandins stimulate calcium-dependent glutamate release in astrocytes. *Nature* **391**, 281-285, doi:10.1038/34651 (1998).
42 Bezzi, P. *et al.* Astrocytes contain a vesicular compartment that is competent for regulated exocytosis of glutamate. *Nature neuroscience* **7**, 613-620, doi:10.1038/nn1246 (2004).
43 Coco, S. *et al.* Storage and release of ATP from astrocytes in culture. *The Journal of biological chemistry* **278**, 1354-1362, doi:10.1074/jbc.M209454200 (2003).
44 Martineau, M., Galli, T., Baux, G. & Mothet, J. P. Confocal imaging and tracking of the exocytotic routes for D-serine-mediated gliotransmission. *Glia* **56**, 1271-1284, doi:10.1002/glia.20696 (2008).
45 Takano, T. *et al.* Receptor-mediated glutamate release from volume sensitive channels in astrocytes. *Proceedings of the National Academy of Sciences of the United States of America* **102**, 16466-16471, doi:10.1073/pnas.0506382102 (2005).
46 Petravicz, J., Fiacco, T. A. & McCarthy, K. D. Loss of IP3 receptor-dependent Ca2+ increases in hippocampal astrocytes does not affect baseline CA1 pyramidal neuron

synaptic activity. *The Journal of neuroscience : the official journal of the Society for Neuroscience* **28**, 4967-4973, doi:10.1523/JNEUROSCI.5572-07.2008 (2008).
47 Petravicz, J., Boyt, K. M. & McCarthy, K. D. Astrocyte IP3R2-dependent Ca(2+) signaling is not a major modulator of neuronal pathways governing behavior. *Frontiers in behavioral neuroscience* **8**, 384, doi:10.3389/fnbeh.2014.00384 (2014).
48 Agulhon, C., Fiacco, T. A. & McCarthy, K. D. Hippocampal short- and long-term plasticity are not modulated by astrocyte Ca2+ signaling. *Science* **327**, 1250-1254, doi:10.1126/science.1184821 (2010).
49 Srinivasan, R. *et al.* Ca(2+) signaling in astrocytes from Ip3r2(-/-) mice in brain slices and during startle responses in vivo. *Nature neuroscience* **18**, 708-717, doi:10.1038/nn.4001 (2015).
50 Panatier, A. *et al.* Astrocytes are endogenous regulators of basal transmission at central synapses. *Cell* **146**, 785-798, doi:10.1016/j.cell.2011.07.022 (2011).
51 Perea, G. & Araque, A. Properties of synaptically evoked astrocyte calcium signal reveal synaptic information processing by astrocytes. *The Journal of neuroscience : the official journal of the Society for Neuroscience* **25**, 2192-2203, doi:10.1523/JNEUROSCI.3965-04.2005 (2005).
52 Martin, R., Bajo-Graneras, R., Moratalla, R., Perea, G. & Araque, A. Circuit-specific signaling in astrocyte-neuron networks in basal ganglia pathways. *Science* **349**, 730-734, doi:10.1126/science.aaa7945 (2015).
53 Tanaka, M. *et al.* Astrocytic Ca2+ signals are required for the functional integrity of tripartite synapses. *Molecular brain* **6**, 6, doi:10.1186/1756-6606-6-6 (2013).
54 Bull, C. *et al.* Rat nucleus accumbens core astrocytes modulate reward and the motivation to self-administer ethanol after abstinence. *Neuropsychopharmacology : official publication of the American College of Neuropsychopharmacology* **39**, 2835-2845, doi:10.1038/npp.2014.135 (2014).
55 Adermark, L. *et al.* Implications for glycine receptors and astrocytes in ethanol-induced elevation of dopamine levels in the nucleus accumbens. *Addiction biology* **16**, 43-54, doi:10.1111/j.1369-1600.2010.00206.x (2011).
56 Lee, M. R. *et al.* Striatal adenosine signaling regulates EAAT2 and astrocytic AQP4 expression and alcohol drinking in mice. *Neuropsychopharmacology : official publication of the American College of Neuropsychopharmacology* **38**, 437-445, doi:10.1038/npp.2012.198 (2013).
57 Scofield, M. D. *et al.* Cocaine Self-Administration and Extinction Leads to Reduced Glial Fibrillary Acidic Protein Expression and Morphometric Features of Astrocytes in the Nucleus Accumbens Core. *Biological psychiatry* **80**, 207-215, doi:10.1016/j.biopsych.2015.12.022 (2016).
58 Knackstedt, L. A., Melendez, R. I. & Kalivas, P. W. Ceftriaxone restores glutamate homeostasis and prevents relapse to cocaine seeking. *Biological psychiatry* **67**, 81-84, doi:10.1016/j.biopsych.2009.07.018 (2010).
59 Turner, J. R., Ecke, L. E., Briand, L. A., Haydon, P. G. & Blendy, J. A. Cocaine-related behaviors in mice with deficient gliotransmission. *Psychopharmacology* **226**, 167-176, doi:10.1007/s00213-012-2897-4 (2013).

60 Bland, S. T., Hutchinson, M. R., Maier, S. F., Watkins, L. R. & Johnson, K. W. The glial activation inhibitor AV411 reduces morphine-induced nucleus accumbens dopamine release. *Brain, behavior, and immunity* **23**, 492-497, doi:10.1016/j.bbi.2009.01.014 (2009).
61 Wu, J., Zhao, R., Guo, L. & Zhen, X. Morphine-induced inhibition of Ca(2+) -dependent d-serine release from astrocytes suppresses excitability of GABAergic neurons in the nucleus accumbens. *Addiction biology* **22**, 1289-1303, doi:10.1111/adb.12417 (2017).
62 Narita, M. *et al.* Direct evidence of astrocytic modulation in the development of rewarding effects induced by drugs of abuse. *Neuropsychopharmacology : official publication of the American College of Neuropsychopharmacology* **31**, 2476-2488, doi:10.1038/sj.npp.1301007 (2006).
63 Wise, R. A. Drug-activation of brain reward pathways. *Drug and alcohol dependence* **51**, 13-22 (1998).
64 Koob, G. F. & Le Moal, M. Drug addiction, dysregulation of reward, and allostasis. *Neuropsychopharmacology : official publication of the American College of Neuropsychopharmacology* **24**, 97-129, doi:10.1016/S0893-133X(00)00195-0 (2001).
65 Miyazaki, I., Asanuma, M., Diaz-Corrales, F. J., Miyoshi, K. & Ogawa, N. Direct evidence for expression of dopamine receptors in astrocytes from basal ganglia. *Brain research* **1029**, 120-123, doi:10.1016/j.brainres.2004.09.014 (2004).
66 Bal, A. *et al.* Evidence for dopamine D2 receptor mRNA expression by striatal astrocytes in culture: in situ hybridization and polymerase chain reaction studies. *Brain research. Molecular brain research* **23**, 204-212 (1994).
67 Nagatomo, K. *et al.* Dopamine D1 Receptor Immunoreactivity on Fine Processes of GFAP-Positive Astrocytes in the Substantia Nigra Pars Reticulata of Adult Mouse. *Frontiers in neuroanatomy* **11**, 3, doi:10.3389/fnana.2017.00003 (2017).
68 Khan, Z. U., Koulen, P., Rubinstein, M., Grandy, D. K. & Goldman-Rakic, P. S. An astroglia-linked dopamine D2-receptor action in prefrontal cortex. *Proceedings of the National Academy of Sciences of the United States of America* **98**, 1964-1969, doi:10.1073/pnas.98.4.1964 (2001).
69 Mladinov, M., et al. . Astrocyte expression of D2-like dopamine receptors in the prefrontal cortex. *Translational Neuroscience* **1.3**, 238-243 (2010).
70 Reuss, B. & Unsicker, K. Atypical neuroleptic drugs downregulate dopamine sensitivity in rat cortical and striatal astrocytes. *Molecular and cellular neurosciences* **18**, 197-209, doi:10.1006/mcne.2001.1017 (2001).
71 Hansson, E. & Ronnback, L. Neurons from substantia nigra increase the efficacy and potency of second messenger arising from striatal astroglia dopamine receptor. *Glia* **1**, 393-397, doi:10.1002/glia.440010606 (1988).
72 Zanassi, P., Paolillo, M., Montecucco, A., Avvedimento, E. V. & Schinelli, S. Pharmacological and molecular evidence for dopamine D(1) receptor expression by striatal astrocytes in culture. *Journal of neuroscience research* **58**, 544-552 (1999).
73 Jennings, A. *et al.* Dopamine elevates and lowers astroglial Ca(2+) through distinct pathways depending on local synaptic circuitry. *Glia* **65**, 447-459, doi:10.1002/glia.23103 (2017).

74 Liu, J. *et al.* Activation of phosphatidylinositol-linked novel D1 dopamine receptor contributes to the calcium mobilization in cultured rat prefrontal cortical astrocytes. *Cellular and molecular neurobiology* **29**, 317-328, doi:10.1007/s10571-008-9323-9 (2009).
75 Vaarmann, A., Gandhi, S. & Abramov, A. Y. Dopamine induces Ca2+ signaling in astrocytes through reactive oxygen species generated by monoamine oxidase. *The Journal of biological chemistry* **285**, 25018-25023, doi:10.1074/jbc.M110.111450 (2010).
76 Reyes, R. C. & Parpura, V. Models of astrocytic Ca dynamics and epilepsy. *Drug discovery today. Disease models* **5**, 13-18, doi:10.1016/j.ddmod.2008.07.002 (2008).
77 Bosson, A., Boisseau, S., Buisson, A., Savasta, M. & Albrieux, M. Disruption of dopaminergic transmission remodels tripartite synapse morphology and astrocytic calcium activity within substantia nigra pars reticulata. *Glia* **63**, 673-683, doi:10.1002/glia.22777 (2015).
78 Johnson, S. W. & North, R. A. Opioids excite dopamine neurons by hyperpolarization of local interneurons. *The Journal of neuroscience : the official journal of the Society for Neuroscience* **12**, 483-488 (1992).
79 Nicola, S. M. & Malenka, R. C. Dopamine depresses excitatory and inhibitory synaptic transmission by distinct mechanisms in the nucleus accumbens. *The Journal of neuroscience : the official journal of the Society for Neuroscience* **17**, 5697-5710 (1997).
80 Nicola, S. M., Kombian, S. B. & Malenka, R. C. Psychostimulants depress excitatory synaptic transmission in the nucleus accumbens via presynaptic D1-like dopamine receptors. *The Journal of neuroscience : the official journal of the Society for Neuroscience* **16**, 1591-1604 (1996).
81 Harvey, J. & Lacey, M. G. Endogenous and exogenous dopamine depress EPSCs in rat nucleus accumbens in vitro via D1 receptors activation. *The Journal of physiology* **492 (Pt 1)**, 143-154 (1996).
82 Wang, W. *et al.* Regulation of prefrontal excitatory neurotransmission by dopamine in the nucleus accumbens core. *The Journal of physiology* **590**, 3743-3769, doi:10.1113/jphysiol.2012.235200 (2012).
83 Hoffman, A. F. & Lupica, C. R. Direct actions of cannabinoids on synaptic transmission in the nucleus accumbens: a comparison with opioids. *J Neurophysiol* **85**, 72-83, doi:10.1152/jn.2001.85.1.72 (2001).
84 Paukert, M. *et al.* Norepinephrine controls astroglial responsiveness to local circuit activity. *Neuron* **82**, 1263-1270, doi:10.1016/j.neuron.2014.04.038 (2014).
85 Mori, T. *et al.* Inducible gene deletion in astroglia and radial glia--a valuable tool for functional and lineage analysis. *Glia* **54**, 21-34, doi:10.1002/glia.20350 (2006).
86 Narushima, M., Uchigashima, M., Hashimoto, K., Watanabe, M. & Kano, M. Depolarization-induced suppression of inhibition mediated by endocannabinoids at synapses from fast-spiking interneurons to medium spiny neurons in the striatum. *The European journal of neuroscience* **24**, 2246-2252, doi:10.1111/j.1460-9568.2006.05119.x (2006).
87 Uchigashima, M. *et al.* Subcellular arrangement of molecules for 2-arachidonoyl-glycerol-mediated retrograde signaling and its physiological contribution to synaptic

modulation in the striatum. *The Journal of neuroscience : the official journal of the Society for Neuroscience* **27**, 3663-3676, doi:10.1523/JNEUROSCI.0448-07.2007 (2007).

88 Lujan, R., Nusser, Z., Roberts, J. D., Shigemoto, R. & Somogyi, P. Perisynaptic location of metabotropic glutamate receptors mGluR1 and mGluR5 on dendrites and dendritic spines in the rat hippocampus. *The European journal of neuroscience* **8**, 1488-1500 (1996).

89 Luscher, C. & Malenka, R. C. Drug-evoked synaptic plasticity in addiction: from molecular changes to circuit remodeling. *Neuron* **69**, 650-663, doi:10.1016/j.neuron.2011.01.017 (2011).

90 Luscher, C. The Emergence of a Circuit Model for Addiction. *Annual review of neuroscience* **39**, 257-276, doi:10.1146/annurev-neuro-070815-013920 (2016).

91 Kalivas, P. W. & Volkow, N. D. The neural basis of addiction: a pathology of motivation and choice. *The American journal of psychiatry* **162**, 1403-1413, doi:10.1176/appi.ajp.162.8.1403 (2005).

92 Bamford, N. S. *et al.* Repeated exposure to methamphetamine causes long-lasting presynaptic corticostriatal depression that is renormalized with drug readministration. *Neuron* **58**, 89-103, doi:10.1016/j.neuron.2008.01.033 (2008).

93 Harvey, J. & Lacey, M. G. A postsynaptic interaction between dopamine D1 and NMDA receptors promotes presynaptic inhibition in the rat nucleus accumbens via adenosine release. *The Journal of neuroscience : the official journal of the Society for Neuroscience* **17**, 5271-5280 (1997).

94 Kombian, S. B., Ananthalakshmi, K. V., Parvathy, S. S. & Matowe, W. C. Substance P depresses excitatory synaptic transmission in the nucleus accumbens through dopaminergic and purinergic mechanisms. *Journal of neurophysiology* **89**, 728-737, doi:10.1152/jn.00854.2002 (2003).

95 Araque, A., Carmignoto, G. & Haydon, P. G. Dynamic signaling between astrocytes and neurons. *Annual review of physiology* **63**, 795-813, doi:10.1146/annurev.physiol.63.1.795 (2001).

96 Haydon, P. G. & Carmignoto, G. Astrocyte control of synaptic transmission and neurovascular coupling. *Physiological reviews* **86**, 1009-1031, doi:10.1152/physrev.00049.2005 (2006).

97 Perea, G., Navarrete, M. & Araque, A. Tripartite synapses: astrocytes process and control synaptic information. *Trends in neurosciences* **32**, 421-431, doi:10.1016/j.tins.2009.05.001 (2009).

98 Volterra, A., Liaudet, N. & Savtchouk, I. Astrocyte Ca(2)(+) signalling: an unexpected complexity. *Nature reviews. Neuroscience* **15**, 327-335, doi:10.1038/nrn3725 (2014).

99 Navarrete, M. & Araque, A. Endocannabinoids potentiate synaptic transmission through stimulation of astrocytes. *Neuron* **68**, 113-126, doi:10.1016/j.neuron.2010.08.043 (2010).

100 Volterra, A. & Meldolesi, J. Astrocytes, from brain glue to communication elements: the revolution continues. *Nature reviews. Neuroscience* **6**, 626-640, doi:10.1038/nrn1722 (2005).

101 Perea, G. *et al.* Activity-dependent switch of GABAergic inhibition into glutamatergic excitation in astrocyte-neuron networks. *eLife* **5**, doi:10.7554/eLife.20362 (2016).
102 Perea, G. & Araque, A. Astrocytes potentiate transmitter release at single hippocampal synapses. *Science* **317**, 1083-1086, doi:10.1126/science.1144640 (2007).
103 Parri, H. R., Gould, T. M. & Crunelli, V. Spontaneous astrocytic Ca2+ oscillations in situ drive NMDAR-mediated neuronal excitation. *Nature neuroscience* **4**, 803-812, doi:10.1038/90507 (2001).
104 Min, R. & Nevian, T. Astrocyte signaling controls spike timing-dependent depression at neocortical synapses. *Nature neuroscience* **15**, 746-753, doi:10.1038/nn.3075 (2012).
105 Halassa, M. M. & Haydon, P. G. Integrated brain circuits: astrocytic networks modulate neuronal activity and behavior. *Annual review of physiology* **72**, 335-355, doi:10.1146/annurev-physiol-021909-135843 (2010).
106 Covelo, A. & Araque, A. Lateral regulation of synaptic transmission by astrocytes. *Neuroscience* **323**, 62-66, doi:10.1016/j.neuroscience.2015.02.036 (2016).
107 Henneberger, C., Papouin, T., Oliet, S. H. & Rusakov, D. A. Long-term potentiation depends on release of D-serine from astrocytes. *Nature* **463**, 232-236, doi:10.1038/nature08673 (2010).
108 Min, R., Santello, M. & Nevian, T. The computational power of astrocyte mediated synaptic plasticity. *Frontiers in computational neuroscience* **6**, 93, doi:10.3389/fncom.2012.00093 (2012).
109 Martin-Fernandez, M. *et al.* Synapse-specific astrocyte gating of amygdala-related behavior. *Nat Neurosci* **20**, 1540-1548, doi:10.1038/nn.4649 (2017).
110 Jennings, A. *et al.* Dopamine elevates and lowers astroglial Ca2+ through distinct pathways depending on local synaptic circuitry. *Glia* **65**, 447-459, doi:10.1002/glia.23103 (2017).
111 Cui, Q. *et al.* Blunted mGluR Activation Disinhibits Striatopallidal Transmission in Parkinsonian Mice. *Cell reports* **17**, 2431-2444, doi:10.1016/j.celrep.2016.10.087 (2016).
112 Lerner, T. N. *et al.* Intact-Brain Analyses Reveal Distinct Information Carried by SNc Dopamine Subcircuits. *Cell* **162**, 635-647, doi:10.1016/j.cell.2015.07.014 (2015).
113 Saunders, B. T., Richard, J. M., Margolis, E. B. & Janak, P. H. Dopamine neurons create Pavlovian conditioned stimuli with circuit-defined motivational properties. *Nature neuroscience* **21**, 1072-1083, doi:10.1038/s41593-018-0191-4 (2018).
114 Klapoetke, N. C. *et al.* Independent optical excitation of distinct neural populations. *Nature methods* **11**, 338-346, doi:10.1038/nmeth.2836 (2014).
115 Calipari, E. S. & Ferris, M. J. Amphetamine mechanisms and actions at the dopamine terminal revisited. *The Journal of neuroscience : the official journal of the Society for Neuroscience* **33**, 8923-8925, doi:10.1523/JNEUROSCI.1033-13.2013 (2013).
116 Gomez-Gonzalo, M. *et al.* Endocannabinoids Induce Lateral Long-Term Potentiation of Transmitter Release by Stimulation of Gliotransmission. *Cerebral cortex* **25**, 3699-3712, doi:10.1093/cercor/bhu231 (2015).
117 Li, X., Zima, A. V., Sheikh, F., Blatter, L. A. & Chen, J. Endothelin-1-induced arrhythmogenic Ca2+ signaling is abolished in atrial myocytes of inositol-1,4,5-

trisphosphate(IP3)-receptor type 2-deficient mice. *Circulation research* **96**, 1274-1281, doi:10.1161/01.RES.0000172556.05576.4c (2005).
118 Gomez-Gonzalo, M. *et al.* Neuron-astrocyte signaling is preserved in the aging brain. *Glia* **65**, 569-580, doi:10.1002/glia.23112 (2017).
119 Navarrete, M. *et al.* Astrocytes mediate in vivo cholinergic-induced synaptic plasticity. *PLoS biology* **10**, e1001259, doi:10.1371/journal.pbio.1001259 (2012).
120 Surmeier, D. J., Bargas, J., Hemmings, H. C., Jr., Nairn, A. C. & Greengard, P. Modulation of calcium currents by a D1 dopaminergic protein kinase/phosphatase cascade in rat neostriatal neurons. *Neuron* **14**, 385-397 (1995).
121 Zhang, J. M. *et al.* ATP released by astrocytes mediates glutamatergic activity-dependent heterosynaptic suppression. *Neuron* **40**, 971-982 (2003).
122 Martin, E. D. *et al.* Adenosine released by astrocytes contributes to hypoxia-induced modulation of synaptic transmission. *Glia* **55**, 36-45, doi:10.1002/glia.20431 (2007).
123 Pascual, O. *et al.* Astrocytic purinergic signaling coordinates synaptic networks. *Science* **310**, 113-116, doi:10.1126/science.1116916 (2005).
124 Serrano, A., Haddjeri, N., Lacaille, J. C. & Robitaille, R. GABAergic network activation of glial cells underlies hippocampal heterosynaptic depression. *The Journal of neuroscience : the official journal of the Society for Neuroscience* **26**, 5370-5382, doi:10.1523/JNEUROSCI.5255-05.2006 (2006).
125 Scofield, M. D. *et al.* Gq-DREADD Selectively Initiates Glial Glutamate Release and Inhibits Cue-induced Cocaine Seeking. *Biological psychiatry* **78**, 441-451, doi:10.1016/j.biopsych.2015.02.016 (2015).
126 Paulson, P. E. & Robinson, T. E. Amphetamine-induced time-dependent sensitization of dopamine neurotransmission in the dorsal and ventral striatum: a microdialysis study in behaving rats. *Synapse* **19**, 56-65, doi:10.1002/syn.890190108 (1995).
127 Kalivas, P. W., Lalumiere, R. T., Knackstedt, L. & Shen, H. Glutamate transmission in addiction. *Neuropharmacology* **56 Suppl 1**, 169-173, doi:10.1016/j.neuropharm.2008.07.011 (2009).
128 Kalivas, P. W. & Stewart, J. Dopamine transmission in the initiation and expression of drug- and stress-induced sensitization of motor activity. *Brain research. Brain research reviews* **16**, 223-244 (1991).
129 O'Daly, O. G. *et al.* Amphetamine sensitization alters reward processing in the human striatum and amygdala. *PloS one* **9**, e93955, doi:10.1371/journal.pone.0093955 (2014).
130 Childs, E. & de Wit, H. Amphetamine-induced place preference in humans. *Biological psychiatry* **65**, 900-904, doi:10.1016/j.biopsych.2008.11.016 (2009).
131 Olds, J. & Milner, P. Positive reinforcement produced by electrical stimulation of septal area and other regions of rat brain. *Journal of comparative and physiological psychology* **47**, 419-427 (1954).
132 Sora, I. *et al.* Cocaine reward models: conditioned place preference can be established in dopamine- and in serotonin-transporter knockout mice. *Proceedings of the National Academy of Sciences of the United States of America* **95**, 7699-7704 (1998).
133 Hnasko, T. S., Sotak, B. N. & Palmiter, R. D. Cocaine-conditioned place preference by dopamine-deficient mice is mediated by serotonin. *The Journal of neuroscience : the*

official journal of the Society for Neuroscience **27**, 12484-12488, doi:10.1523/JNEUROSCI.3133-07.2007 (2007).
134 Hnasko, T. S., Sotak, B. N. & Palmiter, R. D. Morphine reward in dopamine-deficient mice. *Nature* **438**, 854-857, doi:10.1038/nature04172 (2005).
135 Miner, L. L., Drago, J., Chamberlain, P. M., Donovan, D. & Uhl, G. R. Retained cocaine conditioned place preference in D1 receptor deficient mice. *Neuroreport* **6**, 2314-2316 (1995).
136 Pierce, R. C. & Kalivas, P. W. A circuitry model of the expression of behavioral sensitization to amphetamine-like psychostimulants. *Brain research. Brain research reviews* **25**, 192-216 (1997).
137 Hearing, M., Graziane, N., Dong, Y. & Thomas, M. J. Opioid and Psychostimulant Plasticity: Targeting Overlap in Nucleus Accumbens Glutamate Signaling. *Trends in pharmacological sciences* **39**, 276-294, doi:10.1016/j.tips.2017.12.004 (2018).
138 Vanderschuren, L. J., Schoffelmeer, A. N., Wardeh, G. & De Vries, T. J. Dissociable effects of the kappa-opioid receptor agonists bremazocine, U69593, and U50488H on locomotor activity and long-term behavioral sensitization induced by amphetamine and cocaine. *Psychopharmacology* **150**, 35-44 (2000).
139 Stein, C. The control of pain in peripheral tissue by opioids. *New England Journal of Medicine* **332**, 1685-1690 (1995).
140 Christie, M. J., Connor, M., Vaughan, C. W., Ingram, S. L. & Bagley, E. E. Cellular actions of opioids and other analgesics: implications for synergism in pain relief. *Clinical and Experimental Pharmacology and Physiology* **27**, 520-523 (2000).
141 Wise, R. A. Opiate reward: sites and substrates. *Neuroscience & Biobehavioral Reviews* **13**, 129-133 (1989).
142 Strain, E. (Uptodate, 2015).
143 Nam, M. H. *et al.* Expression of micro-Opioid Receptor in CA1 Hippocampal Astrocytes. *Experimental neurobiology* **27**, 120-128, doi:10.5607/en.2018.27.2.120 (2018).
144 Woo, D. H. *et al.* Activation of Astrocytic mu-opioid Receptor Elicits Fast Glutamate Release Through TREK-1-Containing K2P Channel in Hippocampal Astrocytes. *Frontiers in cellular neuroscience* **12**, 319, doi:10.3389/fncel.2018.00319 (2018).
145 Smart, D., Smith, G. & Lambert, D. G. mu-Opioid receptor stimulation of inositol (1,4,5)trisphosphate formation via a pertussis toxin-sensitive G protein. *Journal of neurochemistry* **62**, 1009-1014 (1994).
146 Ventura, R. & Harris, K. M. Three-dimensional relationships between hippocampal synapses and astrocytes. *The Journal of neuroscience : the official journal of the Society for Neuroscience* **19**, 6897-6906 (1999).
147 Parpura, V. & Zorec, R. Gliotransmission: exocytotic release from astrocytes. *Brain research reviews* **63**, 83-92 (2010).
148 Halassa, M. M., Fellin, T. & Haydon, P. G. The tripartite synapse: roles for gliotransmission in health and disease. *Trends in molecular medicine* **13**, 54-63 (2007).
149 Durkee, C. A. & Araque, A. Diversity And Specificity Of Astrocyte-Neuron Communication. *Neuroscience* (2018).

150 Verkhratsky, A., Rodríguez, J. J. & Parpura, V. Calcium signalling in astroglia. *Molecular and cellular endocrinology* **353**, 45-56 (2012).
151 Perea, G., Navarrete, M. & Araque, A. Tripartite synapses: astrocytes process and control synaptic information. *Trends in neurosciences* **32**, 421-431 (2009).
152 Parpura, V. & Haydon, P. G. Physiological astrocytic calcium levels stimulate glutamate release to modulate adjacent neurons. *Proceedings of the National Academy of Sciences* **97**, 8629-8634 (2000).
153 Araque, A., Sanzgiri, R. P., Parpura, V. & Haydon, P. G. Calcium elevation in astrocytes causes an NMDA receptor-dependent increase in the frequency of miniature synaptic currents in cultured hippocampal neurons. *The Journal of neuroscience : the official journal of the Society for Neuroscience* **18**, 6822-6829 (1998).
154 Gómez-Gonzalo, M. *et al.* Neuron–astrocyte signaling is preserved in the aging brain. *Glia* **65**, 569-580 (2017).
155 Pekny, M. & Nilsson, M. Astrocyte activation and reactive gliosis. *Glia* **50**, 427-434, doi:10.1002/glia.20207 (2005).
156 Ozawa, T., Nakagawa, T., Shige, K., Minami, M. & Satoh, M. Changes in the expression of glial glutamate transporters in the rat brain accompanied with morphine dependence and naloxone-precipitated withdrawal. *Brain research* **905**, 254-258 (2001).
157 Nakagawa, T. *et al.* Inhibition of morphine tolerance and dependence by MS-153, a glutamate transporter activator. *European journal of pharmacology* **419**, 39-45 (2001).
158 Khakh, B. S. & Sofroniew, M. V. Diversity of astrocyte functions and phenotypes in neural circuits. *Nature neuroscience* **18**, 942-952, doi:10.1038/nn.4043 (2015).
159 Kofuji, P. & Araque, A. *Neuron* (In Press).
160 Angulo, M. C., Kozlov, A. S., Charpak, S. & Audinat, E. Glutamate released from glial cells synchronizes neuronal activity in the hippocampus. *The Journal of neuroscience : the official journal of the Society for Neuroscience* **24**, 6920-6927, doi:10.1523/JNEUROSCI.0473-04.2004 (2004).
161 Snider, S. E., Hendrick, E. S. & Beardsley, P. M. Glial cell modulators attenuate methamphetamine self-administration in the rat. *European journal of pharmacology* **701**, 124-130, doi:10.1016/j.ejphar.2013.01.016 (2013).
162 Rolan, P., Hutchinson, M. & Johnson, K. Ibudilast: a review of its pharmacology, efficacy and safety in respiratory and neurological disease. *Expert opinion on pharmacotherapy* **10**, 2897-2904, doi:10.1517/14656560903426189 (2009).
163 Monai, H. *et al.* Calcium imaging reveals glial involvement in transcranial direct current stimulation-induced plasticity in mouse brain. *Nature communications* **7**, 11100, doi:10.1038/ncomms11100 (2016).
164 Monai, H. & Hirase, H. Astrocytes as a target of transcranial direct current stimulation (tDCS) to treat depression. *Neuroscience research* **126**, 15-21, doi:10.1016/j.neures.2017.08.012 (2018).
165 Frey, B. N. *et al.* Evidence of astrogliosis in rat hippocampus after d-amphetamine exposure. *Progress in neuro-psychopharmacology & biological psychiatry* **30**, 1231-1234, doi:10.1016/j.pnpbp.2006.03.016 (2006).

166 Chai, H. *et al.* Neural Circuit-Specialized Astrocytes: Transcriptomic, Proteomic, Morphological, and Functional Evidence. *Neuron* **95**, 531-549 e539, doi:10.1016/j.neuron.2017.06.029 (2017).
167 Adamsky, A. *et al.* Astrocytic Activation Generates De Novo Neuronal Potentiation and Memory Enhancement. *Cell* **174**, 59-71 e14, doi:10.1016/j.cell.2018.05.002 (2018).